Investigating the impact of extracellular vesicles on mitochondrial function in human skeletal muscle cells

M S Lota

2022

Investigating the impact of extracellular vesicles on mitochondrial function in human skeletal muscle cells

Manraj Singh Lota

A thesis submitted in fulfilment of the requirements of Manchester Metropolitan University for the degree of Master of Science (by Research)

School of Healthcare Science, Department of Life Sciences, Musculoskeletal Science & Sports Medicine Research Centre

2022

Declaration of Academic Integrity:

With the exception of any statements to the contrary, all the data presented in this report are the results of my own efforts. In addition, no parts of this report have been copied from other sources. I understand that any evidence of plagiarism and / or the use of unacknowledged third-party data will be dealt with as a very serious matter.

Submitted in accordance with the requirements for the degree of:

Master of Science (By Research) (Life Science)

Manchester Metropolitan University

All Saints Building, All Saints, Manchester M15 6BH

Signed: Manraj S Lota

Date: September 2022

Contents page

Table n page

Table 1.
Data showing the measured protein concentrations for both the Horse Serum (HS) and Serum Free (SF) C2C12 samples against a control (0 ng/ml) and varied TNF-α concentrations (10,25 and 50 ng/ml). These were applied under both 72- and 24-hour incubation periods with the absorbance measured at 280 nm.

Table 2.
Data showing the measured RNA amounts for both the Horse Serum (HS) and Serum Free (SF) C2C12 samples against a control (0 ng/ml) and varied TNF-α concentrations (10,25 and 50 ng/ml). These were applied under both 72- and 24-hour incubation periods and the absorbance were measured at A260/A280 nm to determine the purity of nucleic acids.

Table 3.
Data showing the measured Double stranded DNA antibodies (dsDNA) for both the Horse Serum (HS) and Serum Free (SF) C2C12 samples against a control (0 ng/ml) and varied TNF-α concentrations (10,25 and 50 ng/ml). These were applied under both 72- and 24-hour incubation periods and the absorbance were measured at A260/A280 nm.

Figure n page

Figure 1.

The translocation of phosphatidylserine to the outer membrane with signalling factor ADP-ribosylation factor 6 (ARF6) which helps in signalling the cascade needed for the phospholipase D. Allowing for activation of myosin light chain kinase (MLCK) needed for the budding and release of microvesicles (Akers et al., 2013).

Figure 2.

The process that takes place during apoptosis in order for the formation of apoptotic bodies for occur (Akers et al., 2013).

Figure 3.

The capability tetraspanins have with regard to interacting with many receptors and signalling molecules (Andreu and Yáñez-Mó, 2014).

Figure 4.

The formation of exosomes during the two key stages. Left image displaying the fusion of the endocytic vesicles with the late endosome. The image on the right showing the recognition of tetraspanins which are reorganised into enriched microdomains (Akers et al., 2013).

Figure 5.

Multiple examples of how exosomal miRNAs play a role in skeletal muscle myogenesis (Yue et al., 2020).

Figure 6.

The difference in cell culture growth for C2C12 P6 cells over a 24-hour period in two separate flasks.

Figure 7.

The difference in cell culture growth for C2C12 P6 cells over a 72-hour period in two separate flasks.

Figure 8.

The orientation of the 72-hour incubation samples with the specific cell culture media and stimulatory agent concentrations.

Figure 9.

The orientation of the 24-hour incubation samples with the specific cell culture media and stimulatory agent concentrations.

Figure 10.

The orientation of the differentiated samples (Both 72-hour and 24-hour incubation samples) with the specific cell culture media and stimulatory agent concentrations.

Figure 11.

The prepared serial dilutions

Figure 12.

The 96-well plate arrangement.

Figure 13.1.
Difference in C2C12 morphology before and after different TNF-α concentration and different incubation periods in the presence of either serum free or horse serum growth media.

Figure 13.2.
The elevation in Extracellular vesicle / Exosome markers (CD63 and CD81) from TNF-α treated cells. Blot representative of 3 independent experiments.

Figure 14.
Data showing measured non-mitochondrial function from cells treated with varying levels of TNF-α (C, 10, 25 and 50 ng/ml) to promote EV release which have been added with Horse serum (HS) growth media under a 72-hour incubation period. Data is presented as mean of n=3.

Figure 15.
Data showing measured non-mitochondrial function from cells treated with varying levels of TNF-α (C, 10, 25 and 50 ng/ml) to promote EV release which have been added with Serum free (SF) growth media under a 72-hour incubation period. Data is presented as mean of n=3.

Figure 16.
Data showing measured non-mitochondrial function from cells treated with varying levels of TNF-α (C, 10, 25 and 50 ng/ml) to promote EV release which have been added with Horse serum (HS) growth media under a 24-hour incubation period. Data is presented as mean of n=3.

Figure 17.
Data showing measured non-mitochondrial function from cells treated with varying levels of TNF-α (C, 10, 25 and 50 ng/ml) to promote EV release which have been added with Serum free (SF) growth media under a 24-hour incubation period. Data is presented as mean of n=3.

Figure 18.
Data showing measured basal respiration from cells treated with varying levels of TNF-α (C, 10, 25 and 50 ng/ml) to promote EV release which have been added with Horse serum (HS) growth media under a 72-hour incubation period. Data is presented as mean of n=3.

Figure 19.
Data showing measured basal respiration from cells treated with varying levels of TNF-α (C, 10, 25 and 50 ng/ml) to promote EV release which have been added with Serum free (SF) growth media under a 72-hour incubation period. Data is presented as mean of n=3.

Figure 20.
Data showing measured basal respiration from cells treated with varying levels of TNF-α (C, 10, 25 and 50 ng/ml) to promote EV release which have been added with Horse serum (HS) growth media under a 24-hour incubation period. Data is presented as mean of n=3.

Figure 21.
Data showing measured basal respiration from cells treated with varying levels of TNF-α (C, 10, 25 and 50 ng/ml) to promote EV release which have been added with Serum free (SF) growth media under a 24-hour incubation period. Data is presented as mean of n=3.

Figure 22.
Data showing measured maximal respiration from cells treated with varying levels of TNF-α (C, 10, 25 and 50 ng/ml) to promote EV release which have been added with Horse serum (HS) growth media under a 72-hour incubation period. Data is presented as mean of n=3.

Figure 23.
Data showing measured maximal respiration from cells treated with varying levels of TNF-α (C, 10, 25 and 50 ng/ml) to promote EV release which have been added with Serum free (SF) growth media under a 72-hour incubation period. Data is presented as mean of n=3.

Figure 24.
Data showing measured maximal respiration from cells treated with varying levels of TNF-α (C, 10, 25 and 50 ng/ml) to promote EV release which have been added with Horse serum (HS) growth media under a 24-hour incubation period. Data is presented as mean of n=3.

Figure 25.
Data showing measured maximal respiration from cells treated with varying levels of TNF-α (C, 10, 25 and 50 ng/ml) to promote EV release which have been added with Serum free (SF) growth media under a 24-hour incubation period. Data is presented as mean of n=3.

Figure 26.
Data showing measured proton leak from cells treated with varying levels of TNF-α (C, 10, 25 and 50 ng/ml) to promote EV release which have been added with Horse serum (HS) growth media under a 72-hour incubation period. Data is presented as mean of n=3.

Figure 27.
Data showing measured proton leak from cells treated with varying levels of TNF-α (C, 10, 25 and 50 ng/ml) to promote EV release which have been added with Serum free (SF) growth media under a 72-hour incubation period. Data is presented as mean of n=3.

Figure 28.
Data showing measured proton leak from cells treated with varying levels of TNF-α (C, 10, 25 and 50 ng/ml) to promote EV release which have been added with Horse serum (HS) growth media under a 24-hour incubation period. Data is presented as mean of n=3.

Figure 29.
Data showing measured proton leak from cells treated with varying levels of TNF-α (C, 10, 25 and 50 ng/ml) to promote EV release which have been added with Serum free (SF) growth media under a 24-hour incubation period. Data is presented as mean of n=3.

Figure 30.
Data showing measured ATP production from cells treated with varying levels of TNF-α (C, 10, 25 and 50 ng/ml) to promote EV release which have been added with Horse serum (HS) growth media under a 72-hour incubation period. Data is presented as mean of n=3.

Figure 31.
Data showing measured ATP production from cells treated with varying levels of TNF-α (C, 10, 25 and 50 ng/ml) to promote EV release which have been added with Serum free (SF) growth media under a 72-hour incubation period. Data is presented as mean of n=3.

Figure 32.
Data showing measured ATP production from cells treated with varying levels of TNF-α (C, 10, 25 and 50 ng/ml) to promote EV release which have been added with Horse serum (HS) growth media under a 24-hour incubation period. Data is presented as mean of n=3.

Figure 33.
Data showing measured ATP production from cells treated with varying levels of TNF-α (C, 10, 25 and 50 ng/ml) to promote EV release which have been added with Serum free (SF) growth media under a 24-hour incubation period. Data is presented as mean of n=3.

Figure 34.
Data showing measured SRC from cells treated with varying levels of TNF-α (C, 10, 25 and 50 ng/ml) to promote EV release which have been added with Horse serum (HS) growth media under a 72-hour incubation period. Data is presented as mean of n=3.

Figure 35.
Data showing measured SRC from cells treated with varying levels of TNF-α (C, 10, 25 and 50 ng/ml) to promote EV release which have been added with Serum free (SF) growth media under a 72-hour incubation period. Data is presented as mean of n=3.

Figure 36.
Data showing measured SRC from cells treated with varying levels of TNF-α (C, 10, 25 and 50n g/ml) to promote EV release which have been added with Horse serum (HS) growth media under a 24-hour incubation period. Data is presented as mean of n=3.

Figure 37.
Data showing measured SRC from cells treated with varying levels of TNF-α (C, 10, 25 and 50 ng/ml) to promote EV release which have been added with Serum free (SF) growth media under a 24-hour incubation period. Data is presented as mean of n=3.

Figure 38.
Data showing measured coupling efficiency from cells treated with varying levels of TNF-α (C, 10, 25 and 50 ng/ml) to promote EV release which have been added with Horse serum (HS) growth media under a 72-hour incubation period. Data is presented as mean of n=3.

Figure 39.
Data showing measured coupling efficiency from cells treated with varying levels of TNF-α (C, 10, 25 and 50 ng/ml) to promote EV release which have been added with Serum free (SF) growth media under a 72-hour incubation period. Data is presented as mean of n=3.

Figure 40.
Data showing measured coupling efficiency from cells treated with varying levels of TNF-α (C, 10, 25 and 50 ng/ml) to promote EV release which have been added with Horse serum (HS) growth media under a 24-hour incubation period. Data is presented as mean of n=3.

Figure 41.
Data showing measured coupling efficiency from cells treated with varying levels of TNF-α (C, 10, 25 and 50 ng/ml) to promote EV release which have been added with Serum free (SF) growth media under a 24-hour incubation period. Data is presented as mean of n=3.

Figure 42.
Data showing measured non-mitochondrial respiration from differentiated cells treated with varying levels of TNF-α (C, 10, 25 and 50 ng/ml) to promote EV release which have been added with Horse serum (HS) growth media under a 72-hour incubation period. Data is presented as mean of n=3.

Figure 43.
Data showing measured non-mitochondrial respiration from differentiated cells treated with varying levels of TNF-α (C, 10, 25 and 50 ng/ml) to promote EV release which have been added with Serum free (SF) growth media under a 72-hour incubation period. Data is presented as mean of n=3.

Figure 44.
Data showing measured non-mitochondrial respiration from differentiated cells treated with varying levels of TNF-α (C, 10, 25 and 50 ng/ml) to promote EV release which have been added with Horse serum (HS) growth media under a 24-hour incubation period. Data is presented as mean of n=3.

Figure 45.
Data showing measured non-mitochondrial respiration from differentiated cells treated with varying levels of TNF-α (C, 10, 25 and 50 ng/ml) to promote EV release which have been added with Serum free (SF) growth media under a 24-hour incubation period. Data is presented as mean of n=3.

Figure 46.
Data showing measured basal respiration from differentiated cells treated with varying levels of TNF-α (C, 10, 25 and 50 ng/ml) to promote EV release which have been added with Horse serum (HS) growth media under a 72-hour incubation period. Data is presented as mean of n=3.

Figure 47.
Data showing measured basal respiration from differentiated cells treated with varying levels of TNF-α (C, 10, 25 and 50 ng/ml) to promote EV release which have been added with Serum free (SF) growth media under a 72-hour incubation period. Data is presented as mean of n=3.

Figure 48.
Data showing measured basal respiration from differentiated cells treated with varying levels of TNF-α (C, 10, 25 and 50 ng/ml) to promote EV release which have been added with Horse serum (HS) growth media under a 24-hour incubation period. Data is presented as mean of n=3.

Figure 49.
Data showing measured basal respiration from differentiated cells treated with varying levels of TNF-α (C, 10, 25 and 50 ng/ml) to promote EV release which have been added with Serum free (SF) growth media under a 24-hour incubation period. Data is presented as mean of n=3.

Figure 50.
Data showing measured maximal respiration from differentiated cells treated with varying levels of TNF-α (C, 10, 25 and 50 ng/ml) to promote EV release which have been added with Horse serum (HS) growth media under a 72-hour incubation period. Data is presented as mean of n=3.

Figure 51.
Data showing measured maximal respiration from differentiated cells treated with varying levels of TNF-α (C, 10, 25 and 50 ng/ml) to promote EV release which have been added with Serum free (SF) growth media under a 72-hour incubation period. Data is presented as mean of n=3.

Figure 52.
Data showing measured maximal respiration from differentiated cells treated with varying levels of TNF-α (C, 10, 25 and 50 ng/ml) to promote EV release which have been added with Horse serum (HS) growth media under a 24-hour incubation period. Data is presented as mean of n=3.

Figure 53.
Data showing measured maximal respiration from differentiated cells treated with varying levels of TNF-α (C, 10, 25 and 50 ng/ml) to promote EV release which have been added with Serum free (SF) growth media under a 24-hour incubation period. Data is presented as mean of n=3.

Figure 54.
Data showing measured proton leak from differentiated cells treated with varying levels of TNF-α (C, 10, 25 and 50 ng/ml) to promote EV release which have been added with Horse serum (HS) growth media under a 72-hour incubation period. Data is presented as mean of n=3.

Figure 55.
Data showing measured proton leak from differentiated cells treated with varying levels of TNF-α (C, 10, 25 and 50 ng/ml) to promote EV release which have been added with Serum free (SF) growth media under a 72-hour incubation period. Data is presented as mean of n=3.

Figure 56.
Data showing measured proton leak from differentiated cells treated with varying levels of TNF-α (C, 10, 25 and 50 ng/ml) to promote EV release which have been added with Horse serum (HS) growth media under a 24-hour incubation period. Data is presented as mean of n=3.

Figure 57.
Data showing measured maximal respiration from differentiated cells treated with varying levels of TNF-α (C, 10, 25 and 50 ng/ml) to promote EV release which have been added with Serum free (SF) growth media under a 24-hour incubation period. Data is presented as mean of n=3.

Figure 58.
Data showing measured ATP production from differentiated cells treated with varying levels of TNF-α (C, 10, 25 and 50 ng/ml) to promote EV release which have been added with Horse serum (HS) growth media under a 72-hour incubation period. Data is presented as mean of n=3.

Figure 59.
Data showing measured ATP production from differentiated cells treated with varying levels of TNF-α (C, 10, 25 and 50 ng/ml) to promote EV release which have been added with Serum free (SF) growth media under a 72-hour incubation period. Data is presented as mean of n=3.

Figure 60.
Data showing measured ATP production from differentiated cells treated with varying levels of TNF-α (C, 10, 25 and 50 ng/ml) to promote EV release which have been added with Horse serum (HS) growth media under a 24-hour incubation period. Data is presented as mean of n=3.

Figure 61.
Data showing measured ATP production from differentiated cells treated with varying levels of TNF-α (C, 10, 25 and 50 ng/ml) to promote EV release which have been added with Serum free (SF) growth media under a 24-hour incubation period. Data is presented as mean of n=3.

Figure 62.
Data showing measured SRC from differentiated cells treated with varying levels of TNF-α (C, 10, 25 and 50 ng/ml) to promote EV release which have been added with Horse serum (HS) growth media under a 72-hour incubation period. Data is presented as mean of n=3.

Figure 63.
Data showing measured SRC from differentiated cells treated with varying levels of TNF-α (C, 10, 25 and 50 ng/ml) to promote EV release which have been added with Serum free (SF) growth media under a 72-hour incubation period. Data is presented as mean of n=3.

Figure 64.
Data showing measured SRC from differentiated cells treated with varying levels of TNF-α (C, 10, 25 and 50 ng/ml) to promote EV release which have been added with Horse serum (HS) growth media under a 24-hour incubation period. Data is presented as mean of n=3.

Figure 65.
Data showing measured SRC from differentiated cells treated with varying levels of TNF-α (C, 10, 25 and 50 ng/ml) to promote EV release which have been added with Serum free (SF) growth media under a 24-hour incubation period. Data is presented as mean of n=3.

Figure 66.
Data showing measured coupling efficiency from differentiated cells treated with varying levels of TNF-α (C, 10, 25 and 50 ng/ml) to promote EV release which have been added with Horse serum (HS) growth media under a 72-hour incubation period. Data is presented as mean of n=3.

Figure 67.
Data showing measured coupling efficiency from differentiated cells treated with varying levels of TNF-α (C, 10, 25 and 50 ng/ml) to promote EV release which have been added with Serum free (SF) growth media under a 72-hour incubation period. Data is presented as mean of n=3.

Figure 68.
Data showing measured coupling efficiency from differentiated cells treated with varying levels of TNF-α (C, 10, 25 and 50 ng/ml) to promote EV release which have been added with Horse serum (HS) growth media under a 24-hour incubation period. Data is presented as mean of n=3.

Figure 69.
Data showing measured coupling efficiency from differentiated cells treated with varying levels of TNF-α (C, 10, 25 and 50 ng/ml) to promote EV release which have been added with Serum free (SF) growth media under a 24-hour incubation period. Data is presented as mean of n=3.

Abbreviations

4E-BPs – eIF4E-binding proteins
AA – Antimycin
ABs – Apoptotic bodies
AMPK – AMP-activated protein kinase
ATP – Adenosine 5'-triphosphate
BCA – Bicinchoninic acid
BMR – Basal metabolic rate
BR – Basal respiration
BSA – Bovine serum albumin
CE – Coupling efficiency
CoQ10 – Coenzyme Q10
CP450 – Cytochrome P450
dH20 – Distilled water
DPBS – Dulbecco's Phosphate-buffered saline
dsDNA – Double stranded DNA
EBV – Epstein-Barr virus
eIF4E – Eukaryotic translation initiation factor 4E
ERK – Extracellular signal-regulated kinase
ESCRTs – Endosomal sorting complexes required for transport
EVs – Extracellular vesicles
FBS – Fetal bovine serum
FCCP – Carbonyl cyanide-4-phenylhydrazone
G6PD – Glucose-6-phosphate dehydrogenase
HUVECs – Human umbilical vein endothelial cells
ikkβ – Inhibitor of nuclear factor kappa-B kinase subunit beta
ILVs – Intraluminal vesicles
MDH – Malate dehydrogenase
MetOH – Methanol
MLCK – Myosin light chain kinase
MMPS – Matrix metalloproteinases
MR – Maximal respiration
mTOR – Mammalian target of rapamycin
MVBs – Multivesicular bodies
MVs – Microvesicles
NADPH – Nicotinamide adenine dinucleotide phosphate
NMR – Non-mitochondrial respiration
NO – Nitric oxide
NOS – Nitric oxide synthase
nSMase2 – Sphingomyelinase-2
OCR – Oxygen consumption rate
PGD – Phosphogluconate dehydrogenase
PIP3 – Phosphatidylinositol 3-phosphate
PL – Proton leak
PR – Proton leak
PTX – Paclitaxel
RA – Rheumatoid arthritis
RANKL – receptor activator of nuclear factor kappa beta ligand
ROS – Reactive oxygen species
ROT – Rotenone

SD – Standard deviation
SDS – PAGE – Sodium dodecyl sulphate–polyacrylamide gel electrophoresis
SKMs – Skeletal muscle cells
SRC – Spare respiratory capacity
TBST – Tris Buffered Saline with Tween
TEMS – Tetraspanins enriched microdomains
TNF-α – Tumour necrosis factor-alpha
TSG101 – Tumour susceptibility gene 101
Tsp – Thrombospondin
UCPs – Uncoupling proteins
VAMP3 – Associated membrane protein 3
WR – Working reagent

Acknowledgments

First and foremost, I would like to thank Manchester Metropolitan University for the last 4 years and for allowing me to be able to complete this Master of Science by research degree in Life Science's. A huge thank you must go out to Glenn Ferris whose technical support, particularly at the beginning of the academic year made this entire process much easier to carry out. For the last 4 years, I have been lucky enough to meet many academics who have provided me with great lessons, however tutor, Adam Lightfoot has given me the greatest teachings.

I have been lucky enough to be taught by Dr Lightfoot during my undergraduate and work alongside him during my final year and more under this master by research degree. With his advice and guidance throughout this tough year, he made this challenge by far the most enjoyable experience I've had and can say confidently that the experiences I've been through will be remembered for years to come but have set me up in a way that I can be successful in any career I choose. I hope the work presented in this project gives an accurate presentation of the amazing work Adam does and shows how significant this study can be.

Thank you.

Abstract

Background: Extracellular vesicles are a class of membrane limited vesicles that withhold the ability to firstly transport and secondly liaise with several cells such as proteins and lipids. There are 3 major classes of extracellular vesicles, those being microvesicles, apoptotic bodies and finally the most notable out the three, Exosomes. Surrounding extracellular vesicles, the main function was thought to be merely the removal of unwanted substances. However, due to its ability to cell to cell communicate, it has been hypothesised that Extracellular vesicles have a key role in both physiological and pathological mechanisms that make up bodily functions. Skeletal muscles are a huge endocrine organ, and its ability isn't primarily related to its mechanisms found for physical movement but include acting like a storage for substrates key in regulating core body temperatures. Extracellular vesicles have additionally been questioned with playing a part in muscle regeneration as well as repair.

Aim: It was to determine whether cells stimulated with Tumour necrosis factor – alpha caused an increase synthesis of extracellular vesicles and the effect the membrane limited vesicle had on skeletal muscle mitochondrial function.

Method: Human skeletal muscle cells were cultured in varying concentrations of Tumour necrosis factor – alpha for either 24 or 72-hour incubations with two different growth medias. RNA, DNA and protein quantifications were carried out with Nanodrop. Changes in mitochondrial function were analysed with Seahorse XFP stress test to determine the effects extracellular vesicle release had on factors such as, non-mitochondrial respiration, maximal respiration and the key marker for muscle mitochondrial dysfunction, proton leak.

Results: It was possible to determine that as the concentration of Tumour necrosis factor – alpha increased treatment on skeletal muscle cells, it did cause an increase synthesis of extracellular vesicles as a result. Through the identification of key hallmark exosomal markers (CD9 and CD81). Furthermore, RNA and DNA concentrations were altered, in some cases positively but also decreases in RNA and DNA were recorded. Regarding mitochondrial function, increases in proton leak and decreases in ATP production were produced indicating that the increase in extracellular vesicle could lead toward muscle dysfunction. However, the stimulation of extracellular vesicles didn't completely disrupt mitochondrial function, in some cases it was seen the improve.

Conclusion: Collectively, the results attained showed that Tumour necrosis factor – alpha treated skeletal muscle cells did cause an increase in synthesis for extracellular vesicle synthesis as well the release augmented mitochondrial function.

1.0 Introduction

1.1 Basic Biology of Extracellular vesicles

Part of the heterogenous class of membrane – limited vesicles, Extracellular vesicles (EVs) are released by most cells however not able to replicate like most others (Mrgolis and Sadovsky, 2019). With its larger size remaining unknown, the double – layer phospholipid membrane ranges from 10-20 nm at the smaller range. Due to the enormously large and diverse types of EVs known and the complexity found within the biogenesis, targeting mechanisms, and vesicle processing (Mrgolis and Sadovsky, 2019) due to being discharged by a variety of cells. The classification surrounding EVs is resulting attributed to its size, location, and method of release. This has made it increasingly difficult to differentiate between established biological features or presumptions.

EVs have the ability to transfers and communicate information between cytosolic proteins, lipids, and RNA (Raposo and Stoorvogel, 2013), affecting the cell's biological behaviour. In fact, the message conveyed can either be for protection or a stimulus to a remote site of vesicular origin (Yáñez-Mó et al., 2015). EVs were originally thought to be a means of waste removal of unwanted substances from cells. But now there is an ever-growing belief that EVs play a vital role in both physiological and pathological functions in both eukaryotes and prokaryotes (Yáñez-Mó et al., 2015) and help dictate homeostatic processes or negate any negative pathological developments (Van Niel et al., 2018).

However, it should be stated that the manner in which EVs assist in physiological and pathology functions is fairly unexplored, this applies also to studies done in both vivo and vitro situations (Van der Pol et al., 2012).

There are currently two methods of release for EVs which help define the classifications. The first involves donor cells being released from the outward budding of the plasma membrane, resulting in the formation of Microvesicles (MVs) (Abels and Breakefield, 2016). The alternate route involves the inward budding of the endosomal membrane, culminating in the formation of multivesicular bodies (MVBs) (Abels and Breakefield, 2016). Coincidently, Exosomes, the most researched heterogenous class is released by the fusion of the outer MVBs membrane with the plasma membrane (Abels and Breakefield, 2016) releasing intraluminal vesicles (exosomes). These 3 classes are determined by the size, morphology, subcellular origin, lipid and protein composition (Van der Pol et al., 2012).

1.2 Microvesicles

Formally known as platelet dust, Microvesicles (MVs) are the smallest type of EVs, measuring in at roughly at 30nm. The biogenesis remains fairly ambiguous due to being associated with several cellular model systems (Abels and Breakefield, 2016). The formation begins with the binding protein, ADP-ribosylation factor 6 (ARF6), this triggers a cascade that stimulates phospholipase D (PLD) (Abels and Breakefield, 2016), an essential enzyme vital for growth factor signalling. The protein, extracellular signal-regulated kinase (ERK) is passed to the plasma membrane where myosin light chain kinase (MLCK) is activated due to ERK phosphorylating (Abels and Breakefield, 2016) causing the release of MVs.

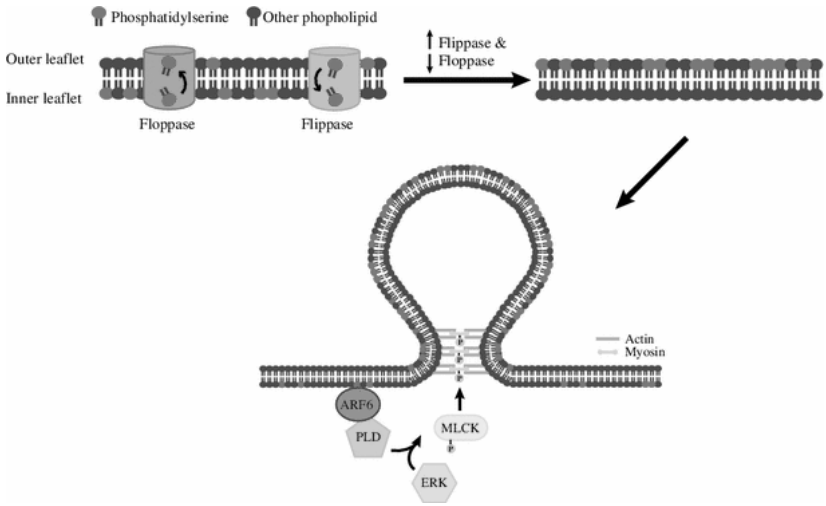

Figure 1: The translocation of phosphatidylserine to the outer membrane with signalling factor ADP-ribosylation factor 6 (ARF6) which helps in signalling the cascade needed for the phospholipase D. Allowing for activation of myosin light chain kinase (MLCK) needed for the budding and release of microvesicles (Akers et al., 2013).

The entire process is carried out by actin to myosin interactions causing a shortening of the cytoskeletal structures (Akers et al., 2013). Many factors help to contribute to the formation of these vesicles such as phospholipids being redistributed and the repositioning of phosphatidylserine to the outer leaflet (Abels and Breakefield, 2016). As mentioned, due to being released from several cell types, the origin of the vesicle dictates their ability to carry out specific functions such as transporting biologically active macromolecules between cells (Meches Jr and Raab-Traub, 2011).

When developing, the microvesicles will contain several definitive virus-like components (Meches Jr and Raab-Traub, 2011) which will dictate their cellular function. For example, when MVs are produced from melanocytes, the vesicles are enriched with associated membrane protein 3 (VAMP3) and B1 integrin receptors (Akers et al., 2013). The functional properties besides transporting molecules involve gene and immune regulation, cell proliferation and invasion (Meches Jr and Raab-Traub, 2011).

1.3 Apoptotic bodies

Apoptotic bodies (ABs) also referred to as apoptotic vesicles and are the largest subtype measuring in at 1 – 5 µm (Meches Jr and Raab-Traub, 2011)**.** Different to the other vesicles, the release of ABs is a by-product of the major mechanism known as Apoptosis, the process characterised by its cell death for normal and cancerous cells (Akers et al., 2013). The development of ABs starts with nuclear chromatin condensing resulting in the membrane blebbing (Akers et al., 2013). The blebbing leads to protrusions of the cell membranes containing cytoplasm being released, leading to disintegration of the cellular contents towards apoptotic bodies (Akers et al., 2013). There are specific changes that occur in order for ABs to be produced, these include changes in oxidation of surface molecules allowing for the binding of Thrombospondin (Tsp) and complement protein C3b (Akers et al., 2013).

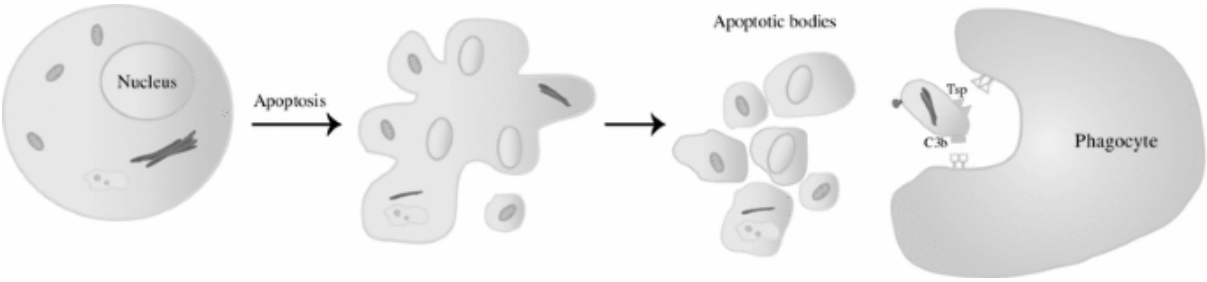

Figure 2: The process that takes place during apoptosis in order for the formation of apoptotic bodies for occur (Akers et al., 2013).

However, it should be mentioned that the clearance of ABs via phagocytosis is vital for keeping bodily functions correct. This mechanism is dictated by recognition receptors on phagocytes (Akers et al., 2013). Failure to do so has been associated with evoking the development of systemic autoimmune diseases (Van der Pol et al., 2012). This is due to when ABs released from the endoplasmic reticulum, they expose immature glycoepitopes (Van der Pol et al., 2012).

As ABs contain cytoplasm as part of their biological structure, it allows for cellular remnants such as DNA fragments and cellular organelles (Meches Jr and Raab-Traub, 2011) to be included which in turn is attributed to their biological function. For example, it has been known that apoptotic bodies are involved in the transfer of oncogenes and DNA between cells (Meches Jr and Raab-Traub, 2011) which helps to regulate and control intercellular communication.

1.4 Exosomes

Exosomes are the more recognised sub-type in regard to Extracellular vesicles. Inheriting a cup-like morphology and a size of 40 – 100nm (Meches Jr and Raab-Traub, 2011). The biogenesis for exosomes takes place and are composed within the intraluminal vesicle (ILV) as well as being **c**ulminated in the inward budding of the endosomal multivesicular bodies (Meches Jr and Raab-Traub, 2011). The **I**LV is key to the generation as it used to degrade and recycle; proteins, lipids and nucleic acids (Abels and Breakefield, 2016). However, it has been suggested that endosomal sorting complexes required for transport (ESCRTs) is essential for the development of MVB formation, vesicle budding, and protein cargo sorting (Zhang et al., 2019). The ESCRT can take 4 different forms which are independently used in cohesion, these include ESCRT 0, 1, 2, and 3.

For the function of ESCRT – 0, 1 and 2, its primary role is to recognise ubiquitinated membrane proteins at the endosomal delimiting membrane (Raposo and Stoorvogel, 2013). Whereas ESCRT – 3 complex is the primary cause for membrane budding and the scission of ILVs (Raposo and Stoorvogel, 2013). However, it should be stated that for the generation of the vesicle, there are numerous routes which can take place involving MVBs. For example, multivesicular bodies can combine with the lysosome for degradation or in this case, with the plasma membrane causing exosomal release (Petrovčíková et al., 2018).

Additionally, cholesterol has been deemed an essential feature for the biogenesis. In a cholesterol rich multivesicular body state, the biogenesis leans more towards secretion of exosomes (Petrovčíková et al., 2018). In comparison, having a low cholesterol yield the MVBs lean towards lysosome degradation (Petrovčíková et al., 2018).

So, the primary step involves the actual formation of ILVs. Tetraspanins are highly enriched membrane bound proteins (Akers et al., 2013) that sort the endosome membrane into specialized sectors which are referred to as tetraspanins enriched microdomains (TEMs). TEMs cluster specific proteins which

enables the formation of ILVs through protein – protein synergy (Akers et al., 2013). The definitive proteins thought to be vital for this interaction are the tetraspanins CD9 and CD63. Tetraspanins are key to biological functions as they are involved in countless processes such as, cell adhesion, invasion, motility, and signalling (Abels and Breakefield, 2016). Tetraspanins can be in 5 distinct location which resulting leads to the specific role they play in biological processes.

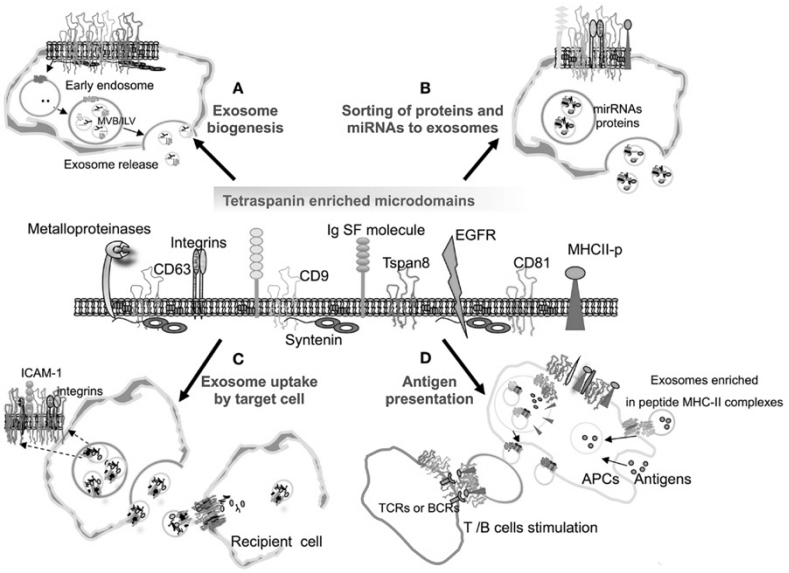

Figure 3: The capability tetraspanins have with regard to interacting with many receptors and signalling molecules (Andreu and Yáñez-Mó, 2014).

The endosome is then marked by a series of abundant phosphatidylinositol 3-phosphate (PIP3) proteins (Akers et al., 2013) which subsequently causes the recruitment of the ESCRT-1 / ESCRT-2 causing the membrane to bud (Akers et al., 2013). Alternate essential proteins are then required for the recruitment of ESCRT-3. One of them is the endo-lysosomal regulator protein (Trioulier et al., 2004), Alix or often referred to as ALP1. The cytoplasmic protein is vital for controlling cell death (Trioulier et al., 2004). The other protein is tumour susceptibility gene 101 (TSG101), which helps reduce derogation. Both work in harmony and are often referred to as exosomal markers alongside the CD9 and CD63 tetraspanins. These help to ensure the completion of the budding and release of exosomes.

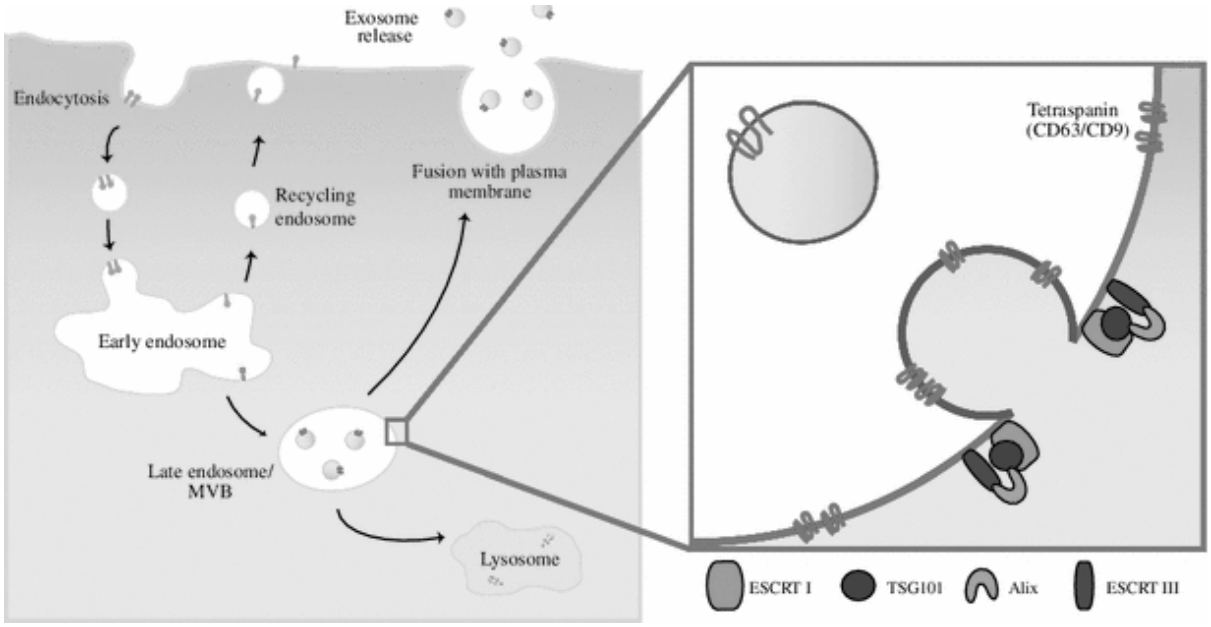

Figure 4: The formation of exosomes during the two key stages. Left image displaying the fusion of the endocytic vesicles with the late endosome. The image on the right showing the recognition of tetraspanins which are reorganised into enriched microdomains (Akers et al., 2013).

Other factors can dictate the biogenesis of exosomes. For example, Hrs, a ESCRT-o protein was shown that in HEK293 cells when reduced caused a reduction in exosomal Wnt3A and Evi secretion (Hessvik and Llorente, 2018). Furthermore, dendritic cells located from the bone marrow were indictive of secreting less exosome – associated flotillin-1 (Hessvik and Llorente, 2018). As well as lipopolysaccharide induced TNF factor or LITAF, a late endosome protein, when involved in MVB formation caused an increase in exosomes (Hessvik and Llorente, 2018). However, in rat adenocarcinoma cells where the release was unaffected, the composition of exosomes did alter, in particular with proteins and mRNAs (Hessvik and Llorente, 2018).

In contrast to other secreted vesicles, exosomes are currently the only known one to arise from internal membranes. Further, exosomes are found in several biological fluids which as a result allows for the vesicle to be counted as a biological biomarker. A few examples of these fluids include saliva, amniotic fluid, urine, plasma and ascites (Meches Jr and Raab-Traub, 2011).

As exosomes can be found and released from many cell types, it is believed that exosomes play a critical role in several processes such as the immune response, tumour progression and

neurodegenerative disorders (Zhang et al., 2015). For example, with the spread of viral infections, exosomes were exposed in the transport of prions and beta – amyloid peptides (Alenquer and Amorim, 2015). This in principle would indicate that exosomes help the progression and spread of infections. Additionally, the vesicle plays a part in the regulation of immunity. When exosomes are released from Epstein-Barr virus (EBV) infected nasopharyngeal carcinoma cells, exosomes contained significant amounts of immunoregulator protein galectin-9 (Alenquer and Amorim, 2015). This resulting leads to the EBV-specific CD4+ T cells apoptosis to be induced. This type of reaction is further seen when exosomes released from EBV-infected B lymphocytes leads to an effect on non-infected B lymphocytes (Alenquer and Amorim, 2015). In fact, it causes the lymphocytes to proliferate and differentiate into plasma blast-like cells (Alenquer and Amorim, 2015).

1.5 What is known in Skeletal muscle cells

More recently, vesicles have been attributed to playing a significant role and having a relationship with the endocrine organ, skeletal muscle. One of the major hypotheses involves extracellular vesicle's ability to communicate and transfer functional cargo to recipient cells during exercise releasing skeletal muscle – specific cytokines (Vechetti Jr et al., 2021). Additionally, they have been proposed in playing a role in the endocrine's organ homeostatic function, specifically regarding the whole-body glucose disposal and locomotion (Rome et al., 2019).

The organ itself is formed from progenitor cells emanating in the somites, specifically forming in the vertebrate limb (Buckingham et al., 2003). The cells then divide into layers from the hypaxial edge of the dorsal part the somites, referred to as the dermomyotome (Buckingham et al., 2003). They then migrate into the limb bud where they are then found to proliferate and express myogenic determination factors, this results in the cells differentiating into skeletal muscles (Buckingham et al., 2003). The muscle is the largest organ found within the body, accounting for roughly 40% (Vechetti Jr et al., 2021). Out of that 40%, 50-75% of all bodily proteins and 30-50% (Frontera and Ochala, 2015) of whole-body protein turnover is found within the endocrine organ.

Primarily skeletal muscle's main function revolves around the ability it has in **a**cting as a storage for a series of substrates, core body temperature maintenance and the most significant, the expenditure of oxygen during physical movement (Frontera and Ochala, 2015). Furthermore, the substrates found in storage within the muscle (amino acids and carbohydrates) have huge implications on the body. For example, the amino acids released contribute to the preservation of blood glucose levels during

conditions such as starvation (Frontera and Ochala, 2015). Highlighting one particular way the importance the endocrine organ has. Not to mention, in terms of disease and health, a reduced skeletal muscle mass results in the body's capability to respond and deal with stress and chronic illness (Frontera and Ochala, 2015).

In regard to extracellular vesicles, previous studies showed the vesicles have a direct relationship with skeletal muscles when actively used. By this, when an hour of cycling was carried out, systemic extracellular vesicles were released significantly and taken up by the liver (Vechetti Jr et al., 2021). In addition to this, 5% of Extracellular vesicles were positive to carrying the protein, α-sarcoglycan and skeletal muscle specific microRNA, miR-206 (Vechetti Jr et al., 2021). Moreover, it has been eluded that extracellular vesicle have a role in muscle regeneration, specifically with the protein Annexin-A1. When cell injury occurs, the protein is released in conjunction with extracellular vesicles and with this causing a reaction to occur on Rac and p120 proteins, ensuring a faster closure of the epithelial wound (Bittel and Jaiswal, 2019).

Previous studies conducted displayed C2C12 cells would release exosomes which would carry mtDNA and some functionally relevant proteins (Yue et al., 2020). Knowing this would support theories that skeletal muscles found within C2C12 could deliver signals to target cells in order to carry out specific actions. Moreover, certain microRNAs are decreased during myoblast proliferation (Yue et al., 2020) indicating that exosomes secreted from skeletal muscles influence the myogenesis for the endocrine organ (Yue et al., 2020). This would further indicate that exosomes liaise with both myoblast and myotubes.

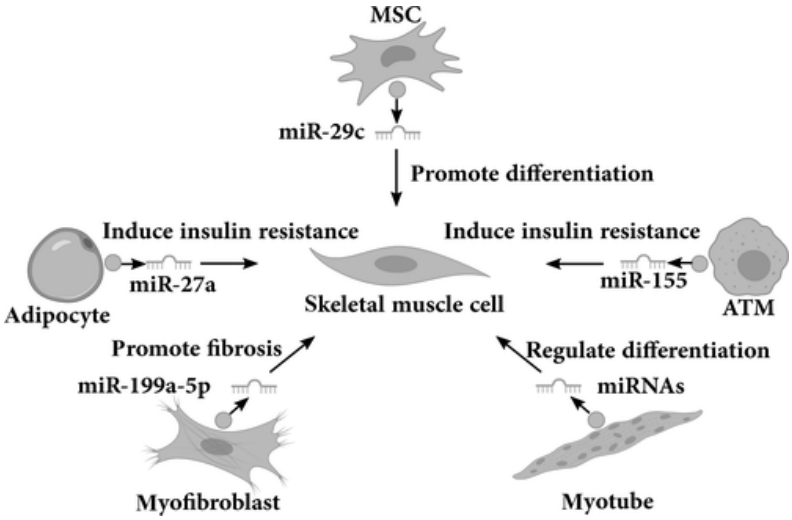

Figure 5: Multiple examples of how exosomal miRNAs play a role in skeletal muscle myogenesis (Yue et al., 2020).

Moreover, skeletal muscle can release specific extracellular vesicles for dealing with specific injuries. For instance, when the muscle is damaged and neutrophils are released, they migrate to the site of injury and cause ectosomes to discharged (Bittel and Jaiswal, 2019). These ectosomes contain properties which work in harmony to increase the inflammatory response. These properties include F-actin, integrins, selectins, matrix metalloproteinases (MMPs) and annexin-5 (Bittel and Jaiswal, 2019). Further, during Duchenne muscular dystrophy related muscle deterioration, exosomes release a series of miRNAs such as CCCU containing miR-133a (Bittel and Jaiswal, 2019). miRNAs such as this are important for intercellular signalling and play a role in the signalling for regeneration and repair mechanism (Bittel and Jaiswal, 2019).

1.6 Stimulatory agents

Many factors influence the biogenesis but also the function of exosomes, these as mentioned can be elements such as bodily homeostasis and stimulatory agents. In this case, Tumour necrosis factor – alpha (TNF-α) has been observed in effecting the production of exosomes. When exosomes were isolated in human umbilical vein endothelial cells (HUVECs) and treated with TNF-α, it led to a reduction in tube formation and increased the rate in which apoptosis occurs (Li et al., 2019). This resulting caused an increase in exosomes in comparison to HUVECs without the stimulation of TNF-α (Li et al., 2019).

The relationship between TNF-α and exosomes is apparent under other settings. For example, with rheumatoid arthritis (RA), a chronic inflammatory autoimmune disease (Console et al., 2019). Exosomes originating from synovial fibroblasts from RA membranes contain a form of TNF-α. This consequently results in exosomes being able to enter anti-CD3-activated T cells, activating AKT and NF-kB (Console et al., 2019). Further after the uptake of exosomes in a RA state, the activate t-cells become resistant to apoptosis (Console et al., 2019).

Regarding mitochondrial function in relation to skeletal muscles, it has been hypothesised that TNF-α hinders myofibrillar proteins by releasing reactive oxygen species (ROS) (McLean J et al., 2013). Although the data is unclear in the manner how it does this, it has been linked to the functions surrounding the electron transport chain (McLean J et al., 2013). With findings like this, it opens the door to try and provide more insight and find out the cause on how it affects mitochondrial functions in skeletal muscles.

1.7 Applications / drug deliverance

Being an endogenous system for intercellular communication, extracellular vesicles have gathered a large amount of interest in terms of their ability to transfer information when it comes to acting as a drug delivery courier. The current interest with EVs surrounding drug delivery surrounds treatments for cancer, particular with chemotherapeutic agents (Vader et al., 2016). When EVs derived from dendritic cells were packaged with integrin for the chemotherapeutic drug doxorubicin, breast tumour growth was significantly reduced along side effects (Vader et al., 2016). The reduced side effects were displayed with a reduction of cardiac damage, a prolific side effect of doxorubicin (Vader et al., 2016). Another example in which exosomes packaged into drugs produced a positive effect is with Paclitaxel (PTX) or as it often referred to, Taxol. The chemotherapy drug when packaged with exosomes displayed a increased level of effectiveness for inhibiting growth of Lewis lung carcinoma (Vader et al., 2016).

For exosomes improving drug delivery capabilities, it has been demonstrated with Parkinson's disease. With this nervous system disorder, it reduces enzymes located in the brain such as catalase and superoxide dismutase (Vader et al., 2016). A test was carried out in which catalase was packaged with EVs and resulted in a reduction of microglial activation and helped in reducing the effect reactive oxygen species (ROS) have on neurons (Vader et al., 2016).

Extracellular vesicles have been suggested to also playing a key part in age-related bone loss as well as bone metabolism. This stems from the knowledge that Osteoblasts synthesize bone whereas Osteoclasts can either break down or re-absorb the bone (Murphy et al., 2018). This mechanical process is factored by several aspects such as hormones and miRNAs (Murphy et al., 2018) and the EVs that originate from bone marrows are known to be involved in bone homeostasis and repair (Murphy et al., 2018). Research was done which did indicate that EVs derived from Osteoblasts helped encourage the formation of Osteoclasts with a beta ligand secreted from Osteoblast-derived EVs called receptor activator of nuclear factor kappa beta ligand (RANKL) (Murphy et al., 2018). This cytokine plays a key role in the bones biogenesis as it determines the maintenance and activation of Osteoclasts (Murphy et al., 2018).

1.8 Aims

The project aims investigate the role Exosomes have on inter-cellular communication in skeletal muscle cells.

As well as determining the effect Tumour necrosis factor – alpha (TNF-α) has on exosomal release from skeletal muscle cells.

Additionally, to characterise their cargo and the ability to transmit and augment the function of adjoining muscle cells.

1.9 Hypothesis

It was hypothesised that numerous pathological stimuli generate specific Exosome populations, which in turn have a pathogenic impact on factors such as muscle growth, development and the metabolism of neighbouring cells.

2.0 Materials and methods

2.1 Cell culture proliferation and differentiation

An immortalised human SkMC line from a 25-year-old donor was gifted from the institute of myology in Paris and was used as the base for all conducted experiments such as isolating the exosomes. C2C12 P6, a subclone of myoblasts were cultured in T75 EasYFlasks with the addition of the growth media made up of; 10 ml L-Glutamine which is an amino acid used for the production of proteins such as lymphocytes, macrophages, and fibroblasts (Miller, 1999), 10 ml of Penicillin and 50 ml of Fetal bovine serum (FBS), a chemical which originates from bovine coagulates with its proteins removed. This is commonly used in culture due to its excessive growth factors. The flasks were kept and stored in 37 degrees; 5% CO_2 humidified atmospheric incubators and were topped up with growth media until the myogenicity of the cell cultures were developed enough for the addition of the stimulatory agents.

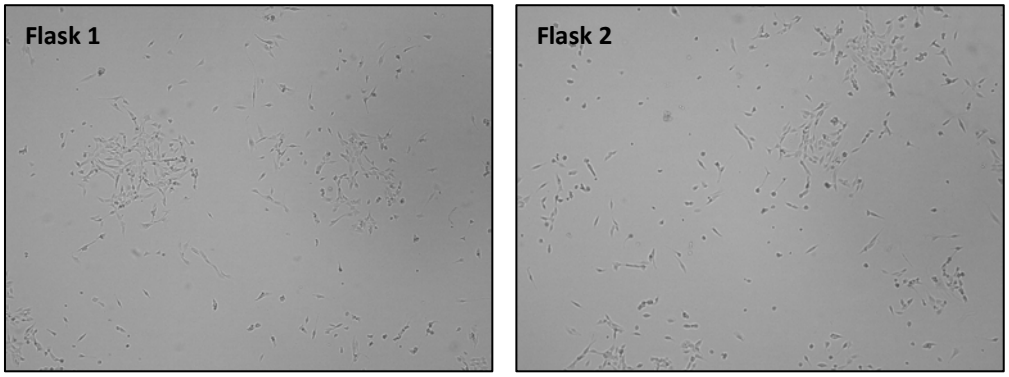

Figure 6: The difference in cell culture growth for C2C12 P6 cells over a 24-hour period in two separate flasks.

In order to keep the growth consistent and reduce the chance of necrosis occurring within the cell flasks, splitting the cells was a necessary requirement. The growth media was removed using SciPette TITAN Automatic Pipette Filler before 5 ml of Dulbecco's Phosphate-buffered saline (DPBS) was used to wash the cells twice. To separate the cells from the surface, trypsin EDTA was supplemented to the flask and then stored in the CO_2 incubator for 5 minutes. It was imperative that the cells weren't stored for ant longer as it could result in the contents becoming toxic. Once the cells were free flowing, growth media was added to inhibit trypsin and then centrifuged at 1000 g, 4 degrees for 5 minutes. Once it had the supernatant, the media was removed and resuspended in growth media and then divided into new flasks.

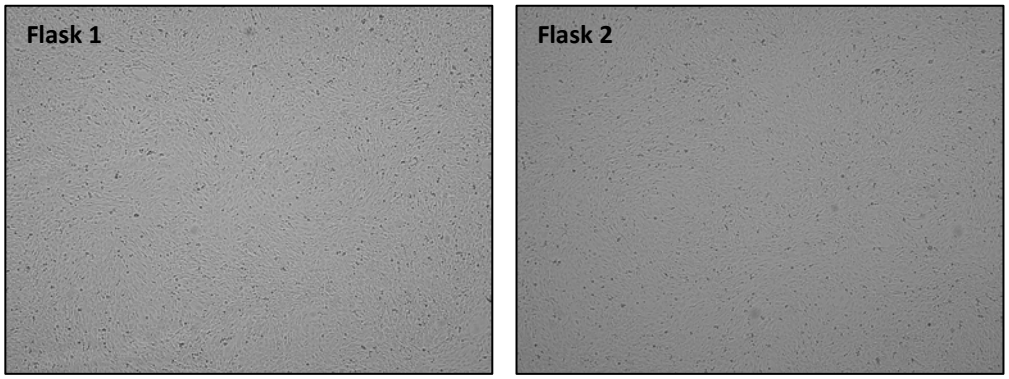

Figure 7: The difference in cell culture growth for C2C12 P6 cells over a 72-hour period in two separate flasks.

The cell cultures displayed in figures 6 and 7 were then split into 16 separate flasks in order to gather enough samples to be able to carry out the necessary tests. To differentiate some of the samples, two measures were taken. One was to incubate half the samples in 2% horse serum growth media, 3 days prior to the addition of the stimulatory agents. This would allow for the cell culture morphology to alter from; spindle shaped to a more cluster and chain like arrangement (Franke et al., 2014). The other method was to use a serum free growth media which would allow for more consistent growth and less variation in shape. Figures 6 and 7 help to show the changes in morphology across the 2 different time periods.

2.2 Sample preparation for stimulatory agents

For the TNF-α, the dosages ranged from; a control which consisted of 0 ng/ml of TNF-α and 10 ml of the chosen incubation media, 10, 25 and 50 ng/ml of TNF-α added with 10 ml of either horse or serum free media. However, half the flasks were stored in incubation for two different period of times. One set was stored in 37 degrees; 5% CO2 humidified atmospheric incubators with the stimulatory agent dosages for 72 – hours. Then in comparison, the other set was stored in the same incubator conditions for 24 – hours.

2.3 Cell scraping and collection

Before scraping the C2C12 cells, the media in each flask was labelled in Argos Technologies conical-bottom centrifuge tubes, 15 ml and stored in the -80-degree freezers. Then one at a time, 1 ml of DPBS was added to each flask and using Fisherbrand cell scrapers, the cells were scraped into one corner.

This was repeated in order to increase the yield and after pipetted into 5 ml test tubes. This process reciprocated for all samples and then stored like the media in the 80-degree freezers.

2.4 Exosome extraction using polymer precipitation

After defrosting the media sample over ice, each one was triturated. 1 ml of each sample was transferred into new 15 ml centrifuge tubes and added with 2 ml of the total exosome isolation kit. The amount added followed the Life Technologies standardise protocol of using a 2:1 reagent media ratio. However, two different incubation periods were taken.

One followed the protocol of a 24 – hour incubation duration but the other was a 72 – hour period. Having two contrasting times would allow us to appraise the current universal standards and see whether extraction yield would be varied.

Once the incubation periods had ended, the mixtures were centrifuged at 4500 g for 90 minutes at 4 degrees celsius. The following pellet was then resuspended in 50 µl of DPBS and then an additional 50 µl was added. Then subsequent mixture and its entire contents were then transferred to 2 ml Eppendorf's for freezer storage.

2.5 RNA, DNA and protein quantification using Nanodrop

For the preparation, it was crucial that the samples were kept on ice throughout the duration of the experiment. Not doing so could have resulted in the exosomes denaturing and therefore effecting the reliability of our recordings.

Just as important, before any measurements were taken, it was vital that the sample reader was cleaned with distilled water and dried with KimWipes. When it came to taking the readings, 2 µl of distilled water was added and used as a blank. For every sample, 2 µl was added. Every time a sample was added and recorded, the reader was then cleaned with distilled water and blanked. Doing this would again reduce the chance of any contamination from previous sample loadings. The A260/A280 and A260/A230 ratios were recorded as well as the amount of RNA (ng/ µl).

2.6 Mitochondrial function analyses

A fresh batch of C2C12 P6 cells were grown in cell culture several days prior to beginning the Seahorse prep. Once the cells were at a stage of confluence where splitting would be the necessary step, the cell culture was stopped, and the normal splitting protocol was followed (as mentioned above). In order to work out the volume of cell media needed where 10,000 cells would be in each well, 40 µl of the cells were added to 40 µl of trypan blue in a 2 ml Eppendorf. The mixture was added to haemocytometer where the volume needed was calculated, in this case 5 µl of the cell culture mixture was added to gather 10,000 cells per well.

For the seahorse XFP cartridges, 20 µl of the calibrant media was added to each well 24 - hours prior to the addition of the media and exosomes. This was to hydrate the cartridge.

To the seahorse XFP plates, the calibrant media was added to the sides to reduce the chance of the contents of the wells from drying out. To the wells, 5 µl of the cell suspension was added alongside the calculated amount of growth media using the data gathered from the nanodrop protocol. Once added, both were left for 1 – hour to adhere to the wells before the calculated volume of exosomes were added. This alongside the cartridge plates were kept in incubation overnight.

For the seahorse assay media, it consisted of; 15 ml of basic basal media, 150 µl of sodium pyruvate and 2.7 µl of glucose. From the incubated seahorse plates, the media in each well was removed with care as agitating the bottom of the well could remove any of the adhered cells. 200 µl of the assay media was added to each well and stored in a non-CO2 incubator for 30 – minutes. The substrates: Oligomycin, Carbonyl cyanide-4-phenylhydrazone (FCCP) and Rotenone/antimycin (ROT/AA) were added with specific amounts of assay media to give specific concentrations. Once the assay media was added to the stock substrates, a new set of mixtures were made using more of the assay media. These new substrates were then added to specific wells on the cartridge plates. 20 µl of Oligomycin was added to well A, 22 µl FCCP to well B and 25 µl ROT/AA to well C. The plates were then placed in the seahorse machine and followed the manufactures instructions for cell mito stress test. Figure 8 and 9 below shows the orientation of the four plates in which this process was carried out for.

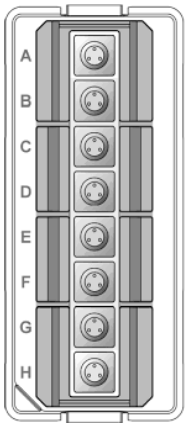

72-hours – HS – Control
72-hours – HS – 10 ng/ml
72-hours – HS – 25 ng/ml
72-hours – HS – 50 ng/ml
72-hours – HS – Control
72-hours – HS – 10 ng/ml
72-hours – HS – 25 ng/ml
72-hours – HS – 50 ng/ml

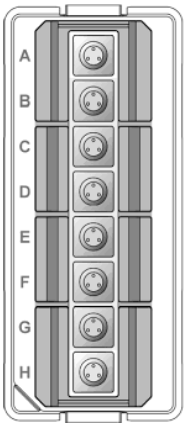

72-hours – SF – Control
72-hours – SF – 10 ng/ml
72-hours – SF – 25 ng/ml
72-hours – SF – 50 ng/ml
72-hours – SF – Control
72-hours – SF – 10 ng/ml
72-hours – SF – 25 ng/ml
72-hours – SF – 50 ng/ml

Figure 8: The orientation of the 72-hour incubation samples with the specific cell culture media and stimulatory agent concentrations.

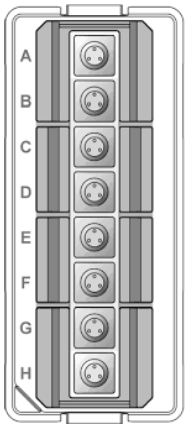

24-hours – HS – Control
24-hours – HS – 10 ng/ml
24-hours – HS – 25 ng/ml
24-hours – HS – 50 ng/ml
24-hours – HS – Control
24-hours – HS – 10 ng/ml
24-hours – HS – 25 ng/ml
24-hours – HS – 50 ng/ml

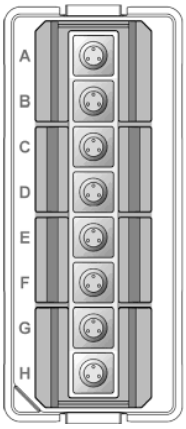

24-hours – SF – Control
24-hours – SF – 10 ng/ml
24-hours – SF – 25 ng/ml
24-hours – SF – 50 ng/ml
24-hours – SF – Control
24-hours – SF – 10 ng/ml
24-hours – SF – 25 ng/ml
24-hours – SF – 50 ng/ml

Figure 9: The orientation of the 24-hour incubation samples with the specific cell culture media and stimulatory agent concentrations.

However, a repeat was carried out for the mitochondrial functional analyses. Where it was a 24 – hour incubation period for the cell suspension, it was changed to a to 72 – hours incubation time period. This did result in the cells in the XFP plates to differentiate and gave us a competitive comparison between myoblast v myotubes. Figure 10 below show the orientation of both plates used for this comparison.

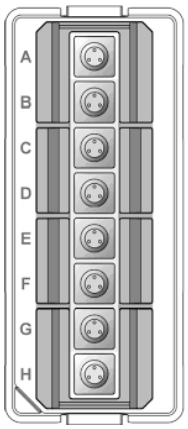

72-hours – HS – Control
72-hours – HS – 10 ng/ml
72-hours – HS – 25 ng/ml
72-hours – HS – 50 ng/ml
72-hours – SF – Control
72-hours – SF – 10 ng/ml
72-hours – SF – 25 ng/ml
72-hours – SF – 50 ng/ml

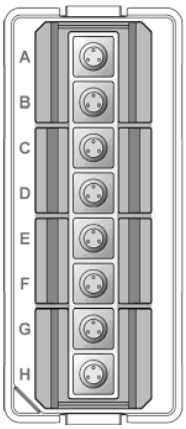

24-hours – HS – Control
24-hours – HS – 10 ng/ml
24-hours – HS– 25 ng/ml
24-hours – HS – 50 ng/ml
24-hours – SF – Control
24-hours – SF – 10 ng/ml
24-hours – SF – 25 ng/ml
24-hours – SF – 50 ng/ml

Figure 10: The orientation of the differentiated samples (Both 72-hour and 24-hour incubation samples) with the specific cell culture media and stimulatory agent concentrations.

2.7 Protein quantification by BCA assay

Each sample was removed from -80-degree storage and left on ice to defrost alongside the Bovine serum albumin (BSA) standard ampoule. The standard was prepared in a 1.5 ml Eppendorf and kept on ice. The serial dilutions were then prepared, figure 11 shows how each sample was arranged. The working reagent (WR) was prepared by mixing a 50:1 reagent A:B ratio, 5 ml of Bicinchoninic acid (BCA) protein assay A was added to a 10 ml test tube alongside 100 µl of BCA protein assay B and vortexed ensuring a thorough mix. 20 µl of each serial dilution was added to its respected well as well as each exosome sample. After the samples were added, 200 µl of the BCA WR reagent was added to every well and then incubation for 30 minutes at 37-degrees. The figure 12 below shows the arrangement of how each sample was added to the 96-well plate.

BSA 1mg/ml (1000ul/ml)	Serial Dilutions	Concentration (µg/ml)
Dil 1:2 50 µl + 50 µl water	S1	500
Dil 1:2 50 µl + 50 µl water	S2	250
Dil 1:2 50 µl + 50 µl water	S3	125
Dil 1:2 50 µl + 50 µl water	S4	62.5
Dil 1:2 50 µl + 50 µl water	S5	31.25
Dil 1:2 50 µl + 50 µl water	S6	15.63
50ul water	B	0

Figure 11: The prepared serial dilutions

	1	2	3	4	5	6	7
A	S1	S1	72hrs-HS-C	72hrs-SF-C	24hrs-HS-C	24hrs-SF-C	
B	S2	S2	72hrs-HS-10	72hrs-SF-10	24hrs-HS-10	24hrs-SF-10	
C	S3	S3	72hrs-HS-25	72hrs-SF-25	24hrs-HS-25	24hrs-SF-25	
D	S4	S4	72hrs-HS-50	72hrs-SF-50	24hrs-HS-50	24hrs-SF-50	
E	S5	S5					
F	S6	S6					
G	B	B					

Figure 12. The 96-well plate arrangement.

After incubation, the plate was read at an absorbance of 562 nm, and a standard curve was created to work out the concentration of each sample's protein quantifications. This was necessary to work out the exact volumes needed for the SDS-Page protocol.

2.8 SDS – PAGE and western blotting

Sodium dodecyl sulphate–polyacrylamide gel electrophoresis (SDS – PAGE) was carried out as followed. 20 µl of the exosomal protein samples were added to 20 µl of Laemmli loading buffer blue, 2x in 1.5 ml Eppendorf's. Each sample was vortexed and then denatured at 95 degrees for 5 minutes and cooled at room temperature. The running buffer was made using 100 ml of 10x Tris/Glycine running buffer, 890 ml of distilled water (dH20) and 10 ml of 10% SDS. The samples as well as the protein ladder were added to the precast Bis-Tris gels (mPAGE®). Electrophoresis was carried out at 150 v for 90 minutes in the pre-made running buffer.

Following electrophoresis, the reagents were prepared. Anode 1 buffer consisted of 36.34 g of Tris Base, 800 ml of dH20 and 200 ml of 20% Methanol (MetOH). Anode 2 buffer was the same except 3.03 g of Tris Base was added. Finally, the cathode buffer included 5.25 g, 40 nM of 6-amino-n-hexanoic acid as well as 800 ml of dH20 and 200 ml of 20% MetOH. The gels were removed from the cassettes and following Bio-Rad Trans – blot turbo transfer system protocol, the gel was stored in anode 2 for 10 minutes to equilibrate. The rest of the protocol was followed and once the system was complete, both gels were placed on the cassette and the conditions were set, 25 v, 1.0 A for 30 minutes.

2.9 Protein detection

Succeeding western blotting, for the protein detection, it followed Bio-Rads protocol. Both membranes were removed from the cassette and rinsed in dH20 for several minutes. They were then

transferred to a shaker whilst ponceau solution was add and left to incubate for 5 minutes. After the stain was removed using dH20, the membranes were placed in blocking solution for 1-hour on a 4-degree shaker. 3 5-minute Tris Buffered Saline with Tween (TBST) washes were done after which was followed by a 60-minute incubation on the 4-degree shaker in the 1ry AB solution, comprised of 5 g Marvel dried skimmed milk and 500 ml of TBST. After the gels were lefts to equilibrate for 15-minutes at room temperature. The blot was again washed 3 times for 5-minutes with TBST, then followed by a secondary antibody wash however this time in a 2ry Ab solution consisting of 15 g of Marvel dried skimmed milk and 500 ml of TBST. This was left to incubate for 60-minutes. The blot was then ready for its final TBST wash.

2.10 Data handling

Due to the time pressures following the pandemic, the user license for the statistical software had expired when the full datasets were finally acquired, therefore it was not possible to continue with the statistical analysis of the data. All data handling was performed using Microsoft Excel version 2021. Where data were presented graphically (Figures 14-69), data were presented as mean. Differences from controls were inspected visually.

3.0 Results

3.1 Characterisation of the Extracellular vesicle preparation

3.1.1 Gross cell morphology

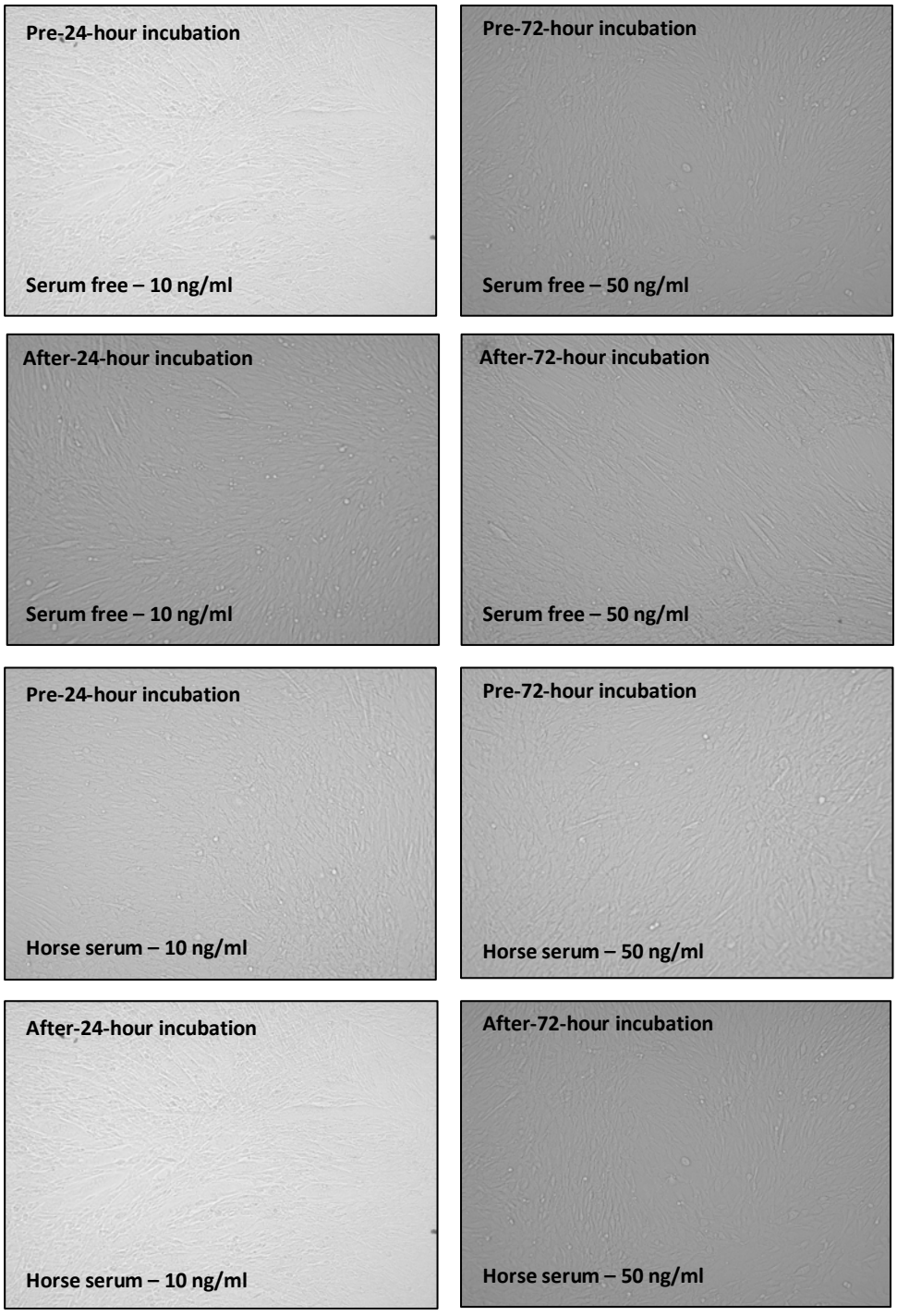

Figure 13.1: Difference in C2C12 morphology before and after different TNF-α concentration and different incubation periods in the presence of either serum free or horse serum growth media.

With figure 13.1, the images of the C2C12 P6 morphology helps to show us how the cells alter against varying TNF-α concentrations as well as the type of serum. In this case, densely packed cells in all samples were presented which could suggest that the cells have undergone several good population doublings. With the clustered cells, it showed more spherical shapes whereas the singular cells depict more thin, elongated features. No clear change can be seen from the varied TNF-α concentrations.

3.1.2 Extracellular vesicle / Exosomal marker expression

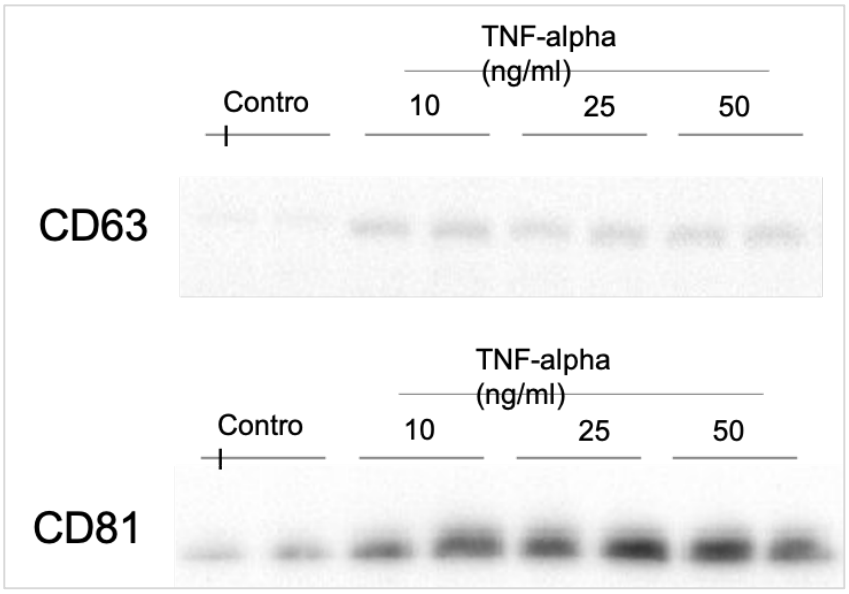

Figure 13.2: The elevation in Extracellular vesicle / Exosome markers (CD63 and CD81) from TNF-α treated cells. Blot representative of 3 independent experiments.

Regarding figure 13.2, as TNF-α increases (10, 25 and 50 ng/µl) so does the expression of CD63 in comparison to the control. As for CD81, this displayed the same pattern however, looking at the figure, it could be said that concentration 25 ng/ml caused the same level of expression of the exosomal markers as 50 ng/ml did.

3.2 Nanodrop protein A280 data set

Table 1: Data showing the measured protein concentrations for both the Horse Serum (HS) and Serum Free (SF) C2C12 samples against a control (0 ng/ml) and varied TNF-α concentrations (10,25 and 50 ng/ml). These were applied under both 72- and 24-hour incubation periods with the absorbance measured at 280 nm.

	Protein A280		
Samples (ng/ml)	**µg/mL**	**A260/A280 (nm)**	**A280 (nm)**
72hrs - HS – C	5.461	5.46	0.98
72hrs - HS – 10	5.81	5.81	0.97
72hrs - HS – 25	6.369	6.37	1.01
72hrs - HS – 50	6.485	1.01	0.46
72hrs - SF – C	0.887	1.17	0.89
72hrs - SF – 10	0.609	1.21	0.61
72hrs - SF – 25	0.769	0.77	0.77
72hrs - SF – 50	0.95	1.22	0.95
24hrs - HS – C	14.357	1.06	14.36
24hrs - HS – 10	6.233	0.97	6.23
24hrs - HS – 25	7.605	0.95	7.61
24hrs - HS – 50	7.01	0.92	7.01
24hrs - SF – C	0.336	1.21	0.34
24hrs - SF – 10	0.419	1.26	0.42
24hrs - SF – 25	0.235	1.25	0.23
24hrs - SF – 50	0.212	1.21	0.21

For both Horse Serum (HS) data sets, a higher protein concentration value was measured in comparison to the Serum Free (SF) data sets. For the 72-hour HS data, a steady increase in results is visible which is the same for the 24-hour HS data, however the control for 24-hour HS gave the highest

recording throughout. For the SF data's, a much lower concentration value is recorded, with all measurements ranging below 1 ng/ml. However, for 24-hour SF, the measurements decreased as the concentration of TNF-α increased which is distinct from all other recordings.

Additionally, for the A260/A280 absorbance readings, the 72hrs - HS – 25 gave the highest recording, however, results over 1.0 nm are indicative of nucleic acid contamination. Going from this, the 24-hour HS data may have provided the most accurate total proteins amounts. With this set also, a steady decrease in values were seen as the concentration of TNF increased.

Regarding the A280 (nm) absorbance results, looking at particular the absorbance of amino acids tyrosine and tryptophan, the 24-hour HS data this time provided the only contrasting results with all values being significantly greater than 1 nm. The rest however provided much more comparative results. No clear trend was present but the 24-hour SF data set, similar to the 72-hour HS data set showed a slight increase from control and then a decrease towards the 50 ng/ml TNF-α

3.3 Nanodrop RNA data set

Table 2: Data showing the measured RNA amounts for both the Horse Serum (HS) and Serum Free (SF) C2C12 samples against a control (0 ng/ml) and varied TNF-α concentrations (10,25 and 50 ng/ml). These were applied under both 72- and 24-hour incubation periods and the absorbance were measured at A260/A280 nm to determine the purity of nucleic acids.

	RNA		
Samples (ng/ml)	**ng/mL**	**A260/A280 (nm)**	**A260/A230 (nm)**
72hrs - HS – C	523.8	0.97	0.38
72hrs - HS – 10	818.2	1	0.47
72hrs - HS – 25	1008	0.99	0.49
72hrs - HS – 50	1029.8	1.02	0.51
72hrs - SF – C	92.4	1.07	0.38
72hrs - SF – 10	52.7	1.09	0.31
72hrs - SF – 25	56.2	1.1	0.30
72hrs - SF – 50	82.2	1.1	0.35
24hrs - HS – C	1239.3	0.99	0.51
24hrs - HS – 10	474.6	0.97	0.36
24hrs - HS – 25	137.6	0.87	0.12
24hrs - HS – 50	513	0.97	0.35
24hrs - SF – C	25.5	1.13	0.21
24hrs - SF – 10	34.8	1.12	0.24
24hrs - SF – 25	19	1.13	0.18
24hrs - SF – 50	17.4	1.12	0.18

The RNA concentration appeared to be at its highest with both HS data sets, with the 72-hour incubation samples proving an increase as the TNF-α concertation increased. This wasn't the case for the 24-hour incubation period as it displayed a significant decrease from the control to 25 ng/ml. For

the serum free data sets, both in comparison to horse serum displayed much lower readings. With the 72-hour set, no real trend was present whereas with the 24-hour set, the 10 ng/ml TNF-α concentration presented the highest RNA concentration, but as the stimulatory agents increased, the concentration of RNA decreased.

For the A260/A280 (nm) collection, measuring the purity of DNA and RNA, all sets of results were comparable with most ranging from 0.9 – 1.2 nm. Each data set didn't present a distinguishing trend or expose a singular result. The A260/A230 (nm) collection, measuring chaotropic salts and non-ionic detergents. The results for serum free sets had similar absorbance readings regardless of the TNF-α concentrations. Whereas for the 24-hour horse serum set, this wasn't the case.

3.4 Nanodrop dsDNA data set

Table 3: Data showing the measured Double stranded DNA antibodies (dsDNA) for both the Horse Serum (HS) and Serum Free (SF) C2C12 samples against a control (0 ng/ml) and varied TNF-α concentrations (10,25 and 50 ng/ml). These were applied under both 72- and 24-hour incubation periods and the absorbance were measured at A260/A280 nm.

	dsDNA		
Samples (ng/ml)	**ng/mL**	**A260/A280 (nm)**	**A260/A230 (nm)**
72hrs - HS – C	268.8	0.93	0.2
72hrs - HS – 10	330.5	0.99	0.22
72hrs - HS – 25	394.5	1	0.22
72hrs - HS – 50	340.2	1.03	0.23
72hrs - SF – C	53.1	1.17	0.22
72hrs - SF – 10	37.3	1.2	0.2
72hrs - SF – 25	41.5	1.18	0.2
72hrs - SF – 50	55.3	1.21	0.23
24hrs - HS – C	256.4	0.92	0.63
24hrs - HS – 10	347.3	0.95	0.22
24hrs - HS – 25	340.9	1.06	0.22
24hrs - HS – 50	248.8	0.89	0.17
24hrs - SF – C	20.9	1.16	0.14
24hrs - SF – 10	23.8	1.21	0.15
24hrs - SF – 25	14.1	1.2	0.11
24hrs - SF – 50	13.3	1.15	0.12

For the double stranded DNA antibodies, both horse serum data sets provided greater concentrations for dsDNA in comparison to both serum free sets. In fact, the HS sets saw an increase from the control.

The horse serum sets however did see an increase but the readings when measured with the TNF-α 50 ng/ml concentration, the concentration for dsDNA decreased.

With the A260/A280 absorbance readings, no clear trend or pattern presented itself for any of the samples. With the 72-hour HS set, the readings took a slight increase, starting from 0.93 for the control and ending with 1.03 for the 50 ng/ml TNF-α concentration. For the 72-hour SF set, similar results were gathered but all ranged above 1.0 nm. The 24-hour HS set provided potentially the most questionable results, were decreased in absorbance were slight, in this case the drop was from 1.06 nm to 0.89 nm for the 25 ng/ml to 50 ng/ml TNF-α dosage.

Regarding the A260/A230 (nm) recordings, both 72-hour horse serum and serum free samples registered nearly identical results. For the 24-hour sets, similar results were again recorded expect for one set, the 24-hour HS control gave a much larger result of 0.63 nm. This was in fact the largest absorbance reading which could imply an error had occurred.

3.5 Mitochondrial function analyses of both horse and serum free cells

3.5.1 Non – Mitochondrial Respiration

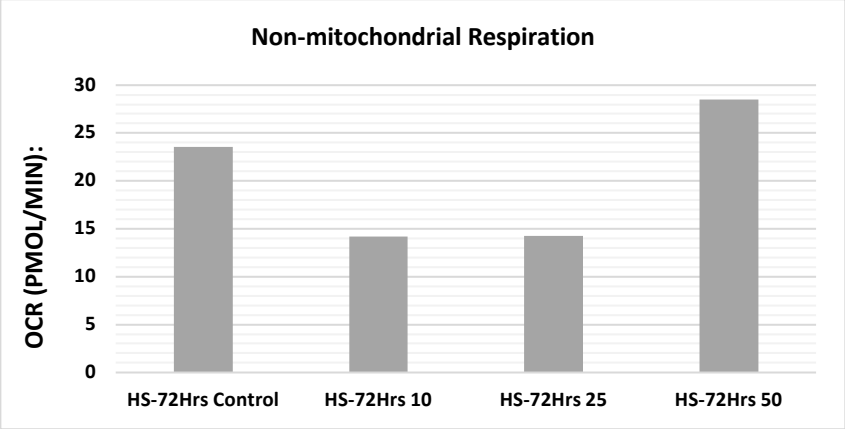

Figure 14: Data showing measured non-mitochondrial function from cells treated with varying levels of TNF-α (C, 10, 25 and 50 ng/ml) to promote EV release which have been added with Horse serum (HS) growth media under a 72-hour incubation period. Data is presented as mean of n=3.

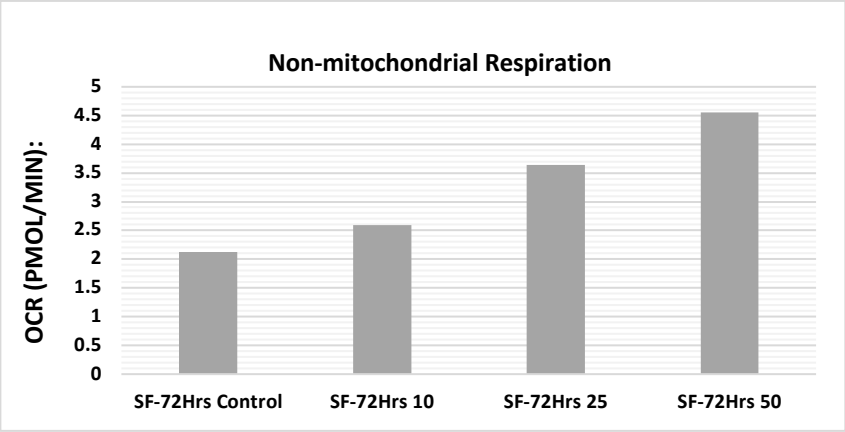

Figure 15: Data showing measured non-mitochondrial function from cells treated with varying levels of TNF-α (C, 10, 25 and 50 ng/ml) to promote EV release which have been added with Serum free (SF) growth media under a 72-hour incubation period. Data is presented as mean of n=3.

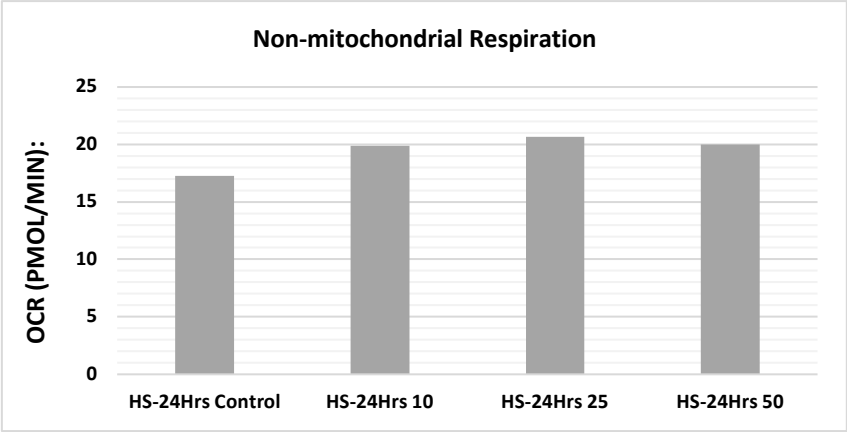

Figure 16: Data showing measured non-mitochondrial function from cells treated with varying levels of TNF-α (C, 10, 25 and 50 ng/ml) to promote EV release which have been added with Horse serum (HS) growth media under a 24-hour incubation period. Data is presented as mean of n=3.

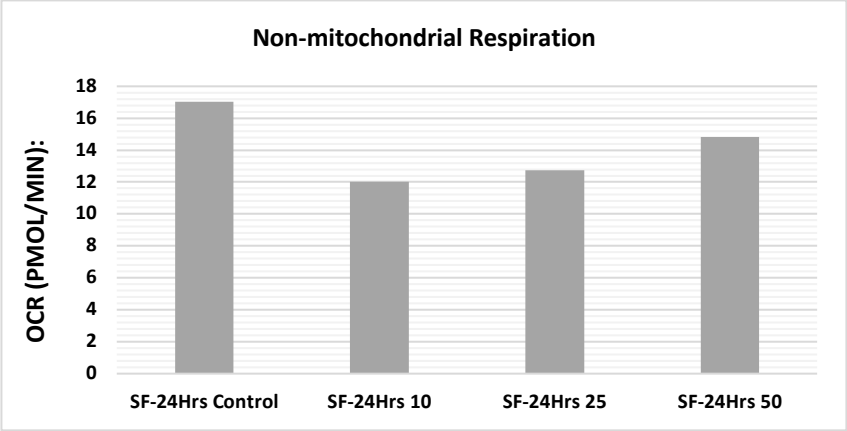

Figure 17: Data showing measured non-mitochondrial function from cells treated with varying levels of TNF-α (C, 10, 25 and 50 ng/ml) to promote EV release which have been added with Serum free (SF) growth media under a 24-hour incubation period. Data is presented as mean of n=3.

For Non-mitochondrial respiration, this is the measurement for how cyclooxygenases, cytochrome P450s or nicotinamide adenine dinucleotide phosphate oxidase (NADPH oxidases) which are pro-oxidant and pro-inflammatory enzymes are affected (Konior et al., 2014). In this case affected by varying levels of TNF-α and type of incubation media. For the 72-hour incubation data set, all the SF results shown in figure 15 displayed a higher inducing OCR effect in comparison to the HS cells displayed in figure 14. In fact, the 72-hour SF control displayed the highest inducing effect. For the horse serum set, 10 ng/ml of TNF-α appeared to effect non-mitochondrial respiration.

For the 24-hour data collection displayed in figure 17, a similar pattern was seen regarding SF presenting a greater effect on the OCR, however in this case, 10 ng/ml had the significant affect. For

figure 16, a slight increase in OCR was recorded as the concentration of TNF-α increased till 25 ng/ml. But the control for HS at 24-hour incubation appeared to show the most notable effect.

3.5.2 Basal Respiration

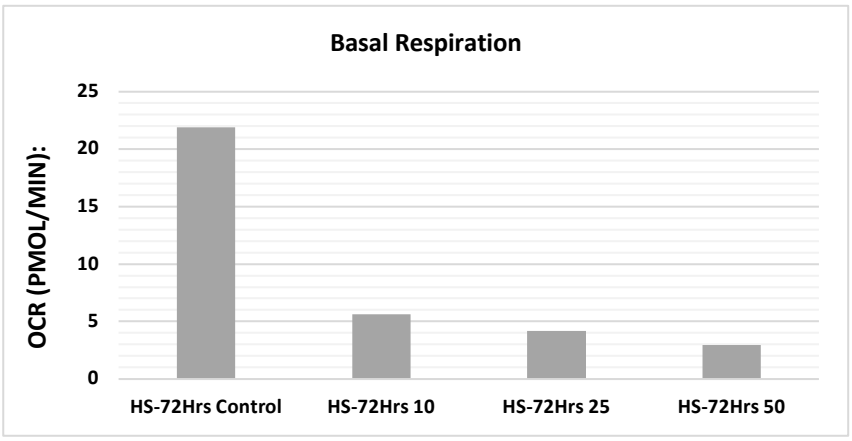

Figure 18: Data showing measured basal respiration from cells treated with varying levels of TNF-α (C, 10, 25 and 50 ng/ml) to promote EV release which have been added with Horse serum (HS) growth media under a 72-hour incubation period. Data is presented as mean of n=3.

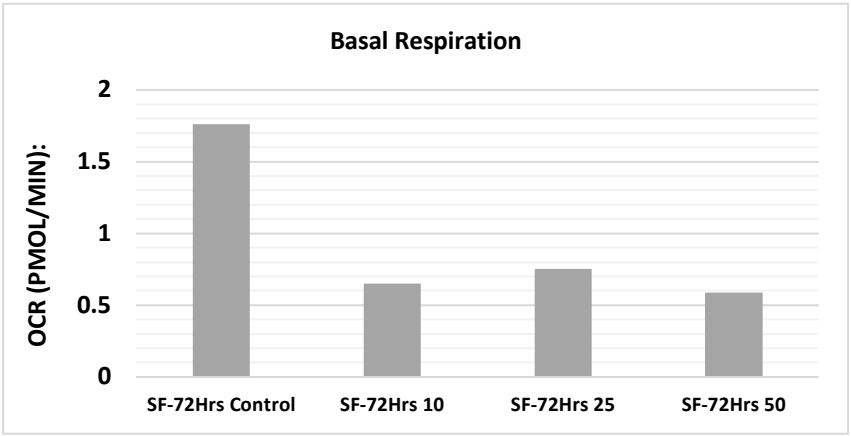

Figure 19: Data showing measured basal respiration from cells treated with varying levels of TNF-α (C, 10, 25 and 50 ng/ml) to promote EV release which have been added with Serum free (SF) growth media under a 72-hour incubation period. Data is presented as mean of n=3.

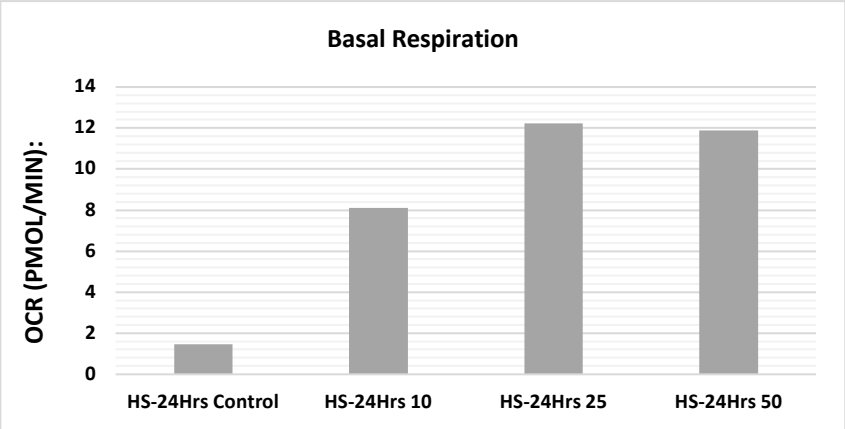

Figure 20: Data showing measured basal respiration from cells treated with varying levels of TNF-α (C, 10, 25 and 50 ng/ml) to promote EV release which have been added with Horse serum (HS) growth media under a 24-hour incubation period. Data is presented as mean of n=3.

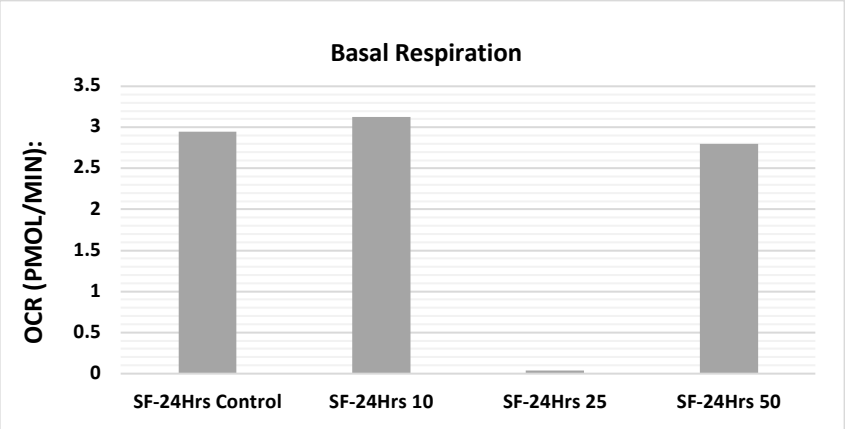

Figure 21: Data showing measured basal respiration from cells treated with varying levels of TNF-α (C, 10, 25 and 50 ng/ml) to promote EV release which have been added with Serum free (SF) growth media under a 24-hour incubation period. Data is presented as mean of n=3.

For basal respiration, it is an indicator on how the minimal rate of metabolism needed to carry out basic body functions essential for bodily maintenance is affected (Larsen et al., 2011). A low OCR value in the graph would imply damage to the C2C12 cells has occurred effecting the basal metabolic rate (BMR). In this case, the entirety of the 72-hour incubation SF data shown in figure 19 displayed results indicating this, with each TNF-α concentration providing an OCR value below 1 PMOL/MIN. With regard to figure 18, it did indicate that as the concentration of TNF-α increased, the BMR decreased.

On the other hand, with the 24-hour incubation period collection, it presented very contrasting results, in fact as the concentration of TNF-α increased in figure 20, the OCR / BMR increased till the 50 ng/ml concentration which then caused a decreased. An increase in OCR would imply a greater minimal rate to support bodily functions. The values themselves were far greater in comparison to the 72-hour incubation periods. Moreover, for figure 21, the results gave similar figures besides the 25 ng/ml.

3.5.3 Maximal Respiration

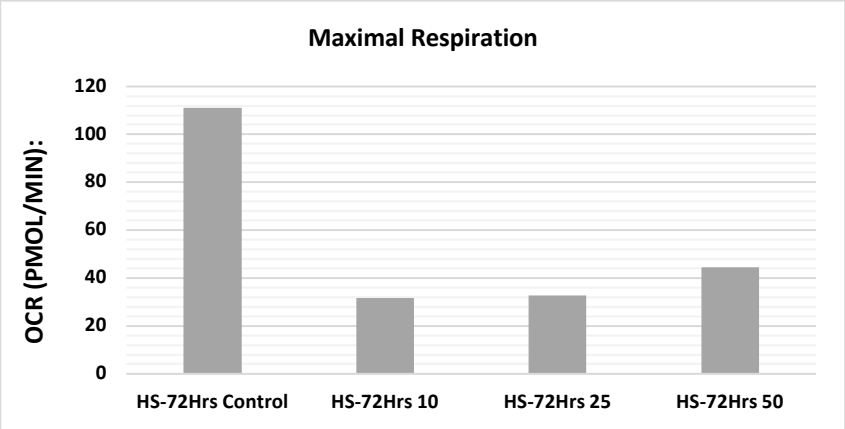

Figure 22: Data showing measured maximal respiration from cells treated with varying levels of TNF-α (C, 10, 25 and 50 ng/ml) to promote EV release which have been added with Horse serum (HS) growth media under a 72-hour incubation period. Data is presented as mean of n=3.

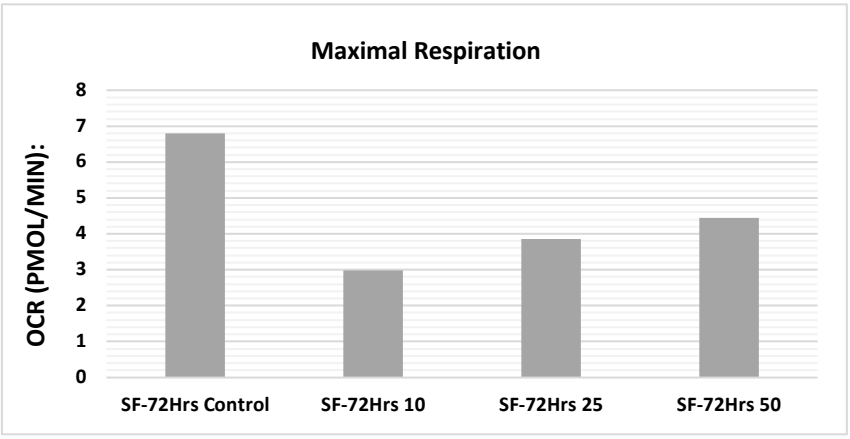

Figure 23: Data showing measured maximal respiration from cells treated with varying levels of TNF-α (C, 10, 25 and 50 ng/ml) to promote EV release which have been added with Serum free (SF) growth media under a 72-hour incubation period. Data is presented as mean of n=3.

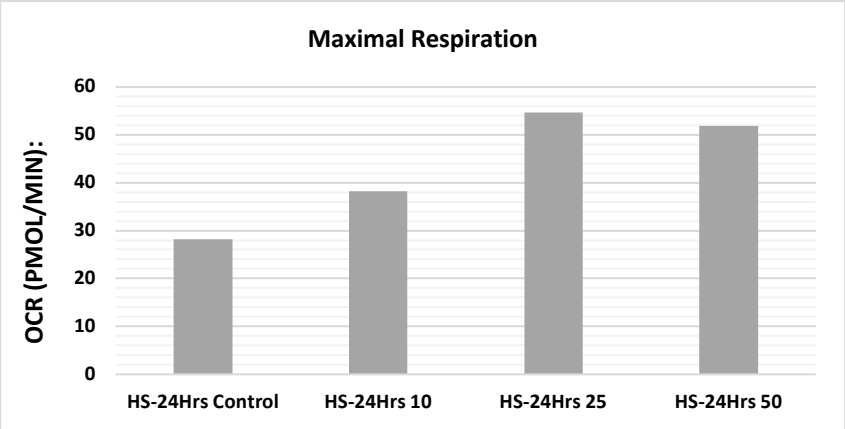

Figure 24: Data showing measured maximal respiration from cells treated with varying levels of TNF-α (C, 10, 25 and 50 ng/ml) to promote EV release which have been added with Horse serum (HS) growth media under a 24-hour incubation period. Data is presented as mean of n=3.

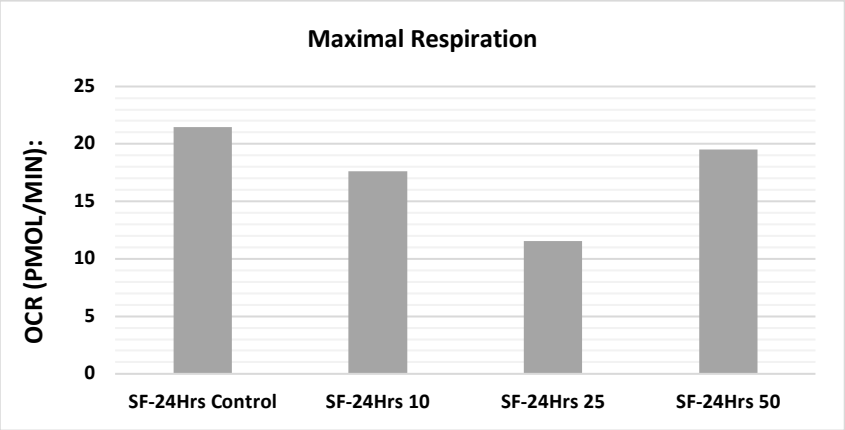

Figure 25: Data showing measured maximal respiration from cells treated with varying levels of TNF-α (C, 10, 25 and 50 ng/ml) to promote EV release which have been added with Serum free (SF) growth media under a 24-hour incubation period. Data is presented as mean of n=3.

For the maximal respiration (MR), this is an indication on the rate which oxygen is used during the maximum work, maximum oxygen consumption. A higher OCR value would indicate a higher MR which can be seen with the HS 72-hour control (figure 22), this isn't the case for the TNF-α treated cells as a clear reduction in OCR is visible. On the other hand, with figure 23, much lower results were recorded indicating that the SF has influenced C2C12 maximum oxygen consumption.

Furthermore, with the 24-hour incubation results shown in figure 24 and 28. The HS exhibited a positive interaction with OCR as the TNF-α concentration increased, with 25 ng/ml displaying a high value. Whereas for the SF result, the 25 ng/ml appears to be the only varying result given.

3.5.4 Proton Leak

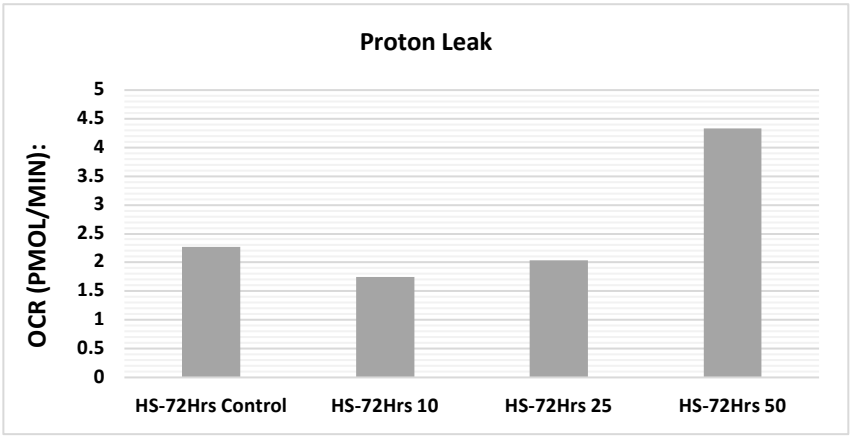

Figure 26: Data showing measured proton leak from cells treated with varying levels of TNF-α (C, 10, 25 and 50 ng/ml) to promote EV release which have been added with Horse serum (HS) growth media under a 72-hour incubation period. Data is presented as mean of n=3.

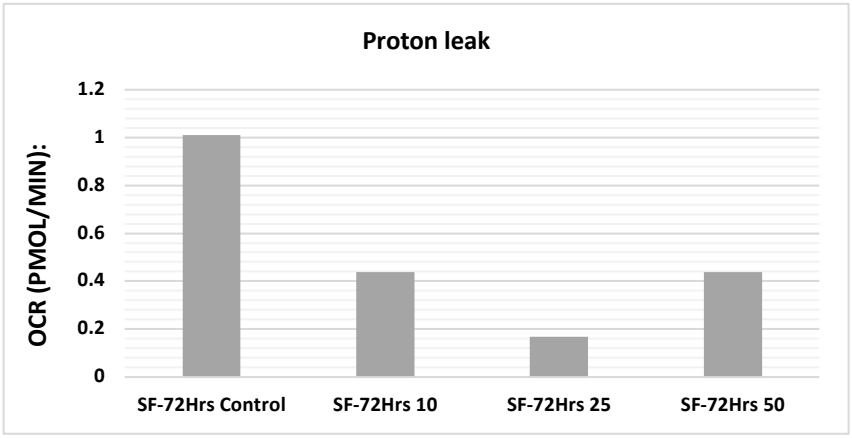

Figure 27: Data showing measured proton leak from cells treated with varying levels of TNF-α (C, 10, 25 and 50 ng/ml) to promote EV release which have been added with Serum free (SF) growth media under a 72-hour incubation period. Data is presented as mean of n=3.

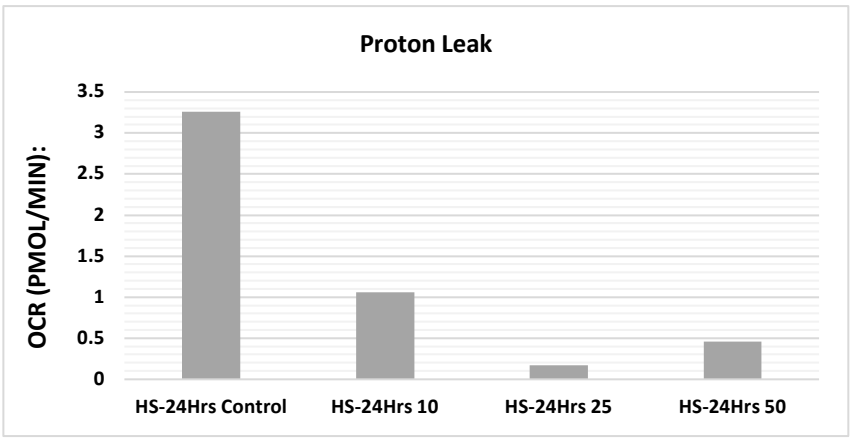

Figure 28: Data showing measured proton leak from cells treated with varying levels of TNF-α (C, 10, 25 and 50 ng/ml) to promote EV release which have been added with Horse serum (HS) growth media under a 24-hour incubation period. Data is presented as mean of n=3.

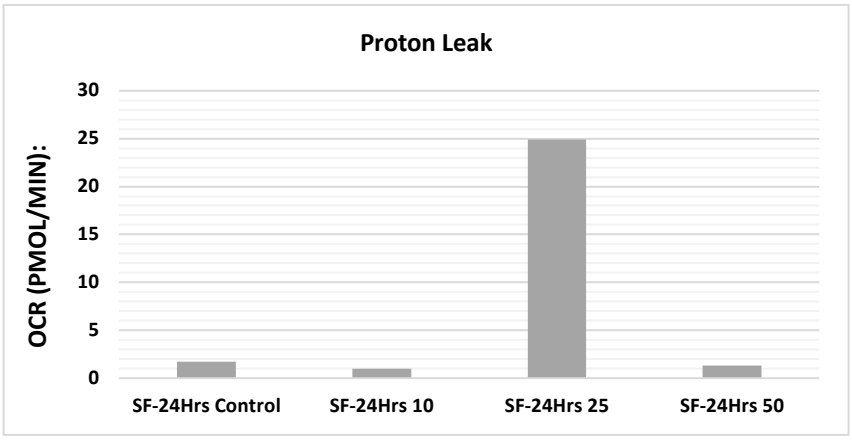

Figure 29: Data showing measured proton leak from cells treated with varying levels of TNF-α (C, 10, 25 and 50 ng/ml) to promote EV release which have been added with Serum free (SF) growth media under a 24-hour incubation period. Data is presented as mean of n=3.

Proton leak (PR) is a measurement on how the dissipation of ΔP in the presence Oligomycin (an ATP synthase inhibitor) in isolated mitochondria and intact cells is affected (Cheng et al., 2017). An increase OCR / PR value would be suggestive of mitochondrial damage. From the data presented in figure 26, it can be seen that the HS results indicate a greater effect on PR in comparison to the SF result (figure 27). With the 50 ng/ml concentration for HS displaying the largest possibility for mitochondrial damage.

Furthermore, when looking at the 24-hour incubation sets. The PR was affected in a similar way to the longer incubation. However, the biggest difference being that the HS media shown in figure 28 didn't indicate a higher PR this time, the SF media did. With figure 28, it shows a decrease in OCR from the control to 25 ng/ml but with the figure 29, the results were similar besides 25 ng/ml.

3.5.5 ATP Production

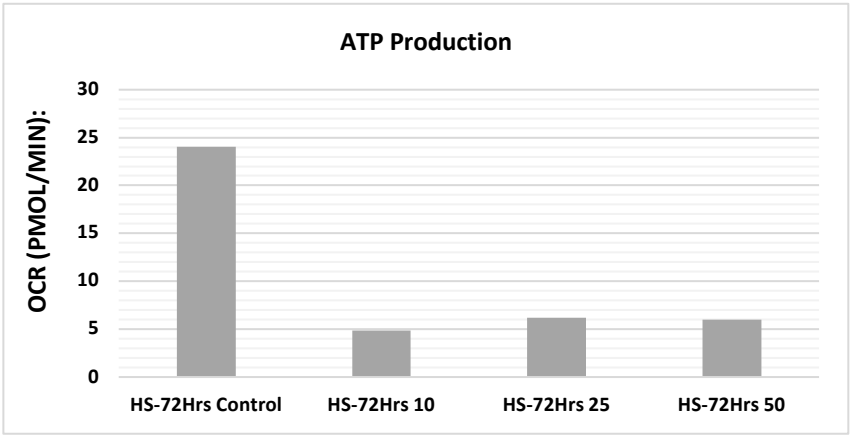

Figure 30: Data showing measured ATP production from cells treated with varying levels of TNF-α (C, 10, 25 and 50 ng/ml) to promote EV release which have been added with Horse serum (HS) growth media under a 72-hour incubation period. Data is presented as mean of n=3.

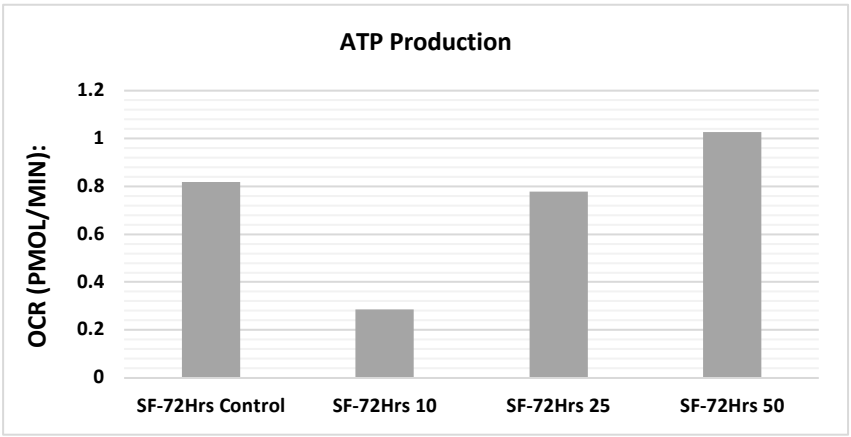

Figure 31: Data showing measured ATP production from cells treated with varying levels of TNF-α (C, 10, 25 and 50 ng/ml) to promote EV release which have been added with Serum free (SF) growth media under a 72-hour incubation period. Data is presented as mean of n=3.

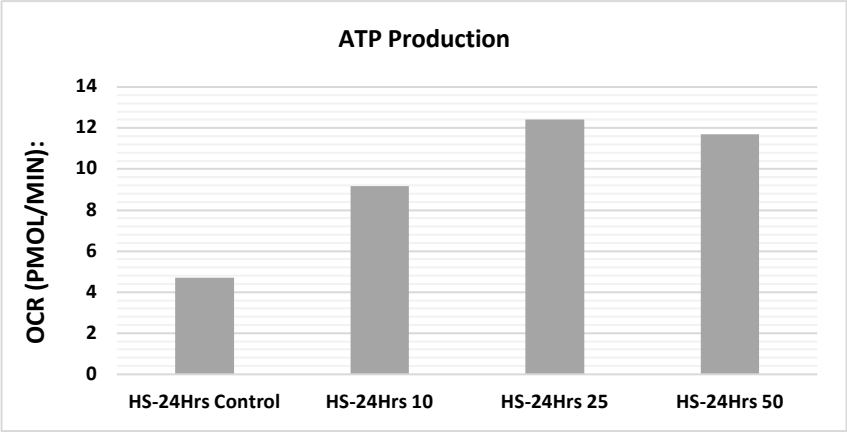

Figure 32: Data showing measured ATP production from cells treated with varying levels of TNF-α (C, 10, 25 and 50 ng/ml) to promote EV release which have been added with Horse serum (HS) growth media under a 24-hour incubation period. Data is presented as mean of n=3.

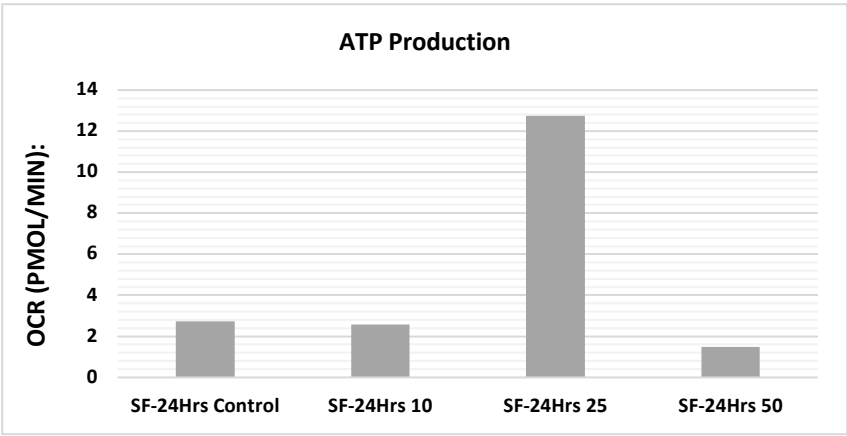

Figure 33: Data showing measured ATP production from cells treated with varying levels of TNF-α (C, 10, 25 and 50 ng/ml) to promote EV release which have been added with Serum free (SF) growth media under a 24-hour incubation period. Data is presented as mean of n=3.

For ATP production, a low OCR value would indicate that the stimulatory agent or incubation media / period has caused a negative effect on the rate of production. From this, it clearly shows that for the 72-hour HS data shown in figure 30, all concentrations caused damaging effect on the rate of production in comparison to the control. For figure 31, the results gained were significantly smaller than HS, clearly indicating that the media type has played a role in the rate ATP is produced.

On the other hand, the 24-hour incubation media results presented very contrasting results. In fact, for the HS set displayed in figure 32, from the control it can be seen that clearly an increase in OCR

PMOL/MIN. A decrease was then recorded from 25 ng/ml to 50 ng/ml. With the SF measurements, the 25 ng/ml produced the highest OCR value potentially indicating that the concentration of TNF-α didn't influence the ATP production.

3.5.6 Spare Respiratory Capacity (SRC)

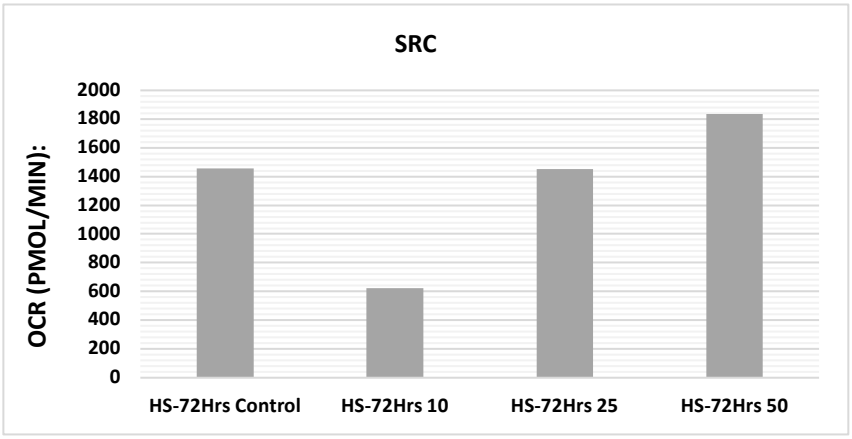

Figure 34: Data showing measured SRC from cells treated with varying levels of TNF-α (C, 10, 25 and 50 ng/ml) to promote EV release which have been added with Horse serum (HS) growth media under a 72-hour incubation period. Data is presented as mean of n=3.

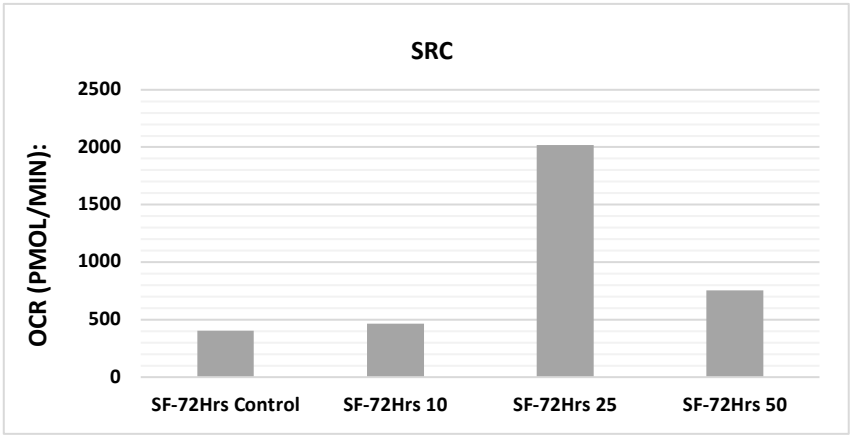

Figure 35: Data showing measured SRC from cells treated with varying levels of TNF-α (C, 10, 25 and 50 ng/ml) to promote EV release which have been added with Serum free (SF) growth media under a 72-hour incubation period. Data is presented as mean of n=3.

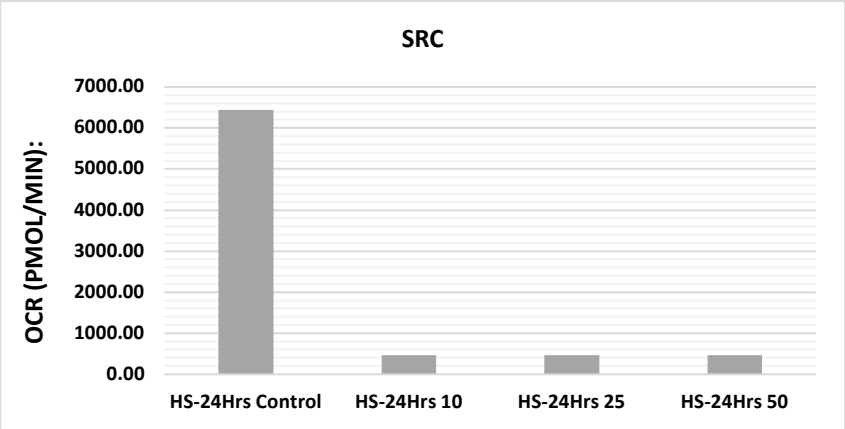

Figure 36: Data showing measured SRC from cells treated with varying levels of TNF-α (C, 10, 25 and 50 ng/ml) to promote EV release which have been added with Horse serum (HS) growth media under a 24-hour incubation period. Data is presented as mean of n=3.

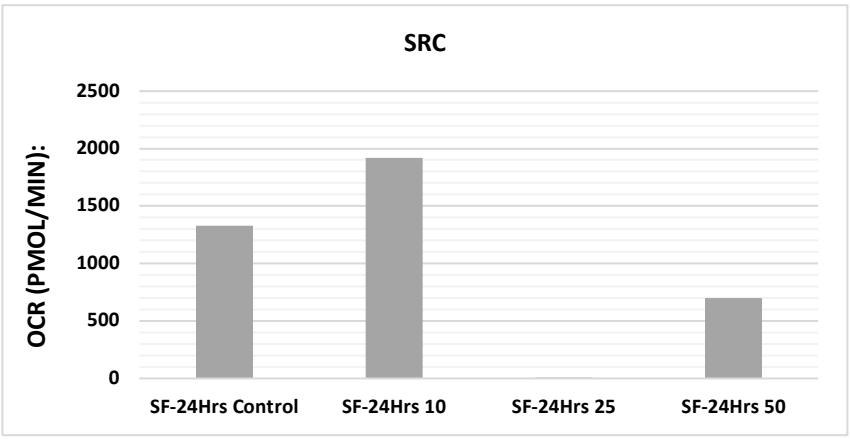

Figure 37: Data showing measured SRC from cells treated with varying levels of TNF-α (C, 10, 25 and 50 ng/ml) to promote EV release which have been added with Serum free (SF) growth media under a 24-hour incubation period. Data is presented as mean of n=3.

Spare respiratory capacity (SRC) is the cells' ability to respond to a sudden energetic demand. A low OCR value seen here would be indicative of mitochondrial stress and looking at the figure 34, it shows that for HS, as the TNF-α concentration increased so did the OCR value. Somewhat implying that the stimulatory agent promotes SRC. However, with figure 35, it doesn't show this clearly. In fact, the 25 ng/ml concentration presented largest value

For the 24-hour results presented in figure 36 and 40, a much greater OCR value was gathered for the control in HS. For the rest of the results for HS, each varying TNF-α concentration gave similar readings

which was different for the 72-hour incubation period. Moreover, for figure 37, it appears that the greater TNF-α concentrations greatly affected the rate in which SRC occurs.

3.5.7 Coupling Efficiency (%)

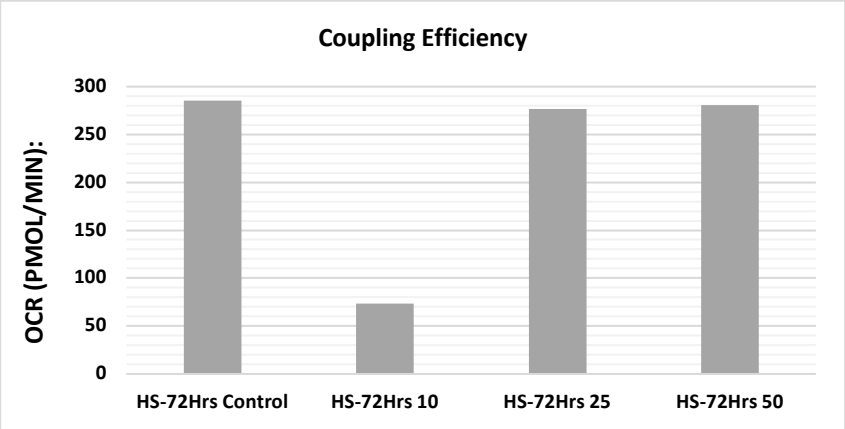

Figure 38: Data showing measured coupling efficiency from cells treated with varying levels of TNF-α (C, 10, 25 and 50 ng/ml) to promote EV release which have been added with Horse serum (HS) growth media under a 72-hour incubation period. Data is presented as mean of n=3.

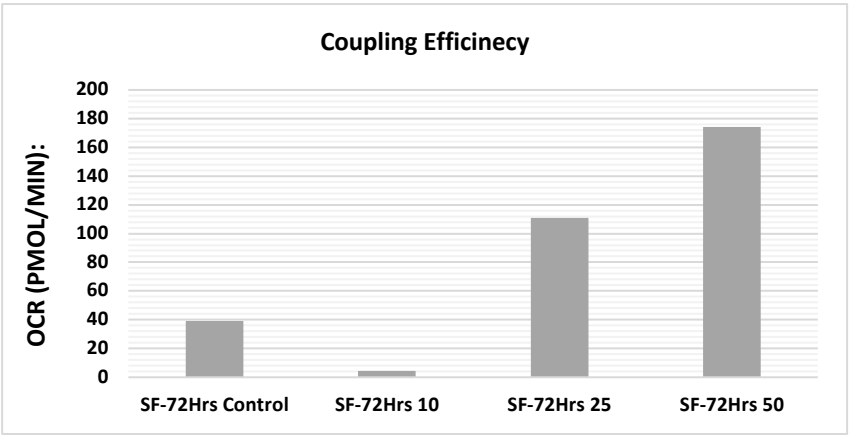

Figure 39: Data showing measured coupling efficiency from cells treated with varying levels of TNF-α (C, 10, 25 and 50 ng/ml) to promote EV release which have been added with Serum free (SF) growth media under a 72-hour incubation period. Data is presented as mean of n=3.

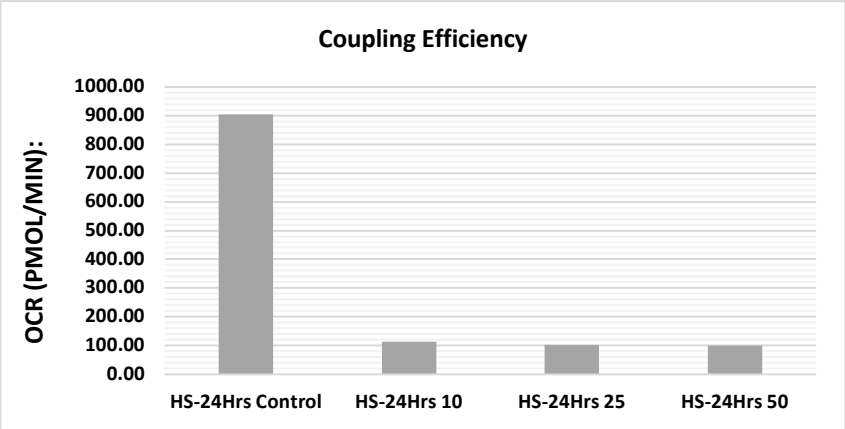

Figure 40: Data showing measured coupling efficiency from cells treated with varying levels of TNF-α (C, 10, 25 and 50 ng/ml) to promote EV release which have been added with Horse serum (HS) growth media under a 24-hour incubation period. Data is presented as mean of n=3.

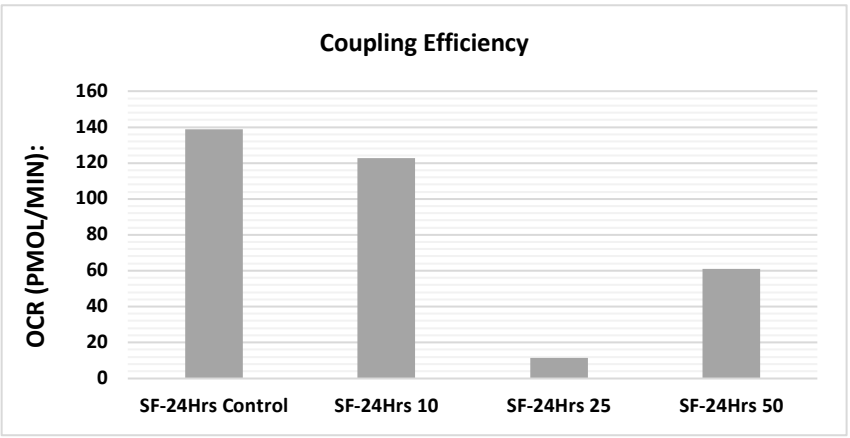

Figure 41: Data showing measured coupling efficiency from cells treated with varying levels of TNF-α (C, 10, 25 and 50 ng/ml) to promote EV release which have been added with Serum free (SF) growth media under a 24-hour incubation period. Data is presented as mean of n=3.

Coupling efficiency percentage is simply the percentage of respiration needed to carry out ATP synthesis (Amo et al., 2008). The muscle myalgia would be the cause of mitochondrial stress that would present itself with a high OCR result. Knowing this, it is shown clearly in figure 39, as the concentration of TNF-α increased, the OCR value did so also indicate that the stimulatory agent negatively effects the coupling efficiency. On the other hand, for HS seen in figure 38, every sample besides 10 ng/ml provided similar results.

For the 24-hour incubation period, it presents varying trends. Firstly, with figure 40, the control transmitted an extremely high OCR value compared to the rest which in comparison gave results in a similar range to the longer incubation period. The results were fairly comparable which only slight variations, expect for 25 ng/ml which resulted in a very low OCR value potentially implying an improvement for coupling efficiency.

3.6 Mitochondrial function analyses of differentiated horse and serum free cells

3.6.1 Non – Mitochondrial Respiration

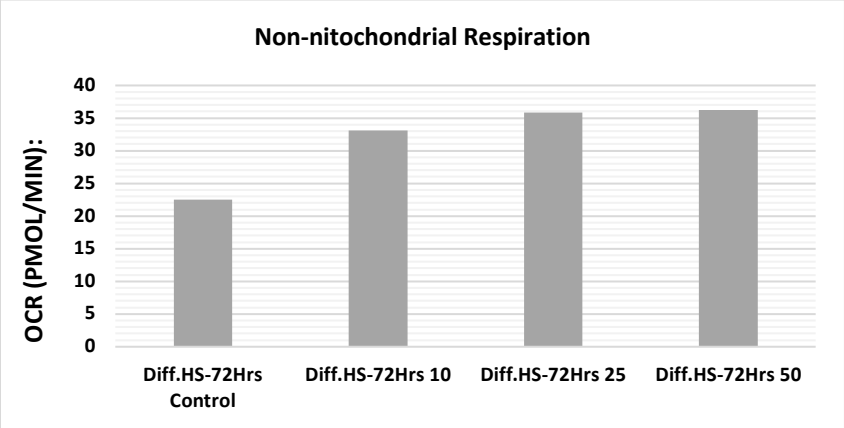

Figure 42: Data showing measured non-mitochondrial respiration from differentiated cells treated with varying levels of TNF-α (C, 10, 25 and 50 ng/ml) to promote EV release which have been added with Horse serum (HS) growth media under a 72-hour incubation period. Data is presented as mean of n=3.

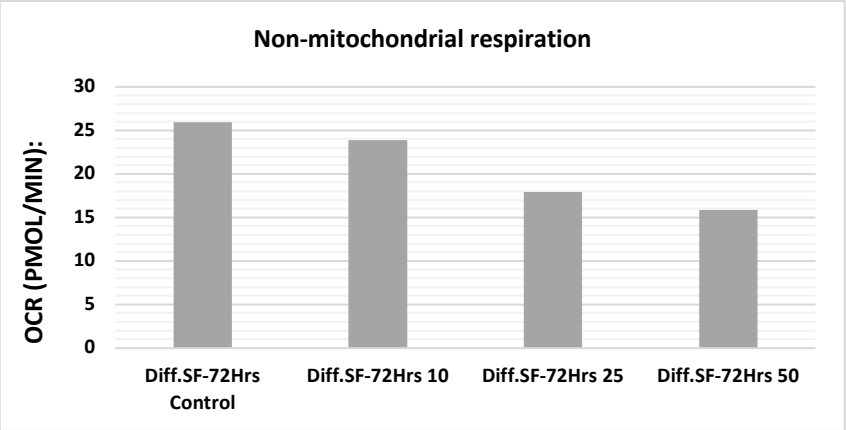

Figure 43: Data showing measured non-mitochondrial respiration from differentiated cells treated with varying levels of TNF-α (C, 10, 25 and 50 ng/ml) to promote EV release which have been added

with Serum free (SF) growth media under a 72-hour incubation period. Data is presented as mean of n=3.

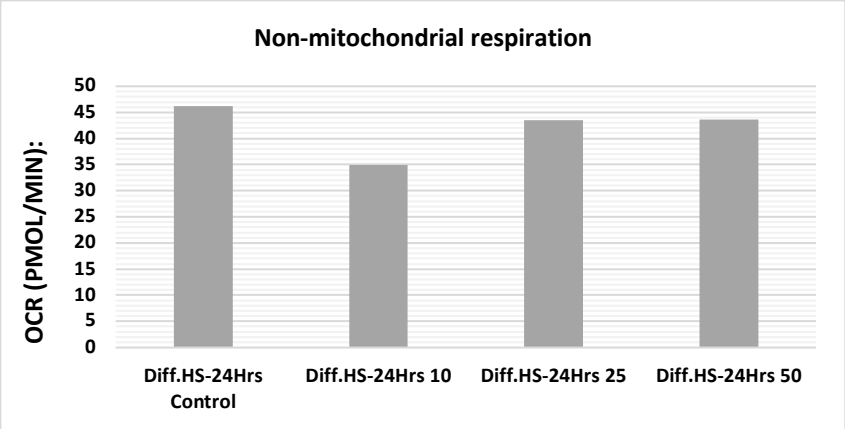

Figure 44: Data showing measured non-mitochondrial respiration from differentiated cells treated with varying levels of TNF-α (C, 10, 25 and 50 ng/ml) to promote EV release which have been added with Horse serum (HS) growth media under a 24-hour incubation period. Data is presented as mean of n=3.

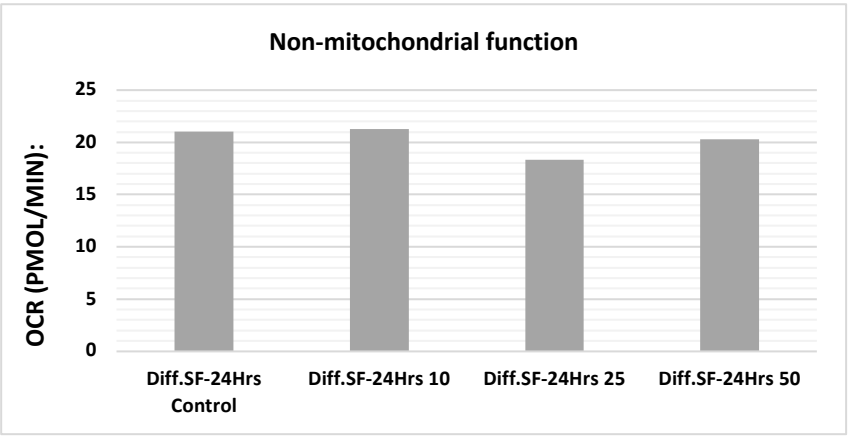

Figure 45: Data showing measured non-mitochondrial respiration from differentiated cells treated with varying levels of TNF-α (C, 10, 25 and 50 ng/ml) to promote EV release which have been added with Serum free (SF) growth media under a 24-hour incubation period. Data is presented as mean of n=3.

Looking at the data presented in figure 43, it shows that the SF results recorded a lower OCR value in comparison to HS (figure 42). Furthermore, a clear opposite in trends is visible with both media types, for example, as the concentration of TNF-α increased for HS it resulted in an increase in OCR. On the

other hand, for SF, it presented a decrease in OCR potentially hinting towards the idea that the increase in the stimulatory agent is causing a greater inducing effect on non-mitochondrial respiration.

With regard to the 24-hour incubation period, it again showed differences in results for HS and SF. As for HS / figure 44, it didn't present a clear trend in comparison to the 72-hour incubation period but rather a standout result. 10 ng/ml appears to be the odd results out of the set as the others gave an OCR value between 40-45 PMOL/MIN. With figure 45, it gave results ranging from 15-20 PMOL/MIN

3.6.2 Basal Respiration

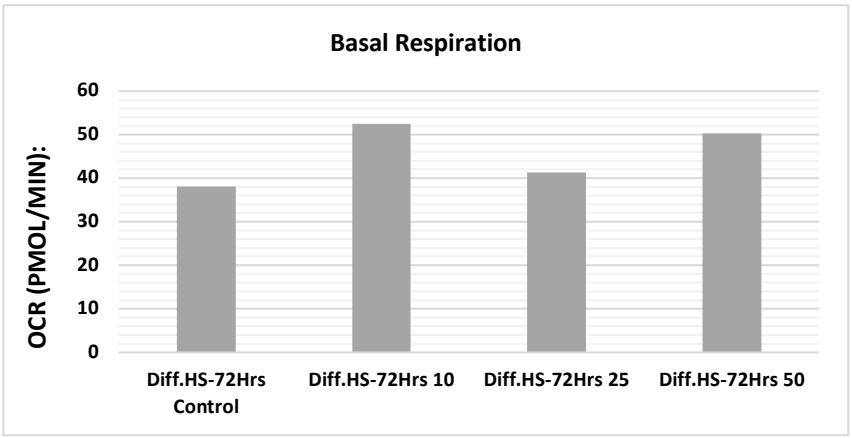

Figure 46: Data showing measured basal respiration from differentiated cells treated with varying levels of TNF-α (C, 10, 25 and 50 ng/ml) to promote EV release which have been added with Horse serum (HS) growth media under a 72-hour incubation period. Data is presented as mean of n=3.

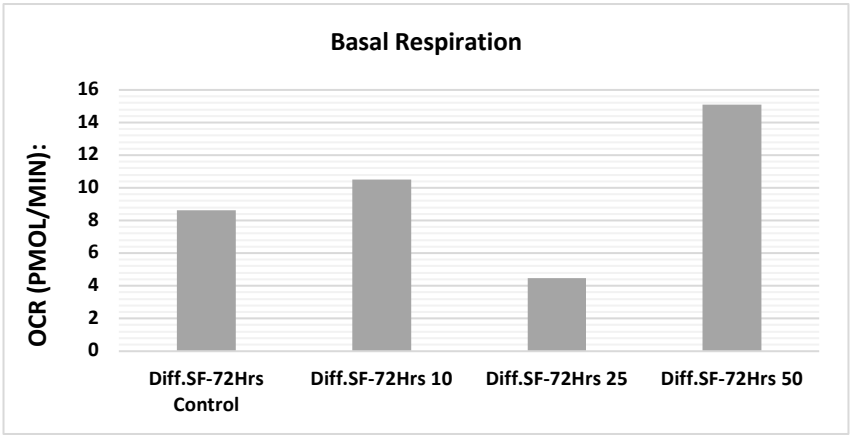

Figure 47: Data showing measured basal respiration from differentiated cells treated with varying levels of TNF-α (C, 10, 25 and 50 ng/ml) to promote EV release which have been added with Serum free (SF) growth media under a 72-hour incubation period. Data is presented as mean of n=3.

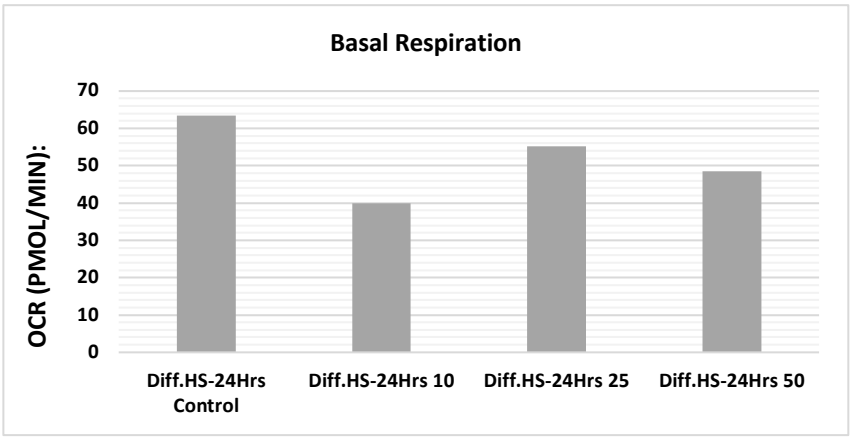

Figure 48: Data showing measured basal respiration from differentiated cells treated with varying levels of TNF-α (C, 10, 25 and 50 ng/ml) to promote EV release which have been added with Horse serum (HS) growth media under a 24-hour incubation period. Data is presented as mean of n=3.

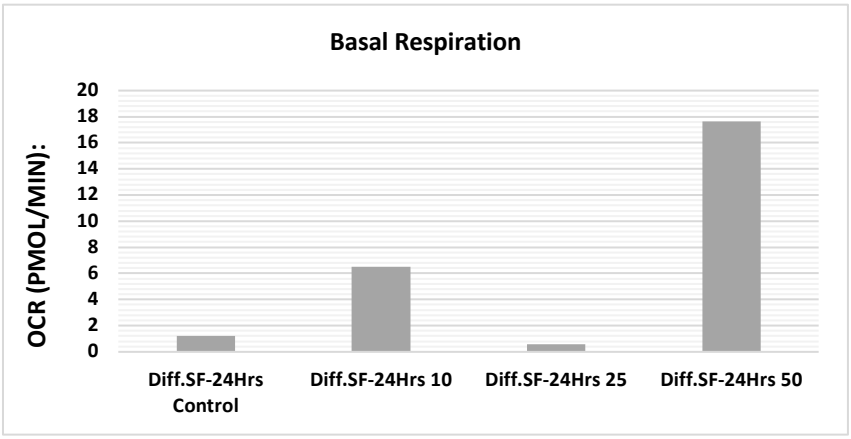

Figure 49: Data showing measured basal respiration from differentiated cells treated with varying levels of TNF-α (C, 10, 25 and 50 ng/ml) to promote EV release which have been added with Serum free (SF) growth media under a 24-hour incubation period. Data is presented as mean of n=3.

Looking at figure 46 and 50 it shows a clear difference with basal respiration for HS and SF. Firstly, the SF medias provided much lower OCR values which are indicative of myopathy occurring, with 24 ng/ml showing the greatest effect. In comparison, the HS results were substantially greater with all OCR values above 30 PMOL/MIN. The control was the lowest and the TNF-α concentration 10 ng/ml gave the highest reading.

Similarly, for the 24-hour incubation periods, SF again displayed a much lower OCR value in comparison to HS, with both the control and 25 ng/ml producing results below 2 PMOL/MIN. Whereas

again, in figure 48, the HS collection have more positive results. 10 ng/ml did the opposite this time however and provided the lowest value potentially indicating that myopathy had occurred.

3.6.3 Maximal Respiration

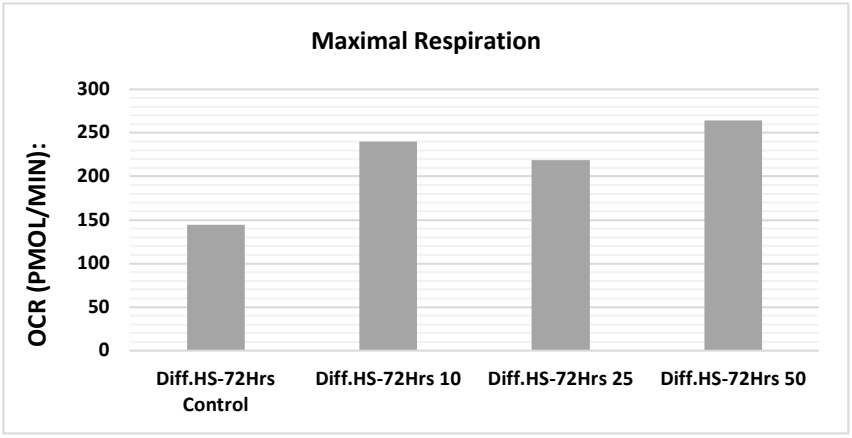

Figure 50: Data showing measured maximal respiration from differentiated cells treated with varying levels of TNF-α (C, 10, 25 and 50 ng/ml) to promote EV release which have been added with Horse serum (HS) growth media under a 72-hour incubation period. Data is presented as mean of n=3.

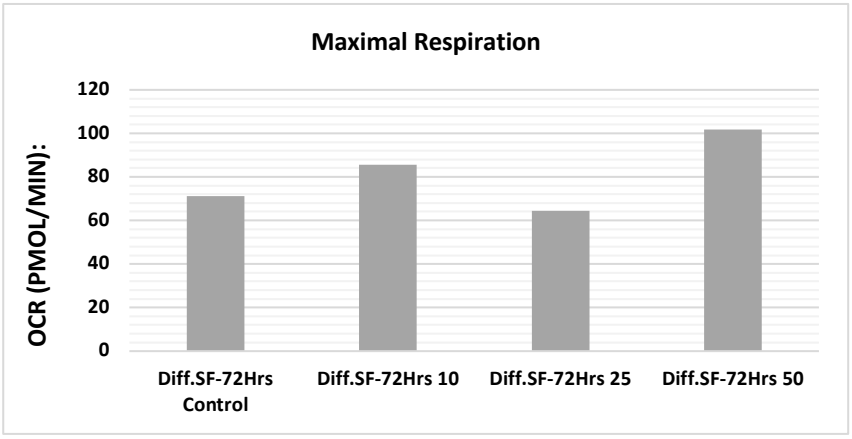

Figure 51: Data showing measured maximal respiration from differentiated cells treated with varying levels of TNF-α (C, 10, 25 and 50 ng/ml) to promote EV release which have been added with Serum free (SF) growth media under a 72-hour incubation period. Data is presented as mean of n=3.

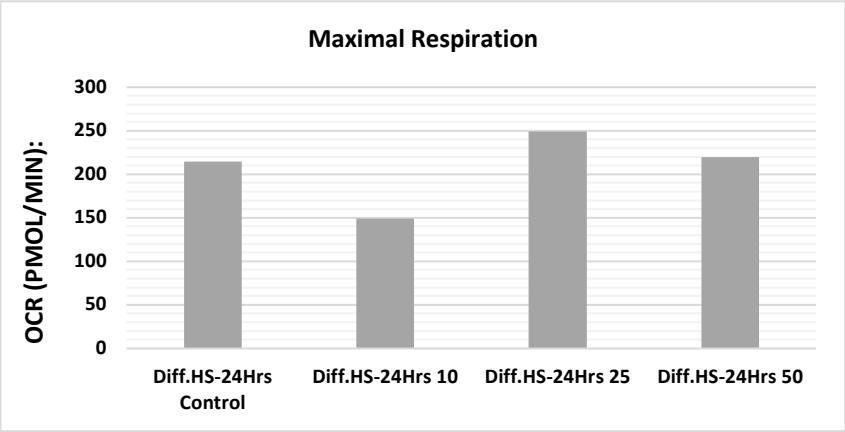

Figure 52: Data showing measured maximal respiration from differentiated cells treated with varying levels of TNF-α (C, 10, 25 and 50 ng/ml) to promote EV release which have been added with Horse serum (HS) growth media under a 24-hour incubation period. Data is presented as mean of n=3.

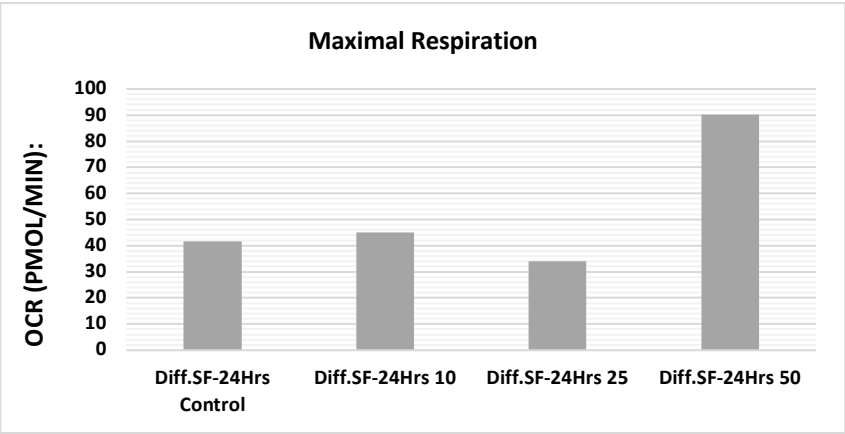

Figure 53: Data showing measured maximal respiration from differentiated cells treated with varying levels of TNF-α (C, 10, 25 and 50 ng/ml) to promote EV release which have been added with Serum free (SF) growth media under a 24-hour incubation period. Data is presented as mean of n=3.

For the data presented in figure 50 for the HS, it shows that the increase in TNF-α has resulted in an increase in OCR regarding maximal respiration compared to the control. However, between 10 and 50ng/ml, only a slight change in OCR is displayed. For figure 51 however, the results display a significant drop, with the OCR for 25 ng/ml displaying the lowest reading. The 50ng/ml concentration didn't present a consequential increase, none the less an increase was shown.

In comparison to the shorter incubation time, the results displayed (figures 52 and 53) didn't show any outstanding changed for both HS and SF. It shows that for HS, the control value gave a result remarkably like TNF-α concentration 50 ng/ml. 10 ng/ml did depict a lower OCR value. Furthermore,

for SF, it shows similar results for figures 50 and 51 where a decrease in OCR is presented. Nevertheless, 50ng/ml did provide an increase in maximal respiration compared to other concentrations.

3.6.4 Proton Leak

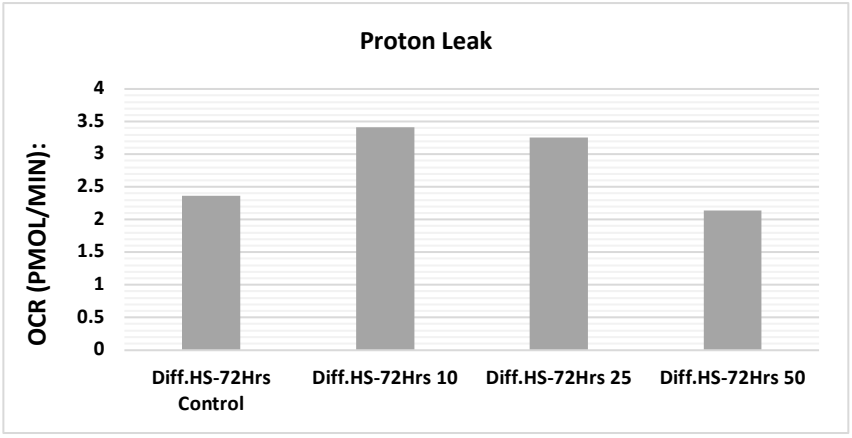

Figure 54: Data showing measured proton leak from differentiated cells treated with varying levels of TNF-α (C, 10, 25 and 50 ng/ml) to promote EV release which have been added with Horse serum (HS) growth media under a 72-hour incubation period. Data is presented as mean of n=3.

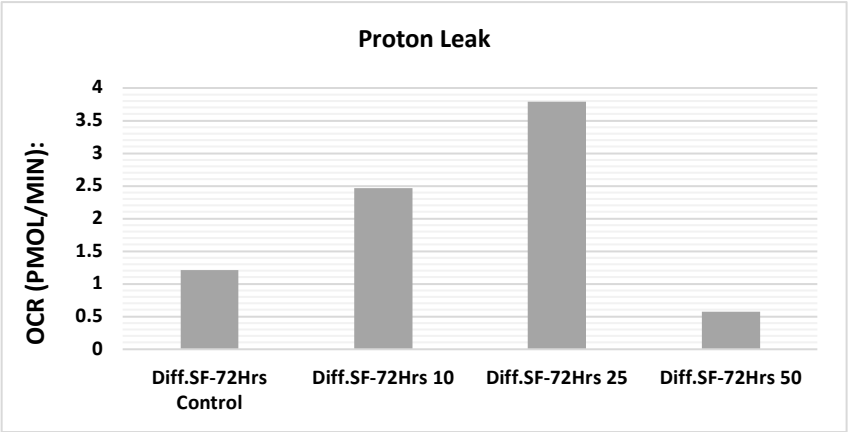

Figure 55: Data showing measured proton leak from differentiated cells treated with varying levels of TNF-α (C, 10, 25 and 50 ng/ml) to promote EV release which have been added with Serum free (SF) growth media under a 72-hour incubation period. Data is presented as mean of n=3.

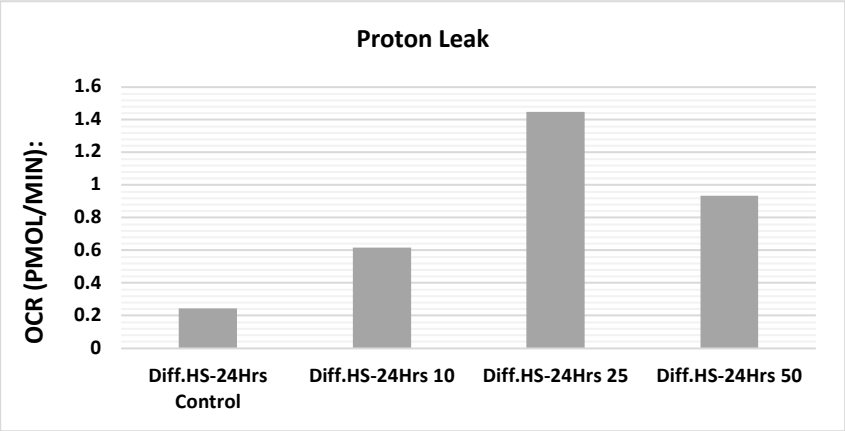

Figure 56: Data showing measured proton leak from differentiated cells treated with varying levels of TNF-α (C, 10, 25 and 50 ng/ml) to promote EV release which have been added with Horse serum (HS) growth media under a 24-hour incubation period. Data is presented as mean of n=3.

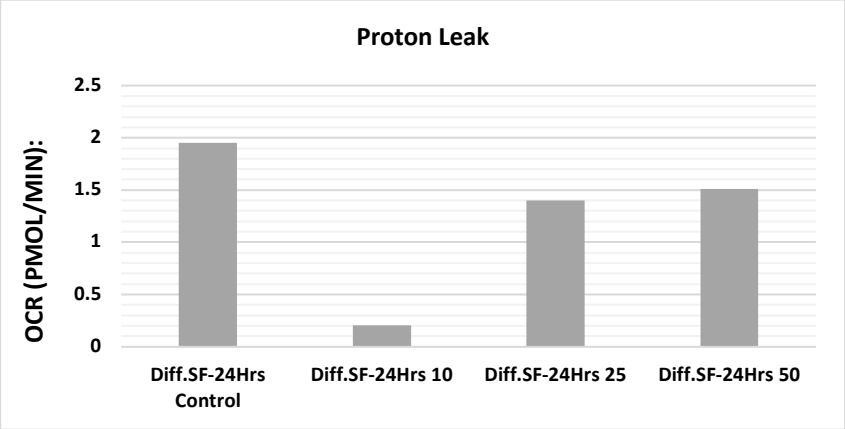

Figure 57: Data showing measured maximal respiration from differentiated cells treated with varying levels of TNF-α (C, 10, 25 and 50 ng/ml) to promote EV release which have been added with Serum free (SF) growth media under a 24-hour incubation period. Data is presented as mean of n=3.

Looking at the results however, the 72-hour incubation results did show a slight trend regarding the increase in stimulatory agent concentration. From the control, an increase in proton leak is presented with both HS and SF set, especially with 10 and 25 ng/ml.

Furthermore, this wasn't the case particularly with figure 57. The control value was highest out of the set and both 25 and 50 ng/ml TNF-α concentrations provided similar results. For the HS set shown in figure 56, a similar trend to the 72-hour incubation set is shown. A clear trend was visible however with 50 ng/ml, it did cause the proton leak / OCR to decrease.

3.6.5 ATP Production

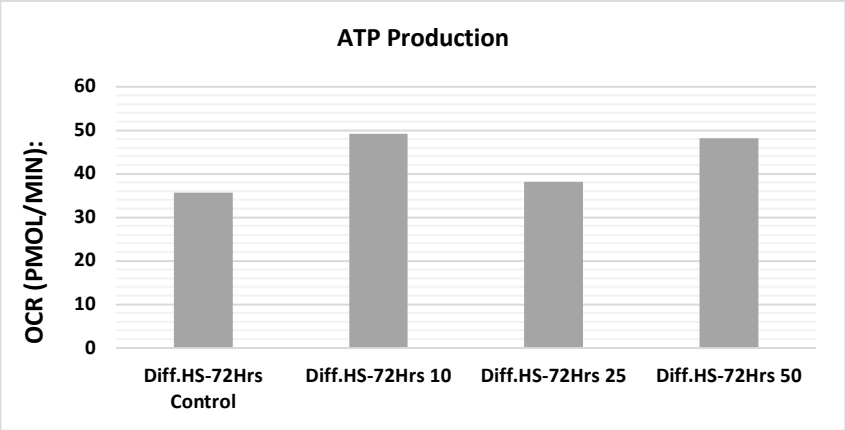

Figure 58: Data showing measured ATP production from differentiated cells treated with varying levels of TNF-α (C, 10, 25 and 50 ng/ml) to promote EV release which have been added with Horse serum (HS) growth media under a 72-hour incubation period. Data is presented as mean of n=3.

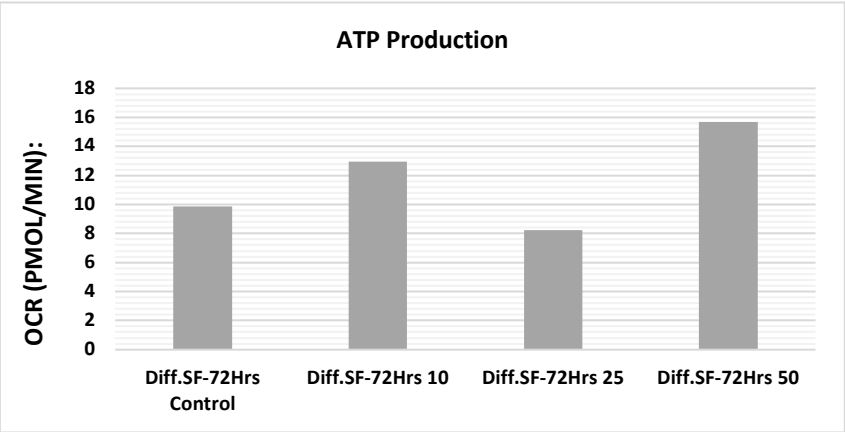

Figure 59: Data showing measured ATP production from differentiated cells treated with varying levels of TNF-α (C, 10, 25 and 50 ng/ml) to promote EV release which have been added with Serum free (SF) growth media under a 72-hour incubation period. Data is presented as mean of n=3.

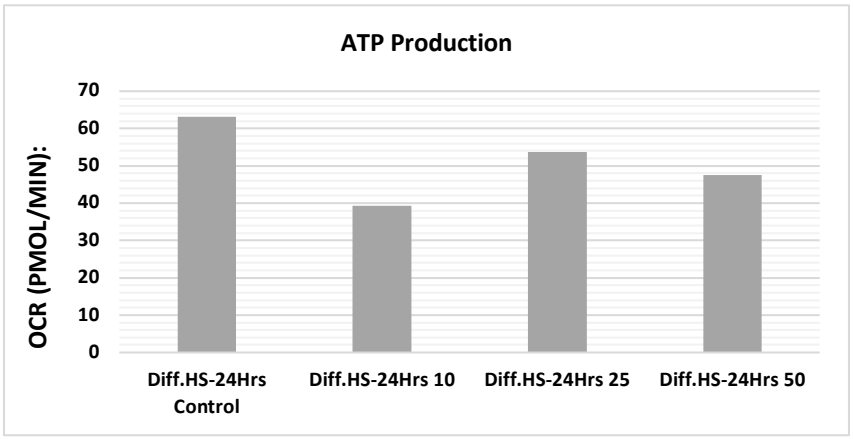

Figure 60: Data showing measured ATP production from differentiated cells treated with varying levels of TNF-α (C, 10, 25 and 50 ng/ml) to promote EV release which have been added with Horse serum (HS) growth media under a 24-hour incubation period. Data is presented as mean of n=3.

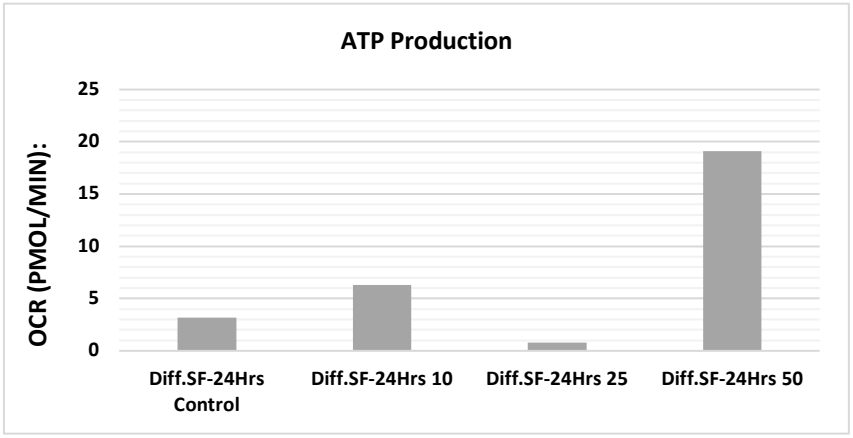

Figure 61: Data showing measured ATP production from differentiated cells treated with varying levels of TNF-α (C, 10, 25 and 50 ng/ml) to promote EV release which have been added with Serum free (SF) growth media under a 24-hour incubation period. Data is presented as mean of n=3.

As for figure 58, the HS data indicates that ATP is much greater in comparison to SF. The control provided a high OCR which then decreased as the 10 ng/ml TNF-α concentration was measured. It should be stated that for the even greater concentrations, the rate of ATP production did increase in comparison to 10 ng/ml. In connection with SF displayed in figure 59, a lower OCR value indicates a higher inducing effect on the ATP production. However, when recording the 50 ng/ml, an increase in ATP production was record.

In comparison, looking at the 24-hour incubation period, similar results were gathered for figure 60. Where the rate of ATP production was at its highest with HS and at its lowest with SF. However, the opposite trend was seen with HS this time, it showed a decrease with 10 ng/ml, this time it was an increase. For figure 61, 25 ng/ml appears to have the highest inducing effect on ATP production recording the lowest result.

3.6.6 Spare Respiratory Capacity (SRC)

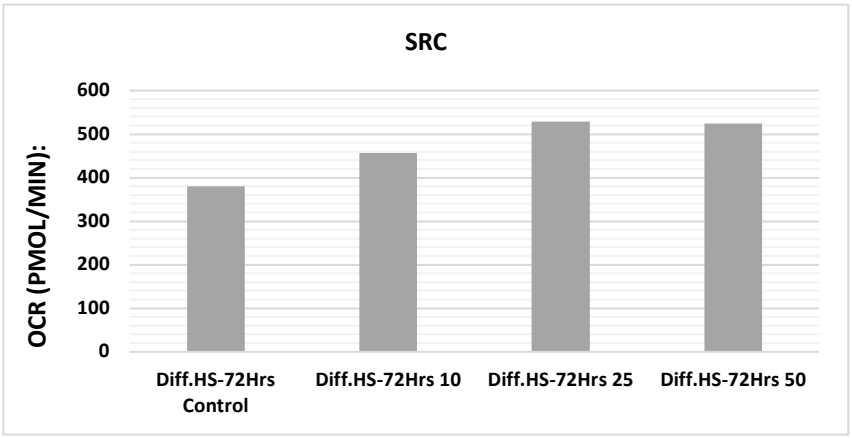

Figure 62: Data showing measured SRC from differentiated cells treated with varying levels of TNF-α (C, 10, 25 and 50 ng/ml) to promote EV release which have been added with Horse serum (HS) growth media under a 72-hour incubation period. Data is presented as mean of n=3.

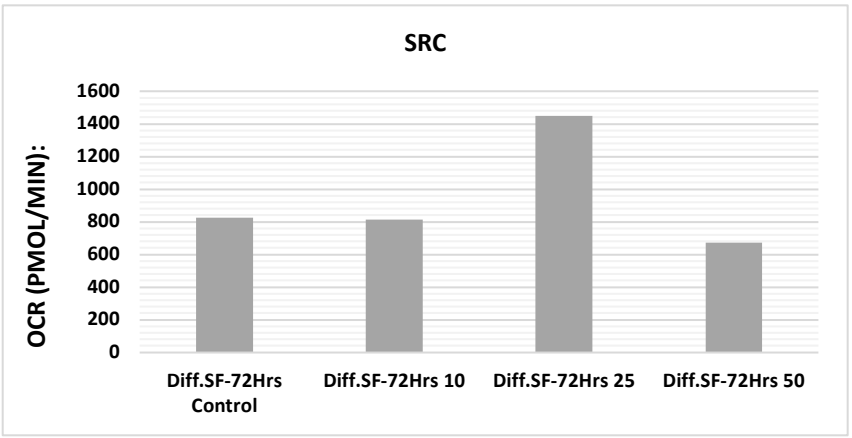

Figure 63: Data showing measured SRC from differentiated cells treated with varying levels of TNF-α (C, 10, 25 and 50 ng/ml) to promote EV release which have been added with Serum free (SF) growth media under a 72-hour incubation period. Data is presented as mean of n=3.

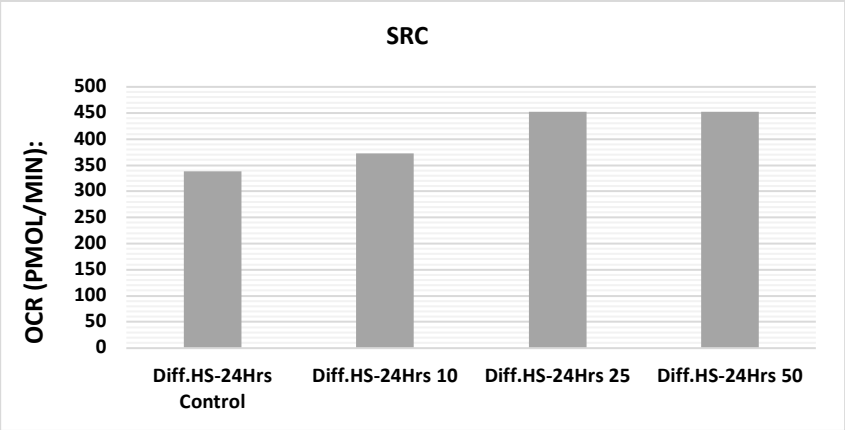

Figure 64: Data showing measured SRC from differentiated cells treated with varying levels of TNF-α (C, 10, 25 and 50 ng/ml) to promote EV release which have been added with Horse serum (HS) growth media under a 24-hour incubation period. Data is presented as mean of n=3.

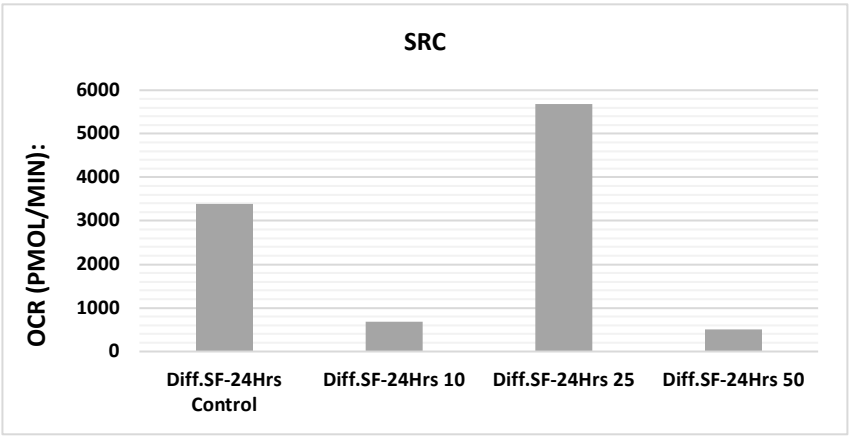

Figure 65: Data showing measured SRC from differentiated cells treated with varying levels of TNF-α (C, 10, 25 and 50 ng/ml) to promote EV release which have been added with Serum free (SF) growth media under a 24-hour incubation period. Data is presented as mean of n=3.

For SRC, with the 72-hour incubation data collection. The HS results given in figure 62 are similar, not presenting any real trend, a slight increase from the control 25 ng/ml can be seen in OCR. On the other hand, with SF results a slight negative trend is presented from the control to 50 ng/ml which would imply that as the concentration of TNF-α increases it induces mitochondrial stress at a higher rate. But 25 ng/ml did display the highest OCR result and dint follow this slight trend.

Moreover, with Figure 65, a similar trend is shown in SF. Concentration 50 ng/ml provided the lowest spare respiratory capacity and again 25 ng/ml provided the highest. With regard to HS, a slight plato and no real increase / decrease is displayed.

3.6.7 Coupling Efficiency (%)

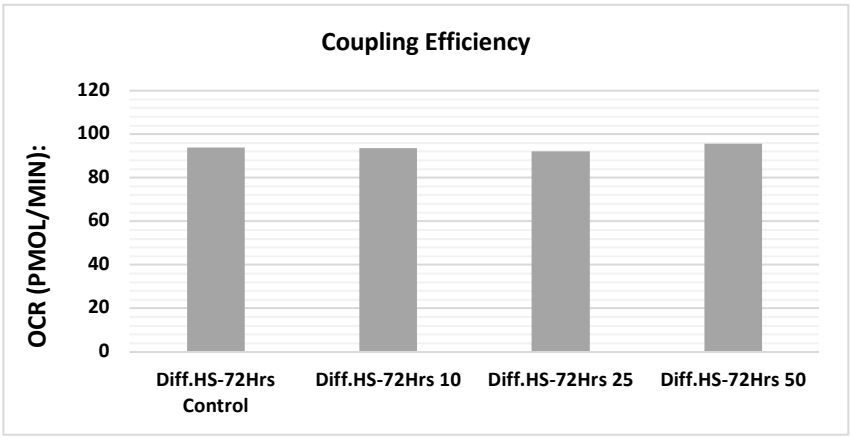

Figure 66: Data showing measured coupling efficiency from differentiated cells treated with varying levels of TNF-α (C, 10, 25 and 50 ng/ml) to promote EV release which have been added with Horse serum (HS) growth media under a 72-hour incubation period. Data is presented as mean of n=3.

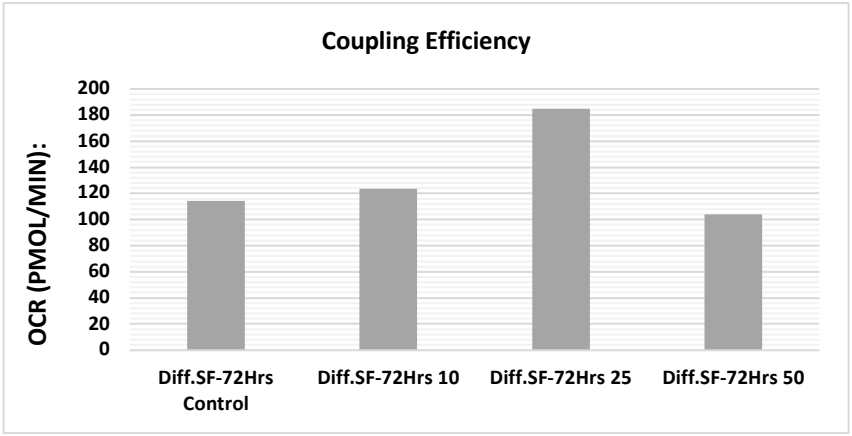

Figure 67: Data showing measured coupling efficiency from differentiated cells treated with varying levels of TNF-α (C, 10, 25 and 50 ng/ml) to promote EV release which have been added with Serum free (SF) growth media under a 72-hour incubation period. Data is presented as mean of n=3.

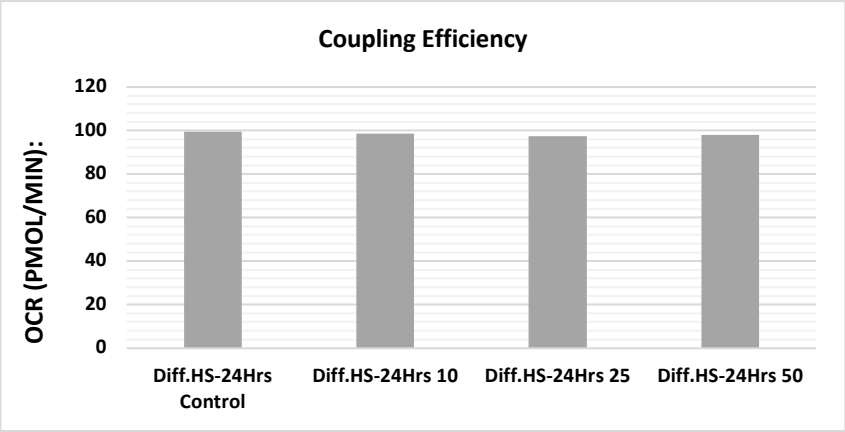

Figure 68: Data showing measured coupling efficiency from differentiated cells treated with varying levels of TNF-α (C, 10, 25 and 50 ng/ml) to promote EV release which have been added with Horse serum (HS) growth media under a 24-hour incubation period. Data is presented as mean of n=3.

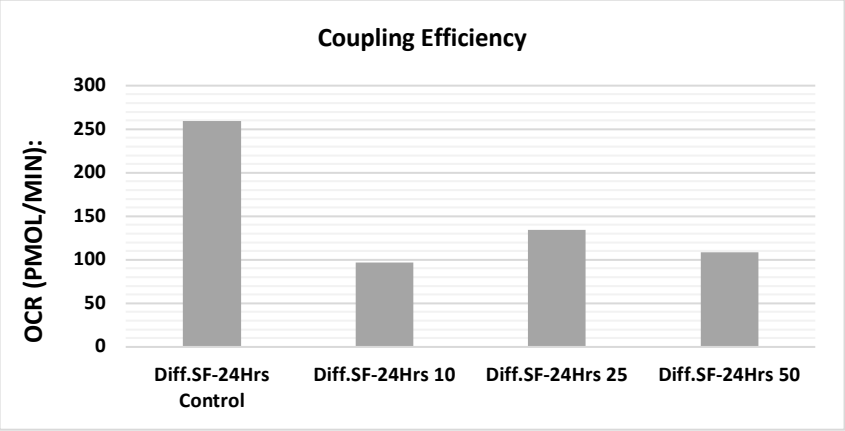

Figure 69: Data showing measured coupling efficiency from differentiated cells treated with varying levels of TNF-α (C, 10, 25 and 50 ng/ml) to promote EV release which have been added with Serum free (SF) growth media under a 24-hour incubation period. Data is presented as mean of n=3.

The data presented in figure 66 and 70, for HS doesn't appear to show any significant trend. However, in terms of SF, it displayed a noteworthy increase in OCR which would indicate mitochondrial stress. From the control too 25 ng/ml an increase is present in OCR PMOL/MIN, yet a decrease then did occur for 50 ng/ml.

For the 24-hour incubation results, figure 68 provided similar readings. Potentially implying that the type of media in this case doesn't appear to induce coupling efficiency regardless of the concentration of TNF-α. Moreover, for the SF control shown in figure 69, a large OCR result was given suggesting

mitochondrial stress. But when the stimulatory agents were added, the percentage of respiration used for ATP synthesis decreased in comparison.

4.0 Discussion

The aim of the study was to investigate the role extracellular vesicles and the effect they have on inter-cellular communication in skeletal muscle cells. This was carried out by determining the effect the stimulatory agent, Tumour necrosis factor – alpha (TNF-α) has on exosomal release from skeletal muscle cells. Further, investigations were carried out to characterise exosomes cargo as well as their ability to disseminate and augment the function of adjoining muscle cells, whether it be its mitochondrial function.

4.1 Characterisation of the Extracellular vesicle preparation

4.1.1 Cell gross morphology

Looking at the data presented in figure 13.1, it displayed no clear change in cell morphology of the C2C12 myotubes with varying levels of TNF-α to promote the synthesis of EVs/ exosomes in either HS or SF growth media. However, with the stimulation of TNF-α, it can lead to increased expression of EVs which causes changes such as hypertension of the muscle-specific ubiquitin ligase atrogin-1, and enhanced activity of the Ca2+-dependent proteolytic system (Bonetto et al., 2011). This further results in increase in myostatin expression as well as a decrease expression of IGF-1 mRNA (Bonetto et al., 2011). Other changes include marginal changes in MyHCF and CK activity (Langen et al., 2001), and these differences could provide insight to how the mitochondrial function is affected with the addition of exosomes.

4.1.2 Extracellular vesicle / Exosomal marker expression

Referring to figure 13.2, the increased expression of extracellular vesicle (EVs) / exosomal markers CD63 and CD81 can be attributed to the ability of TNF-α ability to increase EV / exosomal synthesis. Exosomes in particular are supplemented with several tetraspanins which include, CD9, CD63 and CD81. As a result of been frequently found within, they have been labelled as key markers and used in the characterisation of exosomes (Eldh et al., 2010). So, with an increase in these cell surface proteins, especially CD81 displayed in figure 13.2, with the concentrations of 25ng/ml and 50ng/ml it supports the idea that TNF-α increases the conglomeration of exosomes increases and the hypothesis.

4.2 Impact increased TNF-α concentration has on DNA content from EV fractions.

4.2.1 Protein A280 concentration

The increase in protein concentration presented in table 1 is a direct reflection of the elevated release of extracellular vesicles stimulated by TNF-α, as bioactive exosomes intensify protein generation in SKMs regardless of amino acids (Mobley et al., 2017). The increase in protein concentration could be attributed to the increase in TNF-α stimulating the mammalian target of rapamycin (mTOR) signalling pathway (Mobley et al., 2017), essential to skeletal muscle protein synthesis. As TNF-α increases the stimulation of EVs, it causes the recruitment of protein Wnt-10b towards lipid rafts (Tassew et al., 2017). Lipid rafts, a cell membrane sector regulates receptors and signalling molecules which in turn advance the formation of signalling platforms (Castro et al., 2013), this is key to why an increase in protein concentrations displayed in table 1.

The mechanism which leads to increasing protein yield seen as mentioned involves the protein Wnt-10b. As it is stimulated by the stimulatory agent, it causes the activation of mTORC1, a mTOR subtype. The subtype phosphorylases eukaryotic translation initiation factor 4E (eIF4E)-binding proteins (4E-BPs), a cap-binding protein essential for the uptake of ribosomes and the initiation of the translation mechanism (Amorim et al., 2018). Imperative for the assimilation of mRNA to the ribosome, it allows for the formation of eIF4F complex, which in turn causes an increase in eukaryotic translation initiation, increasing protein yield (Morita et al., 2015). This provides an explanation as to why it produced this increase in protein concentration in the 72-hour incubated, HS and SF samples as TNF-α increases.

The decrease in protein concentration depicted with the 24-hour SF compared to HS incubation data, in particular with the 50 ng/ml concentration of TNF-α could be due to prolonged activation of JNK (Jing and Anning, 2005). Potentially, the 50 ng/ml concentration of the stimulatory agent was able to inhibit caspases and increase the duration of programmed cell death, in turn reducing the quantity of proteins found within SKMs (Jing and Anning, 2005).

4.2.2 RNA concentration

With the data provided for RNA concentration, the increase in Ribonucleic acid exhibited with the increase in TNF-α can be linked to the connection RNA synthesis has with ribosomes. With 80% of skeletal muscle RNA being ribosomal (Millward et al., 1973) which is imperative for the translation mechanism, a fall in RNA synthesis is reflective of a reduced need for cellular RNA modules (Millward

et al., 1973). So, where an increase in RNA concentration demonstrated in table 2, an increased need for ribosomes will also essential.

Additionally, a neutral sphingomyelinase, in particular sphingomyelinase-2 (nSMase2) has a direct relationship with the stimulatory agent, TNF-α. It has been proposed that TNF-α induces late activity of nSMase2 which is a key component in MVB biogenesis (Clarke et al., 2011). Not only that but nSMase2 dictates exosomal miRNA release (Kosaka et al., 2013), which would help explain why when the concentration of TNF-α increased, an increase in RNA was revealed. As the neutral sphingomyelinase would have been highly stimulated to promote miRNA liberation.

4.2.3 dsDNA concentration

The increase in double stranded DNA (dsDNA) following 72-hour incubation with TNF-α (table 3) can be attributed to the stimulatory effect on exosomal biogenesis and release. Firstly, dsDNA is a hallmark feature of exosomes, with studies specifying that dsDNA is found in abundance within exosomes (Kalluri and LeBleu, 2016) as well as TNF-α helping to induce DNA generation (Rolfe et al., 1997). This would provide one explanation as to why it gave an increase in dsDNA concentration in the 72-hour incubated HS and SF samples as the TNF-α concentration increases.

However, it has been reported that dsDNA can be released independent from exosomes and other extracellular vesicles (Jeppesen et al., 2019). A mechanism involving LC3B-PE-positive autophagosomes, engulfs cytoplasmic chromatin (Jeppesen et al., 2019) which resulting leads to the formation of Amphisomes (Jeppesen et al., 2019). Amphisomes are complex organelles key to many endo-lysosomal pathways (Ganesan and Cai, 2021) but in this case, vital for the release of dsDNA as they fuse with plasma membranes (Jeppesen et al., 2019). The formation of amphisomes is stimulated and induced by an inhibitor of nuclear factor kappa-B kinase subunit beta (ikkβ) (Peng et al., 2021).

This subunit has been revealed to be encouraged to be released by the stimulatory agent, TNF-α**.** Tests were carried out which depicted that TNF-α prompted the mRNA and protein expression of IKKβ (Tang et al., 2017). So, an increase in TNF-α, would cause increase in IKKβ, leading to the motivation needed for autophagosomes to fuse with MVBs to form amphisomes (Peng et al., 2021). This would lead to dsDNA to be released, which can seen in the results shown in table 3 following 50 ng/ml TNF-α treatment.

4.3 Impact of Extracellular vesicles on mitochondrial function

4.3.1 Non-mitochondrial respiration

Non-mitochondrial respiration (NMR) is a measurement of how the pro-oxidant and pro-inflammatory enzyme, Nicotinamide adenine dinucleotide phosphate (NADPH) functions. The enzyme is key for the generation of reactive oxygen species (ROS) which enzyme catalyses cytochrome P450 (CP450) and NADPH oxidase (Mittal et al., 2014). CP450 and NADPH are used in vasculature as an electron donor (Margartis et al., 2014).

In figure 14 and 18, the increase in NMR demonstrated following treatment with 50 ng/ml of TNF-α could potentially be due to an increase in enzyme synthesis for glucose-6-phosphate dehydrogenase (G6PD). This enzyme is key for the production of NADPH and TNF-α and is a key factor in improving the biogenesis of G6PD. TNF-α concentrations were seen to elevate G6PD mRNA expression (Spolarics and Wu, 1997) and this cytosolic enzyme is known for inducing the construction of NADPH significantly more than other enzymes such as, phosphogluconate dehydrogenase (PGD) and malate dehydrogenase (MDH) (Frederiks et al., 2007). So, with a greater yield of NADPH, there would be an increase in NMR which is seen with figure 14 and 18 for the 50 ng/ml TNF-α treatment.

Additionally, with the increase in the TNF-α treatment, it leads to an increase in ROS. With mesangial cells, TNF-α causes the release of ROS superoxide as well as hydrogen peroxide (McCarthy et al., 1998). With ROS being a factor in mitochondrial oxidative stress, with increased ROS it would lead to a lower NMR. This can be seen with figures 14 and 17, 10 ng/ml results. With the decreased production of NADPH enzyme and it not being able to reduce ROS adverse influences, it allows for ROS to induce its negative effects at a greater effect.

With regard to the differentiated results displayed in figures 42 and 44, the increase in OCR / NMR rate in comparison to the non-differentiated cells is due to the morphology of mitochondria. When skeletal muscle cells differentiate, the plethora of mitochondria, respiratory chain enzymes and protein respiration increases (Hoffmann et al., 2018). This is also the same for the detached ROS production levels, where an increase in mitochondria is seen, ROS levels increase also (Malinska et al., 2012). This would explain the changes seen in these figures and the increase in NMR, as NADPH expression and activity would be higher.

4.3.2 Basal respiration

Basal respiration (BR) or basal metabolic rate (BMR) is the rate of metabolism necessary to support fundamental body functions that are vital for maintenance (Larsen et al., 2011). The decrease in the rate of metabolism needed for bodily functions / Oxygen consumption rate displayed in the 72-hour incubated set (figure 18 and 22) can be attributed to ROS being far more significant in activating mitochondrial-mediated apoptosis (Kwak et al., 2012). As TNF-α has been added into the samples to express exosome synthesis for longer, it has allowed ROS production and release to be elevated. This in turn reduces the quantity and quality of cells able to functionally carry out metabolic metabolism. However, this effect is not seen following 24-hour incubation as studies have indicated that the ability of TNF-α ability to cause a decrease in cell viability in 24-hours is low (Doll et al., 2015).

On the other hand, the increase / high OCR values presented for basal respiration in figures 20 and 21 may be attributed to the enzyme synthesis of nitic oxide synthase (NOS) caused by TNF-α. The stimulatory agent is key for the induction of nitric oxide (NO) which when provided, sends a signal for the activation of NOS (Fonseca et al., 2003). With an increase of NOS, it causes NADPH oxidase to be inhibited and blocked (Gorabi et al., 2019) as the reaction removes / transfers electrons to NOS from NADPH (Andrew and Mayer et al., 1999). This can also be potentially linked to why it low levels of NMR are seen in figure 19, as NADPH levels are reduced as a result of this reaction. Furthermore, with reduced NADPH levels, it also reduced the amount of ROS, allowing for cells to carry out metabolism.

To add to this, with figures 46 – 49, with the C2C12 cells differentiating, it can potentially causes changes such as an increase in mitochondrial amount and changes in density of protein complexes of mitochondrial cristae (Malinska et al., 2012). These changes result in variation to ROS synthesis, in fact differentiation causes a decrease in mitochondria to capabily to produce ROS (Malinska et al., 2012). This change is presented in figures 46 and 48 with high BR values. As ROS isn't able to induce apoptosis as effectively, basal respiration can be carried out more effectively.

4.3.3 Maximal respiration

With maximal respiration (MR), it is the measurement in which oxygen is used during the maximum work. This is often referred to as maximum oxygen consumption. MR is theorised to be affected by factors key in the positive modulation of several nonsteroidal isoprenoids (Bouitbir et al., 2011). Coincidently, with an increase in EVs treated from varying levels of TNF-α, it results in the generation of ROS as mentioned in section 4.3.1. So, for the 50 µg/ml TNF-α concentration, it can possibly lead to

a greater generation of ROS which has been theorised to heavily reduce isoprenoids which as mentioned above plays a part in the rate in which oxygen is used during maximum work.

With regard to the data collected, the sudden drop in OCR displayed in figure 22 can be attributed to the increased synthesis of extracellular vesicles with treatment of TNF-α which can cause an increase in ROS leading to reducing isoprenoids causing a lowering of maximal respiration. From the control where the theorised yield of ROS is at a low due to no TNF-α stimulating the release of EVs, to 10 ng/ml where it has TNF-α stimulating the synthesis of ROS as a secondary product caused by the formation of EVs , the assembly of isoprenoids would be diminished allowing for one, oxidative stress to impose itself at a greater rate on mitochondria as well as further lowering the rate maximum oxygen is consumed.

However, the increase in MR can be associated with exosomes ability to reduce oxidative stress. In particular its ability to restore bioenergetics and triggering pro-survival signalling which in turn reduces oxidative stress (Arslan et al., 2013). Moreover, with exosomes increasing, it causes factors such as phosphorylated-Akt and phosphorylated-GSK-3β to be increased (Arslan et al., 2013) which are vital for the maintenance of mitochondrial function. With phosphorylated-AKT, it results in the stimulation of cell proliferation and inhibition of apoptosis (Liu et al., 2020). So, with increase proliferation, cell apoptosis within the C2C12 myoblasts is reduced allowing for exosomes to increase maximal respiration. This is seen in figure 24 and figures 50-53.

However, this effect can be seen far more greatly with results from the different cells, as exosome release is significantly higher as well as cell apoptosis greatly reduced due to phosphorylated-AKT. This allowed the MR to be far greater, hence the large OCR value.

4.3.4 Proton leak

Proton leak (PL) is dissipation of ΔP in the presence of Oligomycin, an ATP synthase inhibitor. It can also be defined as the migration of protons into the matrix, regardless of ATP synthase (Cheng et al., 2017). It should also be stated that proton leak is a key marker for mitochondrial dysfunction. Where high levels of ROS induce apoptosis and mitochondrial dysfunction, it has also been theorised that ROS can initiate uncoupling proteins (UCPs). UCPs lead to the uplifting of proton conductance which causes the promotion of proton leak through the activation of that mechanism (Cheng et al., 2017).

However, the significant increase in proton leak displayed in figure 26 with the TNF-α concentration 50 μg/ml can be associated with the relationship exosomes have with reactive oxygen species. A

complicated one, exosomes have been attributed to carry cytochrome P450, a protein family involved in ROS generation (Bodega et al., 2019). So, with TNF-α increasing exosome synthesis in this example, it causes an increase in ROS generation, further leading to an increase in PR.

On the other hand, the low levels of PL recorded, can be related to exosomes accommodating large levels of NADPH oxidase (Bodega et al., 2019). NADPH can serve as an antioxidant, so could potentially reduce the levels of ROS and therefore minimizes its cellular oxidative stress ramifications. Furthermore, other factors have been identified with inhibiting oxidative stress, further reducing PL. These include, Nrf2 mRNA, a transcription factor and other miRNAs (Bodega et al., 2019). Nrf2 mRNAs are involved in antioxidant stress responses which is the same for other miRNAs (Bodega et al., 2019). So, for figures 27 and 28, where it can be seen there in a fall in PL, it could potentially be attributed to NADPH oxidase which from referring to section 4.3.1, it is known that when EVs from NADPH oxidase treated cells causes an increase in NADPH oxidase.

With both the differentiated C2C12 72-hour (figures 54 and 55) and 24-hour (figures 56 and 57) incubation data sets, the environment is greater for the release of exosomes, enabling the extracellular vesicle to influence its mitochondrial effects on the skeletal muscle. A decrease is shown in PL compared to that seen in undifferentiated cells (figures 51 – 54). This is due to a greater synthesis of exosomes, further intensifying the release of NADPH to greater reduce ROS oxidative pressure.

4.3.5 ATP Production

Adenosine triphosphate (ATP) production is simply the cells' ability to meet energetic demands. The increase in ATP production, especially in the HS samples can be associated with exosomes increasing ATP generation. The manner in which this occurs has been related to replenishing decreased glycolytic enzymes (Arslan et al., 2013), which then increases ATP production as well as refurbishing proteins essential for the cellular oxidant mechanism (Arslan et al., 2013). With this, it causes an elevation in ATP and also oxidative phosphorylation (Arslan et al., 2013). This phosphorylation results in a downturn of ROS effectiveness in terms of its ability to induce oxidative stress. The increased ATP is seen clearly in figures 22 and 32 where there is an increase in extracellular vesicles as a result of an increase in TNF-α. Additionally, the results here are further supported with the knowledge that exosomes have been credited with activating the adenosine-mediated RISK pathway, which consequently reduces cell death (Arslan et al., 2013). This would also provide a possible connection with proton leak.

Another explanation to why an increase in ATP is presented can be attributed to the connection coenzyme Q10 (CoQ10) / Ubiquinone has with the stimulation of exosomes caused by TNF-α. C0Q10 is an essential feature for the mechanism regulating mitochondrial function (Beuttner et al., 2016) found within eukaryotic cells containing mitochondria, in this case skeletal muscle cells**.** With two key functional properties, C0Q10 can facilitate the electron transfer needed for the generation of ATP (Marcoff and Thompson, 2007). As well as it can act as an antioxidant by scavenging ROS (Noh et al., 2013), reducing the damage caused by oxidative stress. Having two alternate methods reducing the effect ROS has on mitochondrial function allows for ATP production to increase, which is evident in figure 32.

However, for the low OCR values it can also be attributed to CoQ10 ability to act as a reduction agent. It has been studied that the enzyme can undergo reduction or oxidation (Crane, 2001). In terms of acting as a reduction agent, it would cause ROS to roam more freely and more greatly influence oxidative stress effects. This could be the case for the serum free result in figure 30

Additionally, for the differentiated cells, the higher OCR values throughout can be attributed to the greater area of mitochondria found within the C2C12 cells. With this, ATP production is already heightened as well CoQ10. With greater oxidation of ROS, it will allow for a greater rate in which ATP can be synthesised. However, this is also the same for its ability to act as a reduction agent. Or this disparity in figures 50-52 compared to 53.

4.3.6 Spare Respiratory Capacity (SRC)

With SRC, presented in figures 35 - 37 and 61 - 65, it is the difference between Basals maximal activity and the rate it produces ATP (Yamamoto et al., 2016). With the data already provided in how increased exosome synthesis via TNF-α increase affects ATP production and maximal activity, it helps to understand the changes in SRC seen.

With both factors affected significantly by the release of the extracellular vesicles, the disparity between the two measurements of SRC is then increased. This is due to the mitochondria undergoing stress which causes a surge in energy demand as well as ATP being needed far greater to combat oxidative stress as well as to maintain cellular function. This is shown with the extremely high OCR values in figures 34 and 35.

Furthermore, for the measurement of SRC, it has been speculated that mitochondrial biogenesis and the antioxidant system play a vital role (Yamamoto et al., 2016). For the actual biogenesis of

mitochondria, it is regulated by AMP-activated protein kinase (AMPK) which is regulated the synthesis of exosomes. When the synthesis of **e**xosomes increases, it causes an increase in the p-AMPK/AMPK ratio (Liu et al., 2017). In doing this it causes a stimulation of spare respiratory capacity (Yamamoto et al., 2016). This would explain why slight changes are seen in SRC such as in figure 34. Furthermore, this same effect is clearly presented in the differentiated cells. With the high SRC values being a consequence of exosomes having an effect on ATP production and maximal activity, the slight changes can be assigned to the exosomes ability to increase the p-AMPK/AMPK ratio.

4.3.7 Coupling Efficiency (%)

For the final mitochondrial function analysis, coupling efficiency (CE) is the percentage linked to the generation of ATP at a specific membrane potential (Gnaiger et al., 2015). With all results gathered for this analysis, all displayed high OCR values which would be indicative of oxidative stress. With figure 39, it shows an increase in OCR as TNF-α increases. But it should be stated that the overall arrangement displayed no real change with the stimulation of TNF-α. This can be attributed to the two modes of ATP synthesis.

The first pathway involves NADPH which is further stimulated by the addition of TNF-α. Complex 1 involves NADPH as a substrate alongside complex 2 with succinic acid as a substrate (Zhao et al., 2019). With this reaction, it causes an increase in ATP however results in ROS to be released as a secondary product further resulting in myopathy to occur in the form of oxidative stress. This would explain why it displayed a plato of results with no real distinction.

Moreover, exosomes have been found to contribute to coupling efficiency by restoring complex 1 as well repairing mitochondrial membrane potential (Calabria et al., 2019). This would provide an insight to why significant low OCR values were recorded. On the other hand, as NADPH increases, it also proliferates the synthesis of ROS which in turn will cause higher oxidative stress leading to damage caused on the mitochondrial energy construction (Guo et al., 2013), the result of this is a reduction of ATP production.

Other factors have been also linked to causing a lowering of CE such as the influence reactive oxygen species have on Ca2+ homeostasis. With an increase of CA2+, it causes cytochrome c to be liberated which in turn sets in motion apoptosis (Sirvent et al., 2012). The manner in which it lowers ATP synthesis revolves around the mitochondria's outer membrane rupturing due to osmotic swelling (Sirvent et al., 2012). This reaction is invigorated by the release of ROS.

It shows this slightly in figure 39, where from the control, the OCR values decrease moderately as TNF-α Increases, which naturally increases ROS production. For the differentiated cells, OCR / CE was remarkably lower in comparison to the non-differentiated cells. This was simply due to the increase in mitochondrial yield in these cells, allowing for ROS to impose oxidative stress greater leading to a decrease in ATP production at the specific membrane.

5.0 Conclusion

For the investigation, although procedures were carried out to investigate the role skeletal muscles have on mitochondrial function within skeletal muscle cells. With this, there is a possibility for extracellular vesicles to be used as an effective and more importantly safe therapeutic way of treating mitochondrial dysfunction associated disorders. These could include the likes of diabetes mellitus and external ophthalmoplegia. Furthermore, with the cell-to-cell communication ability that extracellular vesicles withhold, it opens the door for specific drug deliverance to treat a particular disease.

Regarding limitations, one of the major issues was not being able to carry out repeat testing to eliminate experimental errors due to the pandemic. Being limited to the amount of time available in the labs resulted in only being able to carry out one full method plan. This naturally in comparison to repeated tests leads to more inaccurate results, not having multiple repeats removes the ability to work out more defined averages for the results. For example, with figures 27 and 31, the graphs show a large spread of data around the mean. These figures could have been refined with further repeat testing to improve the validity. Not having this level of accuracy doesn't help to indicate whether the chosen method plan was in fact the correct idea as well as highlighting if in fact what was done was correct.

Additionally, this work only investigated the effects of one stimulatory agent, this being TNF-α. In fact, phorbol myristate acetate (PMA), another stimulatory agent, has been shown not to promote exosomal biogenesis but activate ectodomain shedding events located in the plasma membrane (Stoeck et al., 2006). Although having a part in exosomal delivery, no real data has been established. This would have been an opportunity to test this stimulatory agent and see how the results would have altered in comparison to TNF-α. Furthermore, Calcium ionophore (ionomycin) has also been shown to stimulate the release of exosomes. This has been indicated to be carried out in synaptotagmins, a calcium sensor involved in vesicular transport (Hessvik and Llorente, 2018). If able to investigate multiple stimulatory agents, it could've depicted contrasting results to what was gathered and could have even supported conclusions made in this thesis and opened up new avenues for research.

Moreover, with the lack of literature / current research surrounding the topic, it made it increasingly difficult to form accurate theoretical starting points as well as knowing if the results gathered were similar to what was previously recorded in existing research. Having anything related to the thesis

would have helped narrow the scope in terms of the hypothesis being set. Not having this does lower the credibility of the results gathered as there isn't much to compare to and doesn't help when coming against problems. However, the lack of research in this area promotes the novelty of the work presented in this thesis.

For future research, some of the limitations should be addressed such as additional repeats needing to be carried out; as well testing other stimulatory agents. For example, with PMA, it is known that it works in corelation with ADAM 17, a tumour necrosis factor α-converting enzyme (Stoeck et al., 2006). Using this knowledge, it would be a starting point to see how this work together to promote exosomal production and effect factors highlighted in the mitochondrial functional analyses. Having these carried out would naturally help to increase the accuracy of the results gathered as well as potentially open up new avenues of research.

From the data obtained from the investigation, it can be seen that cells stimulated with the stimulatory agent, TNF-α assists and promotes the syntheses of Extracellular vesicles. This was made possible with the data provided for protein expression, displaying an increased expression of hallmark exosomal markers, CD9 and CD81. Moreover, it was possible to conclude that extracellular vesicles were able to augment mitochondrial function with the help of the seahorse mito stress test.

6.0 Reference list

Abels, E.R. and Breakefield, X.O., 2016. Introduction to extracellular vesicles: biogenesis, RNA cargo selection, content, release, and uptake. *Cellular and molecular neurobiology*, *36*(3), pp.301-312.

Akers, J.C., Gonda, D., Kim, R., Carter, B.S. and Chen, C.C., 2013. Biogenesis of extracellular vesicles (EV): exosomes, microvesicles, retrovirus-like vesicles, and apoptotic bodies. *Journal of neuro-oncology*, *113*(1), pp.1-11.

Alenquer, M. and Amorim, M.J., 2015. Exosome biogenesis, regulation, and function in viral infection. *Viruses*, *7*(9), pp.5066-5083.

Amo, T., Yadava, N., Oh, R., Nicholls, D.G. and Brand, M.D., 2008. Experimental assessment of bioenergetic differences caused by the common European mitochondrial DNA haplogroups H and T. Gene, 411(1-2), pp.69-76.

Amorim, I.S., Lach, G. and Gkogkas, C.G., 2018. The role of the eukaryotic translation initiation factor 4E (eIF4E) in neuropsychiatric disorders. *Frontiers in genetics*, *9*, p.561.

Andreu, Z. and Yáñez-Mó, M., 2014. Tetraspanins in extracellular vesicle formation and function. *Frontiers in immunology*, *5*, p.442.

Andrew, P.J. and Mayer, B., 1999. Enzymatic function of nitric oxide synthases. *Cardiovascular research*, *43*(3), pp.521-531.

Arslan, F., Lai, R.C., Smeets, M.B., Akeroyd, L., Choo, A., Aguor, E.N., Timmers, L., van Rijen, H.V., Doevendans, P.A., Pasterkamp, G. and Lim, S.K., 2013. Mesenchymal stem cell-derived exosomes increase ATP levels, decrease oxidative stress and activate PI3K/Akt pathway to enhance myocardial viability and prevent adverse remodeling after myocardial ischemia/reperfusion injury. *Stem cell research*, *10*(3), pp.301-312.

Bittel, D.C. and Jaiswal, J.K., 2019. Contribution of extracellular vesicles in rebuilding injured muscles. *Frontiers in physiology*, *10*, p.828.

Bodega, G., Alique, M., Puebla, L., Carracedo, J. and Ramírez, R.M., 2019. Microvesicles: ROS scavengers and ROS producers. *Journal of extracellular vesicles*, *8*(1), p.1626654.

Bonetto, A., Penna, F., Minero, V.G., Reffo, P., Costamagna, D., Bonelli, G., Baccino, F.M. and Costelli, P., 2011. Glutamine prevents myostatin hyperexpression and protein hypercatabolism induced in C2C12 myotubes by tumor necrosis factor-α. *Amino Acids*, *40*(2), pp.585-594.

Bouitbir, J., Charles, A.L., Rasseneur, L., Dufour, S., Piquard, F., Geny, B. and Zoll, J., 2011. Atorvastatin treatment reduces exercise capacities in rats: involvement of mitochondrial impairments and oxidative stress. Journal of applied physiology, 111(5), pp.1477-1483.

Buckingham, M., Bajard, L., Chang, T., Daubas, P., Hadchouel, J., Meilhac, S., Montarras, D., Rocancourt, D. and Relaix, F., 2003. The formation of skeletal muscle: from somite to limb. *Journal of anatomy*, *202*(1), pp.59-68.

Buettner, C., Greenman, R.L., Ngo, L.H. and Wu, J.S., 2016. Effects of coenzyme Q10 on skeletal muscle oxidative metabolism in statin users assessed using 31P magnetic resonance spectroscopy: a randomized controlled study. *Journal of nature and science*, *2*(8).

Calabria, E., Scambi, I., Bonafede, R., Schiaffino, L., Peroni, D., Potrich, V., Capelli, C., Schena, F. and Mariotti, R., 2019. Ascs-exosomes recover coupling efficiency and mitochondrial membrane potential in an in vitro model of als. *Frontiers in neuroscience*, *13*, p.1070.

Castro, B.M., Torreno-Pina, J.A., van Zanten, T.S. and Garcia-Parajo, M.F., 2013. Biochemical and imaging methods to study receptor membrane organization and association with lipid rafts. *Methods in cell biology*, *117*, pp.105-122.

Cheng, J., Nanayakkara, G., Shao, Y., Cueto, R., Wang, L., Yang, W.Y., Tian, Y., Wang, H. and Yang, X., 2017. Mitochondrial proton leak plays a critical role in pathogenesis of cardiovascular diseases. In Mitochondrial Dynamics in Cardiovascular Medicine (pp. 359-370). Springer, Cham.

Clarke, C.J., Cloessner, E.A., Roddy, P.L. and Hannun, Y.A., 2011. Neutral sphingomyelinase 2 (nSMase2) is the primary neutral sphingomyelinase isoform activated by tumour necrosis factor-α in MCF-7 cells. *Biochemical Journal*, *435*(2), pp.381-390.

Console, L., Scalise, M. and Indiveri, C., 2019. Exosomes in inflammation and role as biomarkers. *Clinica Chimica Acta*, *488*, pp.165-171.

Crane, F.L., 2001. Biochemical functions of coenzyme Q10. *Journal of the American College of Nutrition*, *20*(6), pp.591-598.

Doll, D.N., Rellick, S.L., Barr, T.L., Ren, X. and Simpkins, J.W., 2015. Rapid mitochondrial dysfunction mediates TNF-alpha-induced neurotoxicity. *Journal of neurochemistry*, *132*(4), pp.443-451.

Eldh, M., Ekström, K., Valadi, H., Sjöstrand, M., Olson, B., Jernäs, M. and Lötvall, J., 2010. Exosomes communicate protective messages during oxidative stress; possible role of exosomal shuttle RNA., 5(12), p.e15353.

Fonseca, S.G., Romão, P.R., Figueiredo, F., Morais, R.H., Lima, H.C., Ferreira, S.H. and Cunha, F.Q., 2003. TNF-α mediates the induction of nitric oxide synthase in macrophages but not in neutrophils in experimental cutaneous leishmaniasis. *European journal of immunology*, *33*(8), pp.2297-2306.

Franke, J., Abs, V., Zizzadoro, C. and Abraham, G., 2014. Comparative study of the effects of fetal bovine serum versus horse serum on growth and differentiation of primary equine bronchial fibroblasts. *BMC veterinary research*, *10*(1), pp.1-9.

Frederiks, W.M., Kümmerlin, I.P., Bosch, K.S., Vreeling-Sindelarova, H., Jonker, A. and Noorden, C.J.V., 2007. NADPH production by the pentose phosphate pathway in the zona fasciculata of rat adrenal gland. *Journal of Histochemistry & Cytochemistry*, *55*(9), pp.975-980.

Frontera, W.R. and Ochala, J., 2015. Skeletal muscle: a brief review of structure and function. *Calcified tissue international*, *96*(3), pp.183-195.

Ganesan, D. and Cai, Q., 2021. Understanding amphisomes. *Biochemical Journal*, *478*(10), pp.1959-1976.

Gawlitta, D., Boonen, K.J., Oomens, C.W., Baaijens, F.P. and Bouten, C.V., 2008. The influence of serum-free culture conditions on skeletal muscle differentiation in a tissue-engineered model. *Tissue Engineering Part A*, *14*(1), pp.161-171.

Gnaiger, E., Boushel, R., Søndergaard, H., Munch-Andersen, T., Damsgaard, R., Hagen, C., Díez-Sánchez, C., Ara, I., Wright-Paradis, C., Schrauwen, P. and Hesselink, M., 2015. Mitochondrial coupling and capacity of oxidative phosphorylation in skeletal muscle of Inuit and Caucasians in the arctic winter. Scandinavian journal of medicine & science in sports, 25, pp.126-134.

Gorabi, A.M., Kiaie, N., Hajighasemi, S., Banach, M., Penson, P.E., Jamialahmadi, T. and Sahebkar, A., 2019. Statin-induced nitric oxide signaling: Mechanisms and therapeutic implications. Journal of clinical medicine, 8(12), p.2051.

Guo, C., Sun, L., Chen, X. and Zhang, D., 2013. Oxidative stress, mitochondrial damage and neurodegenerative diseases. Neural regeneration research, 8(21), p.2003

Hessvik, N.P. and Llorente, A., 2018. Current knowledge on exosome biogenesis and release. *Cellular and Molecular Life Sciences*, *75*(2), pp.193-208.

Hettling, H. and van Beek, J.H., 2011. Analyzing the functional properties of the creatine kinase system with multiscale 'sloppy'modeling. *PLoS computational biology*, *7*(8), p.e1002130.

Hoffmann, C., Höckele, S., Kappler, L., de Angelis, M.H., Häring, H.U. and Weigert, C., 2018. The effect of differentiation and TGFβ on mitochondrial respiration and mitochondrial enzyme abundance in cultured primary human skeletal muscle cells. *Scientific reports*, *8*(1), pp.1-12.

Jeppesen, D.K., Fenix, A.M., Franklin, J.L., Higginbotham, J.N., Zhang, Q., Zimmerman, L.J., Liebler, D.C., Ping, J., Liu, Q., Evans, R. and Fissell, W.H., 2019. Reassessment of exosome composition. *Cell*, *177*(2), pp.428-445.

Jing, L.I.U. and Anning, L.I.N., 2005. Role of JNK activation in apoptosis: a double-edged sword. *Cell research*, *15*(1), pp.36-42.

Kalluri, R. and LeBleu, V.S., 2016, January. Discovery of double-stranded genomic DNA in circulating exosomes. In *Cold Spring Harbor symposia on quantitative biology* (Vol. 81, pp. 275-280). Cold Spring Harbor Laboratory Press.

Konior, A., Schramm, A., Czesnikiewicz-Guzik, M. and Guzik, T.J., 2014. NADPH oxidases in vascular pathology. *Antioxidants & redox signaling*, 20(17), pp.2794-2814.

Kosaka, N., Iguchi, H., Hagiwara, K., Yoshioka, Y., Takeshita, F. and Ochiya, T., 2013. Neutral sphingomyelinase 2 (nSMase2)-dependent exosomal transfer of angiogenic microRNAs regulate cancer cell metastasis. *Journal of Biological Chemistry*, *288*(15), pp.10849-10859.

Kwak, H.B., Thalacker-Mercer, A., Anderson, E.J., Lin, C.T., Kane, D.A., Lee, N.S., Cortright, R.N., Bamman, M.M. and Neufer, P.D., 2012. Simvastatin impairs ADP-stimulated respiration and increases mitochondrial oxidative stress in primary human skeletal myotubes. *Free Radical Biology and Medicine*, 52(1), pp.198-207.

Langen, R.C., Schols, A.M., Kelders, M.C., Wouters, E.F. And Janssen-Heininger, Y.M., 2001. Inflammatory cytokines inhibit myogenic differentiation through activation of nuclear factor-κB. *The FASEB Journal*, *15*(7), pp.1169-1180.

Larsen, F.J., Schiffer, T.A., Sahlin, K., Ekblom, B., Weitzberg, E. and Lundberg, J.O., 2011. Mitochondrial oxygen affinity predicts basal metabolic rate in humans. The FASEB Journal, 25(8), pp.2843-2852.

Li, B., Li, L., Zhang, Q., Zhang, H. and Xiu, R., 2019. Effects of tumor necrosis factor-α-induced exosomes on the endothelial cellular behavior, metabolism and bioenergetics. *Microcirculation*, *26*(1), p.e12515.

Liu, L., Jin, X., Hu, C.F., Li, R. and Shen, C.X., 2017. Exosomes derived from mesenchymal stem cells rescue myocardial ischaemia/reperfusion injury by inducing cardiomyocyte autophagy via AMPK and Akt pathways. *Cellular physiology and biochemistry*, *43*(1), pp.52-68.

Liu, M., Huang, X., Tian, Y., Yan, X., Wang, F., Chen, J., Zhang, Q., Zhang, Q. and Yuan, X., 2020. Phosphorylated GSK-3β protects stress-induced apoptosis of myoblasts via the PI3K/Akt signaling pathway. *Molecular medicine reports*, *22*(1), pp.317-327.

Malinska, D., Kudin, A.P., Bejtka, M. and Kunz, W.S., 2012. Changes in mitochondrial reactive oxygen species synthesis during differentiation of skeletal muscle cells. *Mitochondrion*, *12*(1), pp.144-148.

Marcoff, L. and Thompson, P.D., 2007. The role of coenzyme Q10 in statin-associated myopathy: a systematic review. Journal of the American College of Cardiology, 49(23), pp.2231-2237.

Margaritis, M., Channon, K.M. and Antoniades, C., 2014. Statins as regulators of redox state in the vascular endothelium: beyond lipid lowering. *Antioxidants & redox signaling*, 20(8), pp.1198-1215.
Margolis, L. and Sadovsky, Y., 2019. The biology of extracellular vesicles: The known unknowns. *PLoS biology*, *17*(7), p.e3000363.

McCarthy, E.T., Sharma, R., Sharma, M., Li, J.Z., Ge, X.L., Dileepan, K.N. and Savin, V.J., 1998. TNF-alpha increases albumin permeability of isolated rat glomeruli through the generation of superoxide. *Journal of the American Society of Nephrology*, *9*(3), pp.433-438.

McLean J et al., 2013. Tumor necrosis factor-α (TNF) effects on mitochondrial metabolism in C2C12 myotubes. *The FASEB Journal*, 27(S1).

Meckes Jr, D.G. and Raab-Traub, N., 2011. Microvesicles and viral infection. *Journal of virology*, *85*(24), pp.12844-12854.

Miao, C., Zhang, W., Feng, L., Gu, X., Shen, Q., Lu, S., Fan, M., Li, Y., Guo, X., Ma, Y. and Liu, X., 2021. Cancer-derived exosome miRNAs induce skeletal muscle wasting by Bcl-2-mediated apoptosis in colon cancer cachexia. *Molecular Therapy-Nucleic Acids*, *24*, pp.923-938.

Miller, A.L., 1999. Therapeutic considerations of L-glutamine: a review of the literature. *Alternative medicine review: a journal of clinical therapeutic*, *4*(4), pp.239-248.

Millward, D.J., Garlick, P.J., James, W.P.T., Nnanyelugo, D.O. and Ryatt, J.S., 1973. Relationship between protein synthesis and RNA content in skeletal muscle. *Nature*, *241*(5386), pp.204-205.

Mittal, M., Siddiqui, M.R., Tran, K., Reddy, S.P. and Malik, A.B., 2014. Reactive oxygen species in inflammation and tissue injury. *Antioxidants & redox signaling*, 20(7), pp.1126-1167.

Mobley, C.B., Mumford, P.W., McCarthy, J.J., Miller, M.E., Young, K.C., Martin, J.S., Beck, D.T., Lockwood, C.M. and Roberts, M.D., 2017. Whey protein-derived exosomes increase protein synthesis and hypertrophy in C2C12 myotubes. *Journal of dairy science*, *100*(1), pp.48-64.

Morita, M., Gravel, S.P., Hulea, L., Larsson, O., Pollak, M., St-Pierre, J. and Topisirovic, I., 2015. mTOR coordinates protein synthesis, mitochondrial activity and proliferation. *Cell cycle*, *14*(4), pp.473-480.

Murphy, C., Withrow, J., Hunter, M., Liu, Y., Tang, Y.L., Fulzele, S. and Hamrick, M.W., 2018. Emerging role of extracellular vesicles in musculoskeletal diseases. *Molecular aspects of medicine*, *60*, pp.123-128.

Noh, Y.H., Kim, K.Y., Shim, M.S., Choi, S.H., Choi, S., Ellisman, M.H., Weinreb, R.N., Perkins, G.A. and Ju, W.K., 2013. Inhibition of oxidative stress by coenzyme Q10 increases mitochondrial mass and improves bioenergetic function in optic nerve head astrocytes. *Cell death & disease*, *4*(10), pp.e820-e820.

Peng, X., Yang, L., Ma, Y., Li, X., Yang, S., Li, Y., Wu, B., Tang, S., Zhang, F., Zhang, B. and Liu, J., 2021. IKKβ activation promotes amphisome formation and extracellular vesicle secretion in tumor cells. *Biochimica et Biophysica Acta (BBA)-Molecular Cell Research*, *1868*(1), p.118857.

Petrovčíková, E., Vičíková, K. and Leksa, V., 2018. Extracellular vesicles–biogenesis, composition, function, uptake and therapeutic applications. *Biologia*, *73*(4), pp.437-448.

Qin, W. and Dallas, S.L., 2019. Exosomes and extracellular RNA in muscle and bone aging and crosstalk. *Current osteoporosis reports*, *17*(6), pp.548-559.

Raposo, G. and Stoorvogel, W., 2013. Extracellular vesicles: exosomes, microvesicles, and friends. *Journal of Cell Biology*, *200*(4), pp.373-383.

Rolfe, M., James, N.H. and Roberts, R.A., 1997. Tumour necrosis factor alpha (TNF alpha) suppresses apoptosis and induces DNA synthesis in rodent hepatocytes: a mediator of the hepatocarcinogenicity of peroxisome proliferators?. *Carcinogenesis*, *18*(11), pp.2277-2280.

Rome, S., Forterre, A., Mizgier, M.L. and Bouzakri, K., 2019. Skeletal muscle-released extracellular vesicles: state of the art. *Frontiers in physiology*, *10*, p.929.

Sirvent, P., Fabre, O., Bordenave, S., Hillaire-Buys, D., De Mauverger, E.R., Lacampagne, A. and Mercier, J., 2012. Muscle mitochondrial metabolism and calcium signaling impairment in patients treated with statins. Toxicology and applied pharmacology, 259(2), pp.263-268.

Stoeck, A., Kelle r, S., Riedle, S., Sanderson, M.P., Runz, S., Le Naour, F., Gutwein, P., Ludwig, A., Rubinstein, E. and Altevogt, P., 2006. A role for exosomes in the constitutive and stimulus-induced ectodomain cleavage of L1 and CD44. *Biochemical Journal*, 393(3), pp.609-618.

Spolarics, Z. and Wu, J.X., 1997. Tumor necrosis factor alpha augments the expression of glucose-6-phosphate dehydrogenase in rat hepatic endothelial and Kupffer cells. *Life sciences*, *60*(8), pp.565-571.

Tang, D., Tao, D., Fang, Y., Deng, C., Xu, Q. and Zhou, J., 2017. TNF-alpha promotes invasion and metastasis via NF-kappa B pathway in oral squamous cell carcinoma. *Medical science monitor basic research*, *23*, p.141.

Tassew, N.G., Charish, J., Shabanzadeh, A.P., Luga, V., Harada, H., Farhani, N., D'Onofrio, P., Choi, B., Ellabban, A., Nickerson, P.E. and Wallace, V.A., 2017. Exosomes mediate mobilization of autocrine Wnt10b to promote axonal regeneration in the injured CNS. *Cell reports*, *20*(1), pp.99-111.
Trioulier, Y., Torch, S., Blot, B., Cristina, N., Chatellard-Causse, C., Verna, J.M. and Sadoul, R., 2004. Alix, a protein regulating endosomal trafficking, is involved in neuronal death. *Journal of Biological Chemistry*, *279*(3), pp.2046-2052.

Vader, P., Mol, E.A., Pasterkamp, G. and Schiffelers, R.M., 2016. Extracellular vesicles for drug delivery. *Advanced drug delivery reviews*, *106*, pp.148-156.

Van der Pol, E., Böing, A.N., Harrison, P., Sturk, A. and Nieuwland, R., 2012. Classification, functions, and clinical relevance of extracellular vesicles. *Pharmacological reviews*, *64*(3), pp.676-705.

Van Niel, G., d'Angelo, G. and Raposo, G., 2018. Shedding light on the cell biology of extracellular vesicles. *Nature reviews Molecular cell biology*, *19*(4), pp.213-228.

Vechetti Jr, I.J., Valentino, T., Mobley, C.B. and McCarthy, J.J., 2021. The role of extracellular vesicles in skeletal muscle and systematic adaptation to exercise. *The Journal of physiology*, *599*(3), pp.845-861.

Yamamoto, H., Morino, K., Mengistu, L., Ishibashi, T., Kiriyama, K., Ikami, T. and Maegawa, H., 2016. Amla enhances mitochondrial spare respiratory capacity by increasing mitochondrial biogenesis and antioxidant systems in a murine skeletal muscle cell line. Oxidative medicine and cellular longevity, 2016.

Yáñez-Mó, M., Siljander, P.R.M., Andreu, Z., Bedina Zavec, A., Borràs, F.E., Buzas, E.I., Buzas, K., Casal, E., Cappello, F., Carvalho, J. and Colás, E., 2015. Biological properties of extracellular vesicles and their physiological functions. *Journal of extracellular vesicles*, *4*(1), p.27066

Yue, B., Yang, H., Wang, J., Ru, W., Wu, J., Huang, Y., Lan, X., Lei, C. and Chen, H., 2020. Exosome biogenesis, secretion and function of exosomal miRNAs in skeletal muscle myogenesis. *Cell Proliferation*, *53*(7), p.e12857.

Zhang, J., Li, S., Li, L., Li, M., Guo, C., Yao, J. and Mi, S., 2015. Exosome and exosomal microRNA: trafficking, sorting, and function. *Genomics, proteomics & bioinformatics*, *13*(1), pp.17-24.

Zhang, Y., Liu, Y., Liu, H. and Tang, W.H., 2019. Exosomes: biogenesis, biologic function and clinical potential. *Cell & bioscience*, *9*(1), pp.1-18.

Zhao, R.Z., Jiang, S., Zhang, L. and Yu, Z.B., 2019. Mitochondrial electron transport chain, ROS generation and uncoupling. International journal of molecular medicine, 44(1), pp.3-15.